الجمهورية الجزائرية الديمقراطية الشعبية

République Algérienne Démocratique et Populaire

Ministère de L'Enseignement Supérieur et de la Recherche Scientifique

Université Ferhat ABBAS Sétif 1

UNIVERSITÉ FERHAT ABBAS - SETIF1

FACULTÉ DE TECHNOLOGIE

THÈSE

Présentée au Département de Génie des Procèdes

Pour l'obtention du diplôme de

DOCTORAT

Domaine : Sciences et Technologie

Filière: Génie des Procédés **Option: Matériaux Polymères**

Par

MAHDI Billal

THÈME

Synthèse et caractérisation d'un matériau hybride organique-inorganique à base PVA/SiO_2 par la méthode sol-gel

Soutenue le 06/07/2023 devant le Jury:

GUESSOM Melia	**Professeur**	**Univ. Ferhat Abbas Sétif 1**	**Président**
ROUABAH Farid	**Professeur**	**Univ. Ferhat Abbas Sétif 1**	**Directeur de thèse**
HELLATI Abdelhak	**Professeur**	**Univ. Bordj Bou Arreridj**	**Examinateur**
DOUFNOUNE Rachida	**Professeur**	**Univ. Ferhat Abbas Sétif 1**	**Examinatrice**

الجمهورية الجزائرية الديمقراطية الشعبية
Democratic and Popular Republic of Algeria
Ministry of Higher Education and Scientific Research

University of Ferhat ABBAS- Setif-1

FACULTY OF TECHNOLOGY

THESE

Presented to the Process Engineering Department

For obtaining of the diploma of

DOCTORAT

Domain : Science and technology

Sector: Process Engineering **Option: Polymeric materials**

By

MAHDI Billal

THEME

Synthesis and characterization of an organic-inorganic hybrid material based on PVA/SiO$_2$ by the sol-gel method

Defended on 06/07/2023 Front of the Jury:

GUESSOM Melia	**Professor**	**Univ. Ferhat Abbas Sétif 1**	**President**
ROUABAH Farid	**Professor**	**Univ. Ferhat Abbas Sétif 1**	**Supervisor**
HELLATI Abdelhak	**Professor**	**Univ. Bordj Bou Arreridj**	**Examiner**
DOUFNOUNE Rachida	**Professor**	**Univ. Ferhat Abbas Sétif 1**	**Examiner**

DEDICATION

I dedicate this thesis to my family and many friends. A special feeling of gratitude to my loving parents, whose words of encouragement and push for tenacity still ring in my ears.

To my faithful brothers and sisters, who have never left my side and are very special.

I also dedicate this dissertation to everyone who has supported me in one way or the other.

B. MAHDI

Acknowledgments

This research has been conducted at the Laboratory of Physico-Chemistry of High Polymers (LPCHP), University Ferhat Abbas of Setif-1, Department of Process Engineering under the supervision of **Prof. F. ROUABAH**.

First and foremost, I would like to express my deep and sincere gratitude to my supervisor **Prof. F. ROUABAH** for his continuous support during my Ph.D. study and research, as well as for his patience, motivation, and immense knowledge. He was an exceptional supervisor, providing precious guidance, patience, and enthusiasm. Whenever I had questions or problems, he was always there to provide effective assistance.

I am very thankful to him for giving me such an interesting project that opened up a whole new world of science to me. His intelligence and rich knowledge always inspired and encouraged me.

I would also like to thank all members of my jury, **Prof. M. GUESSOM**, **Prof. R. DOUFNOUNE** and **Prof. A. HELLATI** for taking the time to read, assess, and judge my thesis. Your suggestions have made this work even better and more valuable.

My special acknowledgments go to **Prof. N. HADAOUI** for his precious help and services, as well as to all the professors and staff of Department of Process Engineering.

I express my sincere gratitude to miss **Ibtisam** Engineer at the Laboratory of LPCHP, as well as to all the other members of the lab for their technical and administrative assistance.

B. MAHDI

Table of contents

Literature Review

Chapter III: Overviews of the Materials Used……...…………...………………...…...………..42

The Experimental Part

List of Acronyms and Symbols

CVD: Chemical vapor deposition

DI: Deionized water

DSC: Differential Scanning Calorimetry

FTIR: Fourier transform infrared

FHD: Flame hydrolysis deposition

PVA: Poly (vinyl alcohol)

Silica: Silicon dioxide

SiO_2: Silicon dioxide

TiO_2: Titanium dioxide

TEOS: Tetraethyl Ortho silicate

TGA: Thermogravimetric analysis

UV-Vis: Ultraviolet-visible spectrometry

XRD: X-ray diffraction

List of Figures

List of tables

Introduction

1. Introduction

Organic-inorganic hybrid materials especially the compounds doped with nanoparticles including various metal oxides or clays are now being studied extensively and attract much research attention because of their properties originating from the organic part (flexibility, easy processability, light weight) combined with those of the inorganic part (stiffness, high strength, dimensional stability, chemical resistance, and thermal stability) [1–6]. This makes them high-quality and multifunctional materials in addition to their unique optical properties and switching capacity. Hybrid materials have a wide range of applications in different fields like optics [7], electronics [8], Ionics [9], mechanics [10], energy [11], environment [12], biology [13], medicine [14] and many more.

To obtain hybrid materials doped with different nanoparticles, several methods have been developed and used, including flame hydrolysis deposition (FHD) [15], thermal oxidation [16], chemical vapor deposition (CVD) [17].

As a consequence of their expensive and time-consuming protocols, these methods are effective but, difficult to implement for large-scale processing due to high reaction temperatures, lengthy reaction times, and the usage of toxic reagents.

In contrast to these methods, the sol-gel method is the best one for synthesizing hybrid materials because it is simple, easy to handle, and inexpensive [18,20]. The process of sol-gel enables the preparation of materials in various configurations such as monoliths [21], coatings [22], foams [23], powders [24], and fibers [25].

The sol-gel method offers many advantages, including the possibility to monitor reaction structure and stoichiometry, the possibility to add different functional groups, and the possibility to fill with nanoparticles, at ambient pressure, and temperatures below 100°C under the so-called soft chemistry conditions [26].

Via hydrolysis-condensation reactions, the sol-gel method converts a substance from the liquid state (Sol) to a gel state (Gel). The sol is a solid dispersion of colloidal particles which are often alkoxides with [$M(OR)_4$] form or polymers dissolved in a solvent.

Polyvinyl Alcohol (PVA) is a semi-crystalline, biocompatible, and biodegradable polymer but, typically cannot be used alone in many applications [27], due to its poor mechanical properties, high humidity absorption, and low water resistance. PVA has been used in various studies to prepare thin films [28], fibers [29], and hydrogels [30].

As stated in several studies [31], adding silica to polyvinyl alcohol (PVA) improves the properties of the latter. Bandyopadhyay et al [4] synthesized a PVA/Silica (TEOS) with various ratios, reported an increase in PVA water resistance, and mechanical properties, and noticed that the PVA with 40% of TEOS exhibited the highest tensile strength. Pingan *et al* [32] synthesized PVA/SiO_2 (50/50%) adhesive to study the effect of the H_2O/TEOS ratio. They reported that the PVA/silica composite has excellent mechanical properties and thermal stability with high transparency compared to neat PVA. They also found that the best molar ratio of water to TEOS is equal to unity (1) which induces a lower crystallinity and better dispersion.

Nakane *et al* [33] reported that the PVA/SiO_2 composites containing more than 60 wt % of silica become brittle. In general, films prepared by blending organic polymers and inorganic particles at low concentrations exhibit better properties than those of the unfilled polymer [34]. Nano-TiO_2 is commonly used in air purification in wastewater treatment, product processing, and several other uses. TiO_2 has many special properties, including its high chemical stability, antibacterial activity, photocatalytic properties, UV-Rays resistance, non-toxicity, biocompatibility, and low commercial cost [35]. It exists in three distinct crystalline forms: anatase, brookite, and Rutile which is the most stable phase. Due to its strong scattering influence, rutile TiO_2 offers excellent ultraviolet light shielding. Nanoparticles have a significant ability to accumulate in water owing to their high surface energy. When they are aggregated, their performance plummets [33].

The dispersion of nanoparticles throughout a medium may be carried out by using an incorporating dispersant or an ultrasonic technique [36–38]. Ultrasonic agitation is a lot more powerful tool for deagglomeration than magnetic stirring since it generates shock waves that produce a rough atmosphere in which any chemical reaction with the polymer and nanoparticles can easily occur producing a better dispersion accompanied by fewer agglomerations [39–41].

This work aims to synthesize and characterize a hybrid material based on poly (vinyl alcohol)/ silica gel at different levels (1, 3, and 5%wt (by weight)) of nano-TiO_2 by using the sol-gel process, and ultrasonic agitation to obtain a better dispersion, and to study the consequences on their thermal and physico-chemical properties.

The originality of this research is: This work is focused on the preparation and characterization of poly (vinyl alcohol)/silica gel/Nano-TiO_2, and the study of titanium dioxide (TiO_2) nanoparticles (from 1 to 5%) on the properties of poly (vinyl alcohol)/silica films, unlike previous researchers, who used TiO_2 from precursor to poly (vinyl alcohol)/silica gel, that has not been studied before.

The literature review in **Chapters I, II, and III** will delve into the different classes of hybrid materials and the sol-gel process, including its various parameters and their impact on the final product. Additionally, general information on PVA, silicon dioxide, and titanium dioxide will be provided, including their properties, synthesis methods, and intended applications.

Chapters IV and V focus on the experimental study. **Chapter IV's** first part discusses the materials used and the development of sols for hybrid film preparation. The second part covers the techniques of structural, thermal, and physical characterization of hybrid materials, which will enable us to study their properties and determine their performances.

Chapter V presents the results of the characterization of the hybrids, which are analyzed with consideration of various effects, such as the impact of the inorganic part on pure PVA and the effect of TiO_2 content on PVA/SiO_2 films.

Finally, the thesis concludes with a general conclusion and recommendations for future work.

References

[1] Higuchi M, Otsuka Y, Shomura R, Kurth D G, Syntheses of novel bis-terpyridine and cyclic phenylazomethine as organic modules in organic–metallic hybrid materials, Thin Solid Films. 516 (2008) 2416–20.

[2] Markovic G, Visakh P M, 1 - Polymer blends: State of art Recent Developments In Polymer Macro, Micro and Nano Blend ed P M Visakh, G Markovic and D Pasquini (Woodhead Publishing). (2017) pp 1–15.

[3] Kim C, Huan T D, Krishnan S, Ramprasad R, A hybrid organic-inorganic perovskite dataset Scientific Data, Volume 4, id. 170057 (2017). 4 170057

[4] Bandyopadhyay A, De Sarkar M, Bhowmick A K, Poly (vinyl alcohol)/silica hybrid nanocomposites by sol-gel technique: Synthesis and properties, J Mater Sci. 40 (2005) 5233–41.

[5] Kanie K, Muramatsu A, Organic-Inorganic Hybrid Liquid Crystals: Innovation Toward "Suprahybrid Material" Nanohybridization of Organic-Inorganic Materials Advances in Materials Research ed A Muramatsu and T Miyashita, (Berlin, Heidelberg: Springer). (2009) pp 41–53.

[6] Rosato D V, Di Mattia D P, Rosato D V, The Properties of Plastics Designing with Plastics and Composites: A Handbook ed D V Rosato, D P Di Mattia, and D V Rosato, (Boston, MA: Springer US). (1991) pp 405–588.

[7] Serbin J, Egbert A, Ostendorf A, Chichkov B N, Houbertz R, Domann G, Schulz J, Cronauer C, Fröhlich L and Popall M, Femtosecond laser-induced two-photon polymerization of inorganic–organic hybrid materials for applications in photonics, Opt. Lett., OL. 28 (2003) 301–3.

[8] Houbertz R, Schulz J, Fröhlich L, Domann G, Popall M, Inorganic-organic hybrid materials for polymer electronic applications, MRS Online Proceedings Library Archive. 769 (2003).

[9] Lai Q, Zhang L, Li Z, Stickle W F, Williams R S, Chen Y, Ionic/Electronic Hybrid Materials Integrated in a Synaptic Transistor with Signal Processing and Learning Functions, Advanced Materials. 22 (2010) 2448–53.

[10] Wei Y, Jin D, Xu J, Baran G, Qiu K-Y, Mechanical properties of interface-free polyacrylate-silica hybrid sol-gel materials for potential dental applications, Polymers for Advanced Technologies. 12 (2001) 361–8.

[11] Choudhary N, Islam M A, Kim J H, Ko T-J, Schropp A, Hurtado L, Weitzman D, Zhai L, Jung Y, Two-dimensional transition metal dichalcogenide hybrid materials for energy applications, Nano Today. 19 (2018) 16–40.

[12] Ruiz-Hitzky E, Aranda P, Darder M, Rytwo G, Hybrid materials based on clays for environmental and biomedical applications, J. Mater. Chem. 20 (2010) 9306–21.

[13] Catauro M, Raucci M G, Ausanio G, Ambrosio L, Sol-gel Synthesis, Characterization and Bioactivity of Poly(Ether-Imide)/TiO_2 Hybrid Materials, Journal of Applied Biomaterials and Biomechanics. (2018) 41-48.

[14] Vallet-Regí M, Colilla M, González B, Medical applications of organic-inorganic hybrid materials within the field of silica-based bioceramics, Chem. Soc. Rev. 40 (2011) 596–607.

[15] Huang Y, Zheng L, Zhang H, Zhang G, Jiang L, Design and optimization of substrate placement for large-sized and high-quality fused silica glass by SiCl4 flame hydrolysis deposition International, Journal of Heat and Mass Transfer. 111 (2017) 917–32.

[16] Gao Y, Pu X, Zhang D, Ding G, Shao X, Ma J, Combustion synthesis of graphene oxide–TiO2 hybrid materials for photodegradation of methyl orange, Carbon. 50 (2012) 4093–101.

[17] Van Chuc N, Thanh C T, Van Tu N, Phuong V T Q, Thang P V, Thanh Tam N T, A Simple Approach to the Fabrication of Graphene-Carbon Nanotube Hybrid Films on Copper Substrate by Chemical Vapor Deposition, Journal of Materials Science & Technology. 31 (2015) 479–83

[18] Pomogailo A D, Polymer Sol-Gel Synthesis of Hybrid Nanocomposites, Colloid J. 67 (2005) 658–77.

[19] Dippong T, Toloman D, Levei E-A, Cadar O, Mesaros A, A possible formation mechanism and photocatalytic properties of $CoFe_2O_4$/PVA-SiO_2 nanocomposites, Thermochimica Acta. 666 (2018) 103–15.

[20] Obregón S, Rodríguez-González V, Photocatalytic TiO_2 thin films and coatings prepared by sol–gel processing: a brief review, Journal of Sol-Gel Science and Technology 102 (2021) 125–141.

[21] Tokudome Y, Fujita K, Nakanishi K, Miura K, Hirao K, Synthesis of Monolithic Al_2O_3 with Well-Defined Macropores and Mesostructured Skeletons via the Sol−Gel Process Accompanied by Phase Separation, Chemistry of Materials. 19 (2007) 3393–8.

[22] Deng Y-H, Wang C-C, Hu J-H, Yang W-L, Fu S-K, Investigation of formation of silica-coated magnetite nanoparticles via sol-gel approach Colloids and Surfaces A, Physicochemical and Engineering Aspects. 262 (2005) 87–93.

[23] Pereira M M, Jones J R, Orefice R L, Hench L L, Preparation of bioactive glass-polyvinyl alcohol hybrid foams by the sol-gel method, J Mater Sci: Mater Med. 16 (2005) 1045–50.

[24] Agrawal K, Singh G, Puri D, Prakash S, Synthesis and Characterization of Hydroxyapatite Powder by Sol-Gel Method for Biomedical Application, Journal of Minerals and Materials Characterization and Engineering. 10 (2011) 727–34.

[25] You Y, Zhang S, Wan L, Xu D, Preparation of continuous TiO_2 fibers by sol-gel method and its photocatalytic degradation on formaldehyde, Applied Surface Science. 258 (2012) 3469–74.

[26] Pooyan S and Box P O, Sol-gel process and its application in Nanotechnology, Journal of Polymer Engineering and Technology. 13 (2005), 38-41.

[27] Singh V, Singh D, Polyvinyl alcohol–silica nanohybrids: An efficient carrier matrix for amylase immobilization Process Biochemistry 48 (2013) 96–102.

[28] Chandar Shekar B, Ranjit Kumar R, Dinesh K.P.B, Sulana Sundar C, Sunnitha S, Punithavathi K, preparation and characterization of polyvinyl alcohol thin films for organic thin-film transistors and biomedical applications, Kongunadu Research Journal. 5 (2018) 16–8.

[29] Chang A R, Preparation and Study of Polyvinyl Alcohol Fiber, Applied Mechanics and Materials. 727–728 (2015) 227–30

[30] Hou Y, Chen C, Liu K, Tu Y, Zhang L, Li Y, Preparation of PVA hydrogel with high-transparence and investigations of its transparent mechanism, RSC Adv. 5 (2015) 24023–30.

[31] Zhao Y-N, Preparation of poly (vinyl alcohol)/silica nanocomposites by sol-gel method, e-Polymers. 13 (2013).

[32] Pingan H, Mengjun J, Yanyan Z, Ling H, A silica/PVA adhesive hybrid material with high transparency, thermostability, and mechanical strength, RSC Adv. 7 (2017) 2450–9.

[33] Nakane K, Yamashita T, Iwakura K, Suzuki F, Properties and structure of poly (vinyl alcohol)/silica composites, Journal of Applied Polymer Science. 74 (1999) 133–8.

[34] Matei A, Cernica I, Cadar O, Roman C Schiopu V, Synthesis and characterization of ZnO – polymer nanocomposites, Int J Mater Form. 1 (2008) 767–70.

[35] Chalal S, Haddadine N, Bouslah N, Souilah S, Benaboura A, Barille R, Haroun A, Preparation Characterization and Thermal Behaviour of Carbopol-TiO_2 Nanocomposites, OJOPM. 04 (2014) 55–64.

[36] García-Lecina E, García-Urrutia I, Díez J A, Fornell J, Pellicer E, Sort J, Codeposition of inorganic fullerene-like WS2 nanoparticles in an electrodeposited nickel matrix under the influence of ultrasonic agitation, Electrochimica Acta. 114 (2013) 859-867.

[37] Kaur I, Ellis L-J, Romer I, Tantra R, Carriere M, Allard S, Mayne-L'Hermite M, Minelli C, Unger W, Potthoff A, Rades S, Valsami-Jones E, Dispersion of Nanomaterials in Aqueous Media: Towards Protocol Optimization, JoVE (Journal of Visualized Experiments). 25 (2017) 56-74.

[38] Goudarzi V, Shahabi-Ghahfarrokhi I, Babaei-Ghazvini A, Preparation of eco-friendly UV-protective food packaging material by starch/TiO_2 bio-nano composite: Characterization, International Journal of Biological Macromolecules. 95 (2017) 306–13.

[39] Chung S J, Leonard J P, Nettleship I, Lee J K, Soong Y, Martello D V, Chyu M K, Characterization of ZnO nanoparticle suspension in water: Effectiveness of ultrasonic dispersion, Powder Technology. 194 (2009) 75-80.

[40] Nguyen V S, Rouxel D, Hadji R, Vincent B, Fort Y, Effect of ultrasonication and dispersion stability on the cluster size of alumina nanoscale particles in aqueous solutions, Ultrasonics Sonochemistry. 18 (2011) 382–8.

[41] Matsuyama K and Mishima K, Particle Coating of Talc with TiO_2 Nanoparticles Using Ultrasonic Irradiation in Liquid CO_2, Industrial & Engineering Chemistry Research. 49 (2010) 1289–96.

Chapter I
Hybrid Materials

Chapter I *Hybrid materials*

I.1. Generality

Hybrid materials have become a topic of great interest among researchers in recent years. These materials are composed of both organic and inorganic components, which give them unique properties such as mechanical strength, thermosensitivity, chemical stability, optical and corrosion resistance, electrical conductivity, and fire retardancy. Due to these properties, hybrid materials have found a wide range of applications in fields such as coatings, catalysis, optics, optoelectronics, biomedical engineering, and nanocomposites.

The importance of hybrid materials is expected to grow in the future, particularly in engineering-related industries such as automotive, solar energy, solid-state lighting, civil engineering, aviation, and aerospace. Therefore, the development of hybrid materials is crucial for modern technologies. In this part, we will explore the definition, method of preparation, and characteristics of hybrid materials [1-3].

I.2. Introduction

Hybrid materials offer endless possibilities for creating novel material properties by combining organic and inorganic parts [4]. Nature provides several examples of hybrid materials, such as bone and shell, which possess excellent hardness and high resistance [5]. Unlike conventional composites that have macroscopic components in the micrometer to millimeter range, hybrid materials have components at the nanoscale level ranging from a few nanometers to tens of nanometers [6].

Hybrid materials synergistically combine the properties of organic materials, such as recyclability, cost-effectiveness, sustainability, and ease of processing, with the properties of inorganic materials, such as excellent dielectric constant, thermal stability, and high charge mobility [7]. By changing their components, the properties of hybrid materials can be tuned, leading to an infinite number of new properties [8]. This unique characteristic makes hybrid materials highly versatile and valuable in various applications, including catalysis, sensors, energy storage, and biomedical engineering.

I.3. Definition of hybrid materials

Hybrid materials are defined as the mixture of two components at the molecular or nanometer level. Many natural materials incorporate inorganic and organic building blocks dispensed on the nanoscale.

The International Union of Pure and Applied Chemistry (IUPAC) provides a definition of hybrid materials as those which are made up of an intimate combination of inorganic and/or organic components that typically intermingle on a scale of less than 1 µm. [9,10].

I.4. Classification of hybrid materials

The classification of Hybrid materials can be done in a variety of ways. Based on their origin, bonding, properties, and formation process. a simplistic classification that is based on how organic and inorganic parts are connected and interact:

Class I corresponds to systems where the two phases are linked only by weak interactions such as Van der Waals interactions, hydrogen bonds, or electrostatic forces.

In class II, organic and inorganic components are linked by strong chemical bonds such as covalent or ion-covalent bonds. Within class I materials, the organic component is trapped in a mineral network; the bonds between the networks are weak, of the Van der Waals, hydrogen, or electrostatic type. Within class II materials, the organic and mineral components are chemically linked by a strong bond of the covalent or io-no-covalent type. Class II materials are divided into three families. Either material of the co-gel type, mesostructured materials, nanostructured materials, or polysilsesquioxanes. [11,12].

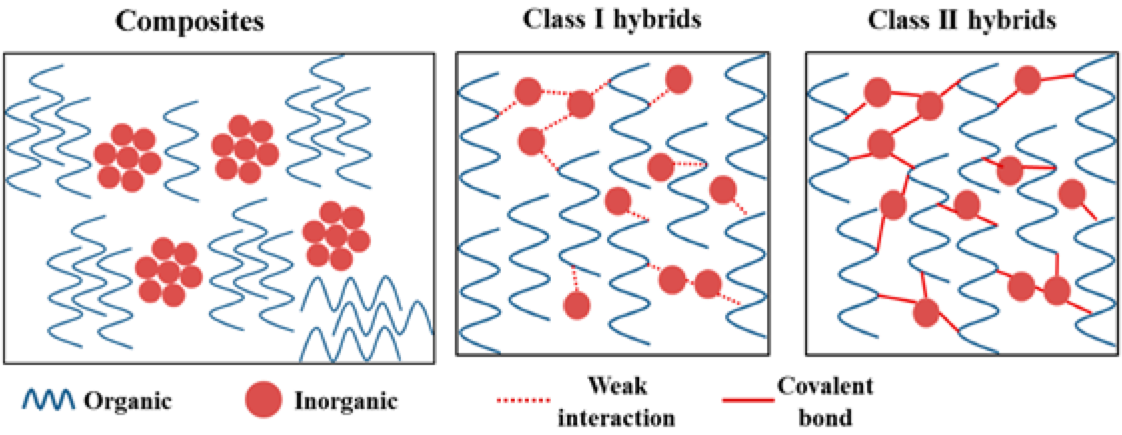

Fig. I.1 Schematic representation of the two classes of hybrid materials [13]

I.5. Synthesis of Hybrid Materials

Hybrid materials can be divided into four categories: composite, nanocomposite, hybrid, and nanohybrid. These materials can be synthesized using a variety of techniques, including blending, sol-gel, emulsion polymerization, photopolymerization, electrocrystallization, hydrothermal wet chemistry, coordination approaches, intercalation, microwave-assisted synthesis, electrochemical synthesis, and block copolymer-mediated synthesis. Since nanomaterials are also considered to be hybrid materials, several additional synthesis methods can be employed, such as solid-state reactions, molten salt synthesis, hydrothermal methods, co-precipitation, thermal evaporation, plasma methods, pulsed laser deposition, magnetron sputtering, and chemical vapor deposition. These methods offer flexibility in the design and fabrication of hybrid materials with tailored properties for various applications, ranging from biomedical engineering to energy storage and conversion [16-24].

I.6. Properties of Hybrid Materials

Hybrid materials can contain a variety of organic and inorganic components. Depending on the material (organic/inorganic), structure, and various component interfaces, the hybrid material's properties change. The ideal combination can improve thermal and chemical stability, mechanical strength and thermosensitivity, optical, anticorrosive, magnetic, electrical, and thermal properties, as well as fire resistance. this makes the properties of hybrid materials superior to those of their counterparts [25].

I.6.1. Physical Properties of Hybrid Materials

Organic-inorganic material hybrids frequently have porous crystalline structures The adsorbent properties are influenced by the porous structure. The majority of hybrid materials have distinctive structural qualities that make them excellent catalysts for chemical reactions. Hybrid materials also have remarkable optical properties. They frequently have either active optical properties, such as photochromic and electrochromic materials, or passive optical properties which are unaffected by environmental excitation [26].

I.6.2. Mechanical Properties of Hybrid Materials

It is still difficult for materials scientists to forecast the mechanical characteristics of hybrid materials. However, hybrid materials have outstanding structural capabilities and fracture resistance due to extrinsic toughening, which shields any crack from applied pressures.

The proportion of organic and inorganic components has an impact on the mechanical characteristics of hybrid materials. Ratio imbalance will have an impact on the elastic-plastic or viscous-elastic behavior. In addition, the contact between organic and inorganic components affects the hybrid material's characteristics.

To ascertain the hybrid materials' elastic properties, the tensile or compression test is used.

Elasticity benefits from the inorganic composition's high content, which is often greater than 15%. favors elastic modulus. This is because when filler levels rise, hybrid materials become more brittle. However, the elastic behavior remains unchanged when the inorganic component is under 15%. Due to its high porosity, the inorganic component makes the material fragile. Additionally, hybrid materials with a significant inorganic percentage have a lower fracture toughness. The inorganic elements' size and content determine the mechanical behavior of the hybrid material. In reality, the type of inorganic components, which frequently include metal oxides of Si, Ti, Zn, and Al, has an impact on fracture toughness. Hardness is a different mechanical characteristic that can be assessed using an indentation test. Wear resistance and hardness are related. Multifunctional materials' hardness is affected by the component morphology during the synthesis [27-32].

I.6.3. Optical Properties

Hybrid materials are characterized by versatility in the optical fields. The optical properties of hybrid materials are often characterized by the RI (Refraction index). In optics, the refractive index (or refraction index) of an optical medium is a dimensionless number that indicates the light-bending ability of that medium. The refractive index determines how much the path of light is bent or refracted when entering a material. the ratio between the velocity of light in a vacuum to its velocity in a specified medium.

The inorganic–organic composites are also versatile in terms of their optical properties. Researchers are actively investigating the optical properties of the hybrid composite to achieve the following objectives: Adjustability of RI over a wide range, Light transmittance over a wide range, Lighter weight compared with the inorganic optical materials, Better heat resistance, and stability compared with the organic materials, Better flexibility compared with the inorganic optical materials.

Through a combination of organic and inorganic materials, the different RI can be modified based on the desired application. The RI of the materials can be related to molar volume (Vm) and polarizability d to the(α) of the materials. The hybrid materials can be tuned to different RI by implementing different heat treatments, types of metal alkoxides, and the weight or volume fraction of inorganic content. Hybrid inorganic–organic materials are a promising system for a variety of applications due to their properties based on the combination of different building blocks [33-36].

I.7. Properties of PVA/SiO_2/TiO_2 Hybrids

Polyvinyl alcohol (PVA)/SiO_2/TiO_2 hybrids are a type of material that has received significant attention in the field of materials science. These materials have unique properties that make them suitable for a wide range of applications, including coatings, sensors, and drug delivery systems. Here are some of the key properties of PVA/SiO_2/TiO_2 hybrids.

Mechanical properties: PVA/SiO_2/TiO_2 hybrids exhibit excellent mechanical properties, such as high tensile strength, good flexibility, and toughness. The addition of SiO_2 and TiO_2 nanoparticles to PVA matrix enhances the mechanical properties of the composite material. The reinforcement of the polymer matrix is due to the strong interfacial interaction between nanoparticles and PVA chains, which leads to stress transfer from the polymer matrix to the nanoparticles. [37]

Thermal properties: PVA/SiO_2/TiO_2 hybrids show good thermal stability, with high decomposition temperatures. The addition of SiO_2 and TiO_2 nanoparticles to PVA matrix also leads to an increase in the glass transition temperature, indicating an enhancement in the thermal stability of the hybrid. [38]

Optical properties: PVA/SiO_2/TiO_2 hybrids exhibit excellent optical properties, such as high transparency and low refractive index. The incorporation of TiO_2 nanoparticles in the PVA/SiO_2 matrix enhances the refractive index of the hybrid material, making it useful for optical applications. [39]

Biocompatibility: PVA/SiO_2/TiO_2 hybrids have been shown to be biocompatible, making them suitable for use in biomedical applications. In vitro studies have demonstrated that PVA/SiO_2/TiO_2 hybrids exhibit no cytotoxicity and good cell viability. [40]

I.8. Hybrid Material Applications

Various inert or active oxides (e.g. silica, TiO_2, etc.) are used as a filler (core) to attend to the desired properties of the hybrid products.

hybrid inorganic-organic materials have emerged to be good candidates in different application fields such as in coating, nanocomposite, medical, optical, and electronic domains, which will be covered later, as a result of the improvement in mechanical and physical properties [41, 42].

I.8.1. Medical Applications

With a focus on hybrid material medical applications that incorporate inherent degradability, cytotoxicity, and biocompatibility, hybrid materials have recently attracted more attention in biomaterials research. Therefore, hybrid materials are significant in the production of bioceramics, which are utilized in medical applications. For example, a stimuli-responsive drug delivery system is used as the local carrier, which is synthesized using charged ionic interaction between carboxylic-modified mesoporous silica and polyelectrolyte solution.

Hybrid materials can also be used for cell targeting. Many hybrid materials were used for cell targeting, either to help with drug delivery or cancer cell imaging [43-47].

I.8.2. Optical Applications

The mechanical flexibility and excellent transparency of inorganic/organic hybrid materials make them suitable for optical applications.

Depending on how it will be used, such as in waveguides and micro-optical devices, hybrid materials' physical and chemical properties can be functionalized.

Waveguide materials, photodetectors, and nonlinear optical materials are examples of hybrid material optical applications. Additionally, hybrid materials have applications in the production of LEDs and photovoltaics, where there is a sizable market for the goods [48-50].

I.8.3. Electronic Applications

Their use of hybrid materials in the electronics industry has increased, due to the development of integrated circuit performance. Hybrid materials are installed in electronic devices, which are resistant to high-temperature use without compromising the device's performance. Electrochemically active hybrid materials have several advantages. For instance, hybrid materials offer stability like solid materials but possess liquid properties at the same time. Hybrid materials can integrate the electrical conductivity of solid materials and the ionic conductivity of liquid materials, which is useful for electronic devices that provide low-k dielectrics. The silicon-derived hybrid material is significant in electronic devices [51-53].

I.9. Conclusion

Modern technology has made significant advancements in various areas, driven by the increased use of hybrid materials. Despite the extensive research conducted on hybrid materials, the reported properties and characteristics are still insufficient. This is because even minor changes in the synthetic methods used can significantly impact the behavior and characteristics of these materials. However, for the benefits of hybrid material technology to be realized by all stakeholders, the challenges in hybrid material synthesis must be addressed.

To refine the production of hybrid materials, further studies are required to enhance their physical and mechanical properties. Research on hybrid materials should be carried out to overcome the obstacles faced in various applications. Although the high inorganic composition of hybrid materials remains a challenge in different environmental conditions such as temperature, their modular composition allows for many components to be involved in an organic/inorganic combination. As a result, there are limitless possibilities for future applications.

References

[1] Anjali Pal, Suman Prabhakar, Jaya Bajpai, A.K. Bajpai, 16 - Antiviral behavior of metal oxide-reinforced polymer nanocomposites, anoparticle-Based Polymer Composites. (2022) Pages 439-467.

[2] García-Martínez JM, Collar EP. Organic-Inorganic Hybrid Materials II: Some Additional Contributions to the Topic. Polymers (Basel). 13(15) (2021) 2390.

[3] Wail Al Zoubi, Muhammad Prisla Kamil, Siti Fatimah, Nisa Nashrah, Young Gun Ko, Recent advances in hybrid organic-inorganic materials with spatial architecture for state-of-the-art applications, Progress in Materials Science. Volume 112, (2020) 100663.

[4] Mobin, R., Rangreez, T.A., Chisti, H.T., Inamuddin, Rezakazemi, M. Organic-Inorganic Hybrid Materials and Their Applications, Cham. (2019) 1020.

[5] Christian Emeka Okafor, et al, Biobased hybrid composite design for optimum hardness and wear resistance, Composites Part C: Open AccessVolume 10 (2023).

[6] Shaoyun Fu, Zheng Sun, Pei Huang, Yuanqing Li, Ning Hu, Some basic aspects of polymer nanocomposites: A critical review, Nano Materials Science, 1 (2019) 2-30.

[7] Krasia-Christoforou, T. Organic–Inorganic Polymer Hybrids: Synthetic Strategies and Applications. In: Kim, CS., Randow, C., Sano, T. (eds) Hybrid and Hierarchical Composite Materials, (2015) 11–63.

[8] Yentl Swolfs, Larissa Gorbatikh, Ignaas Verpoest, Fibre hybridization in polymer composites: A review, Composites Part A: Applied Science and Manufacturing, Volume 67 (2014) Pages 181-200.

[9] Vargas-Bernal R, Introductory Chapter: Hybrid Nanomaterials. Hybrid Nanomaterials - Flexible Electronics Materials. IntechOpen. (2020).

[10] García-Martínez, J.-M.; Collar, E.P. Organic–Inorganic Hybrid Materials. Polymers 13 (2021) 86.

[11] Saveleva MS, Eftekhari K, Abalymov A, Douglas TEL, Volodkin D, Parakhonskiy BV, Skirtach AG. Hierarchy of Hybrid Materials-The Place of Inorganics-*in*-Organics in it, Their Composition and Applications. Front Chem. (2019) 7-17.

[12] Patrick Judeinstein and Clément Sanchez, Hybrid organic–inorganic materials: a land of multidisciplinarity, J. Mater. Chem**.** 6 (1996) 511-525.

[13] Aslankoohi, Neda, Dibakar Mondal, Amin S. Rizkalla, and Kibret Mequanint. "Bone Repair and Regenerative Biomaterials: Towards Recapitulating the Microenvironment" Polymers, 9 (2019) 14-37.

[14] Krasia-Christoforou, T. Organic–Inorganic Polymer Hybrids: Synthetic Strategies and Applications. In: Kim, CS., Randow, C., Sano, T. (eds) Hybrid and Hierarchical Composite Materials. Springer, Cham. (2015).

[15] C. Guillén, J. Herrero, High conductivity and transparent ZnO:Al films prepared at low temperature by DC and MF magnetron sputtering, Thin Solid Films, Volume 515, Issue 2, (2006) Pages 640-643.

[16] S.P. Lim, A. Pandikumar, N.M. Huang, H.N. Lim, Facile synthesis of Au-TiO_2 nanocomposite and its application as a photoanode in dye-sensitized solar cells, RSC Adv. 5 (2015) 44398-44407

[17] Y. Liu, Q. Kou, D. Wang, L. Chen, Y. Sun, Z. Lu, et al., Rational synthesis and tailored optical and magnetic characteristics of Fe_3 O_4-Au composite nanoparticles, J. Mater. Sci. 52 (2017) 10163-10174

[18] H. Li, Y. He, Z. Liu, B. Jiang, Y. Huang, Rapid synthesis of broad band Ag-TiO_2 core-shell nanoparticles for solar energy conversion, Sol. Energy Mater. Sol. Cells 166 (2017) 52-60

[19] R.T. Tom, A. Sreekumaran Nair, N. Singh, M. Aslam, C.L. Nagendra, R. Philip, et al., Freely dispersible Au-TiO_2 , Au-ZrO_2 , Ag-TiO_2, and Ag-ZrO_2 core-shell nanoparticles: one-step synthesis, characterization, spectroscopy, and optical properties, Langmuir 19 (2003) 3439-3445.

[20] M.E.F. Brollo, J.M. Orozco-Henao, R. Lo´ pez-Ruiz, D. Muraca, C.S.B. Dias, K.R. Pirota, et al., Magnetic hyperthermia in brick-like Ag-Fe3O 4 core-shell nanoparticles, J. Magn. Magn. Mater. 397 (2016) 20-27.

[21] J. Zhou, G. Zhao, X. Ren, B. Song, G. Han, Effects of diethanolamine on the evolution of silver/titanium dioxide sol-gel process, J. Sol-Gel Sci. Technol. 58 (2011) 148-155

[22] K.H. Leong, H.Y. Chu, S. Ibrahim, P. Saravanan, Palladium nanoparticles anchored to anatase TiO_2 for enhanced surface plasmon resonance-stimulated, visible-light-driven photocatalytic activity, Beilstein J. Nanotechnol. 6 (2015) 428-437

[23] J. Zhou, G. Zhao, X. Ren, B. Song, G. Han, Effects of diethanolamine on the evolution of silver/titanium dioxide sol-gel process, J. Sol-Gel Sci. Technol. 58 (2011) 148-155

[24] . Huang, Q. Zhang, S. Yuan, Y. Zhang, M. Zhang, One-pot facile synthesis of branched Ag-ZnO hetero- junction nanostructure as highly efficient photocatalytic catalyst, Appl. Surf. Sci. 353 (2015) 949-957.

[25] Saveleva Mariia S et al, Hierarchy of Hybrid Materials—The Place of Inorganics-in-Organics in it, Their Composition and Applications, Frontiers in Chemistry. 7 (2019).

[26] Hüsing, N., Hartmann, S. Inorganic–Organic Hybrid Porous Materials. In: Merhari, L. (eds) Hybrid Nanocomposites for Nanotechnology. Springer, Boston, MA (2009).

[27] Bahrami, M.; Abenojar, J.; Martínez, M.Á. Recent Progress in Hybrid Biocomposites: Mechanical Properties, Water Absorption, and Flame Retardancy. *Materials*. *13* (2020) 45-51.

[28] Paladugu, S.R.M et al, A Comprehensive Review of Self-Healing Polymer, Metal, and Ceramic Matrix Composites and Their Modeling Aspects for Aerospace Applications. *Materials*. *15* (2022) 8521.

[29] Ritchie Robert O, toughening materials: enhancing resistance to fracturePhil. Trans. R. Soc. (2021).

[30] Dubois, G., Volksen, W., Magbitang, T. *et al.* Superior mechanical properties of dense and porous organic/inorganic hybrid thin films. *J Sol-Gel Sci Technol.* 48 (2008) 187–193.

[31] loria Young, et al, Hybrid materials with continuous mechanical property gradients that can be 3D printed, Materials Today Advances, Volume 17 (2023) 100344.

[32] Ahmad Y Al-Maharma1 , Sandeep P Patil1, and Bernd, Effects of porosity on the mechanical properties of additively manufactured components: a critical review* Markert1 Published 2 December, Ltd Materials Research Express. Volume 7, (2020).

[33] R. Houbertz, G, Inorganic–organic hybrid materials for application in optical devices, Thin Solid Films. Volume 442, Issues 1–2, (2003) Pages 194-200.

[34] Plinio Innocenzia and Bénédicte Lebeau, Organic–inorganic hybrid materials for non-linear optics, Journal of Materials Chemistry. 15 (2005) 3821-3831.

[35] Huafang Jiang, Siyong Qin, Hui Dong, An injectable and fast-degradable poly(ethylene glycol) hydrogel fabricated via bioorthogonal strain-promoted azide–alkyne cycloaddition click chemistry, Soft Matter. 11 (2015) 6029-6036.

[36] Jorio, A., Kauppinen, E., Hassanien, A, Carbon-Nanotube Metrology. In: Jorio, A., Dresselhaus, G., Dresselhaus, M.S. (eds) Carbon Nanotubes. Topics in Applied Physics, vol 111 (2007).

[37] Wang, X., Zhang, S., Hu, J., Xu, Y., & Yao, J. Preparation and characterization of PVA/SiO2/TiO2 hybrid membranes with high performance. Materials Science and Engineering: C, 70, (2017) 347-355.

[38] Rajendran, S., & Rajendran, K. Fabrication, characterization and thermal stability of polyvinyl alcohol-silica-titania nanocomposites. Journal of Molecular Liquids, 240, (2017) 206-214.

[39] Sahu, S., Mohanty, S., & Nayak, S. K, Preparation and characterization of polyvinyl alcohol/silica/titania hybrid nanocomposites: effect of titania loading on the optical properties. Materials Research Express, 6(10), (2019) 1050e.

[40] Zhang, J., Huang, Y., Zou, Y., & Zhang, Y, Polyvinyl alcohol/silica/titania hybrid films: Preparation, properties, and biocompatibility. Colloids and Surfaces B: Biointerfaces, 200, (2021) 111601.

[41] Clément Sanchez, Beatriz Julián, Applications of hybrid organic–inorganic nanocomposites* J. Mater. Chem., 15 (2005) 3559-3592.

[42] Yu, Y.-Y.; Yang, C.-H. Preparation and Application of Organic-Inorganic Nanocomposite Materials in Stretched Organic Thin Film Transistors. *Polymers 12*, 1058 (2020).

[43] Jessica M. Rosenholm, et al, Targeting of Porous Hybrid Silica Nanoparticles to Cancer Cells* ACS Nano 3 (1), (2009) 197-206.

[44] Qing Yang, et al, pH-Responsive Carrier System Based on Carboxylic Acid Modified Mesoporous Silica and Polyelectrolyte for Drug Delivery, Chemistry of Materials. 17 (24) (2005) 5999-6003.

[45] María Vallet-Regí, Montserrat Colilla and Blanca González, Medical applications of organic–inorganic hybrid materials within the field of silica-based bioceramics *Chem. Soc. Rev.*, 40 (2011) 596-607.

[46] Ana García, et al, Incorporation of Phosphorus into Mesostructured Silicas: A Novel Approach to Reduce the SiO_2 Leaching in Water, Chemistry of Materials. 21 (18) (2009) 4135-4145.

[47] Kaimin Chen, e al, Hybrid cathode lithium batteries for implantable medical applications, Journal of Power Sources. Volume 162, Issue 2, (2006) Pages 837-840.

[48] Jinghong Li, Jin Z. Zhang, Optical properties and applications of hybrid semiconductor nanomaterials, Coordination Chemistry Reviews. Volume 253, Issues 23–24, (2009) Pages 3015-3041.

[49] Wenfang Sun, Qiu Dai, James G. Worden, and Qun Huo, Optical Limiting of a Covalently Bonded Gold Nanoparticle/Polylysine Hybrid Material, The Journal of Physical Chemistry B. 109 (44) (2005) 20854-20857.

[50] Zhi-Bo Liu, Porphyrin and Fullerene Covalently Functionalized Graphene Hybrid Materials with Large Nonlinear Optical PropertiesThe Journal of Physical Chemistry B. 113 (29) (2009) 9681-9686.

[51] Synthesis of Monodispersed Wurtzite Structure CuInSe2 Nanocrystals and Their Application in High-Performance Organic−Inorganic Hybrid Photodetectors Jian-Jun Wang, Yong-Qing Wang, Fei-Fei Cao, Yu-Guo Guo, and Li-Jun Wan Journal of the American Chemical Society. 132 (35) (2010) 12218-12221.

[52] Jin Wook Park, Jyongsik Jang, Fabrication of graphene/free-standing nano fibrillar PEDOT/P(VDF-HFP) hybrid device for wearable and sensitive electronic skin application, Carbon, Volume 87 (2015) Pages 275-281.

[53] B. Rajesh, K. Electronically conducting hybrid material as high-performance catalyst support for electrocatalytic application, Journal of Power Sources. Volume 141, Issue 1 (2005) Pages 35-38.

Chapter II

Sol-Gel Method

Chapter II *Preparation of Hybrid Materials Using the Sol-Gel Method*

There are various methods for synthesizing hybrid materials, but the sol-gel process is considered the ideal approach for creating hybrid inorganic-organic materials. This process utilizes a molecular precursor as the starting material, which undergoes hydrolysis and condensation reactions to form oxide frameworks [1].

II.1. Introduction

The sol-gel technique is a highly versatile process used to produce a wide range of hybrid materials, including glasses, ceramics, and organo-mineral compounds, from precursors in a solution. This method is particularly useful for generating thin layers comprising metal oxide nanoparticles [2]. Compared to other methods, such as physical deposition, the sol-gel process is a more chemical (wet chemical) approach, making it ideal for synthesizing various nanostructures, including metal oxide nanoparticles.

In the sol-gel process, a molecular precursor (typically a metal alkoxide) is dissolved in water or alcohol and heated and stirred until it forms a gel. Since this is a low-temperature solution process, the decomposition of the organic component can be minimized. The majority of organic-inorganic hybrid materials are synthesized using the sol-gel method [3].

The term "sol-gel" comes from the abbreviation "gelation solution." Essentially, a "sol" is a colloidal suspension of oligomers with a diameter of just a few nanometers. This "sol" evolves through a series of chemical reactions, eventually forming a network with infinite viscosity known as a "gel" [4]. The basic principle of the sol-gel process is to transform a liquid-phase solution of precursors into a solid through a series of chemical reactions (hydrolysis and condensation), often at room temperature, making it a "soft" chemistry method [5]. The time it takes for the solution to turn into a solid is called the freezing time (or freezing point). There are two routes for sol-gel synthesis [6]:

Aqueous sol-gel method: obtained from metallic salts (chlorides, nitrates, oxychlorides) in an aqueous solution. This route is inexpensive and difficult to control, which is why it is still very little used. However, it is the preferred way to obtain ceramic materials.

Nonaqueous sol-gel method: obtained from metal alkoxides in organic solutions. It is relatively expensive but allows fairly easy control of the particle size. In both cases, the reaction is initiated by hydrolysis (addition of water for the alkoxy route and change of pH to form hydroxides for the inorganic route) allowing the formation of M-OH groups then occurs the condensation allowing the formation of bonds M-O-M [7].

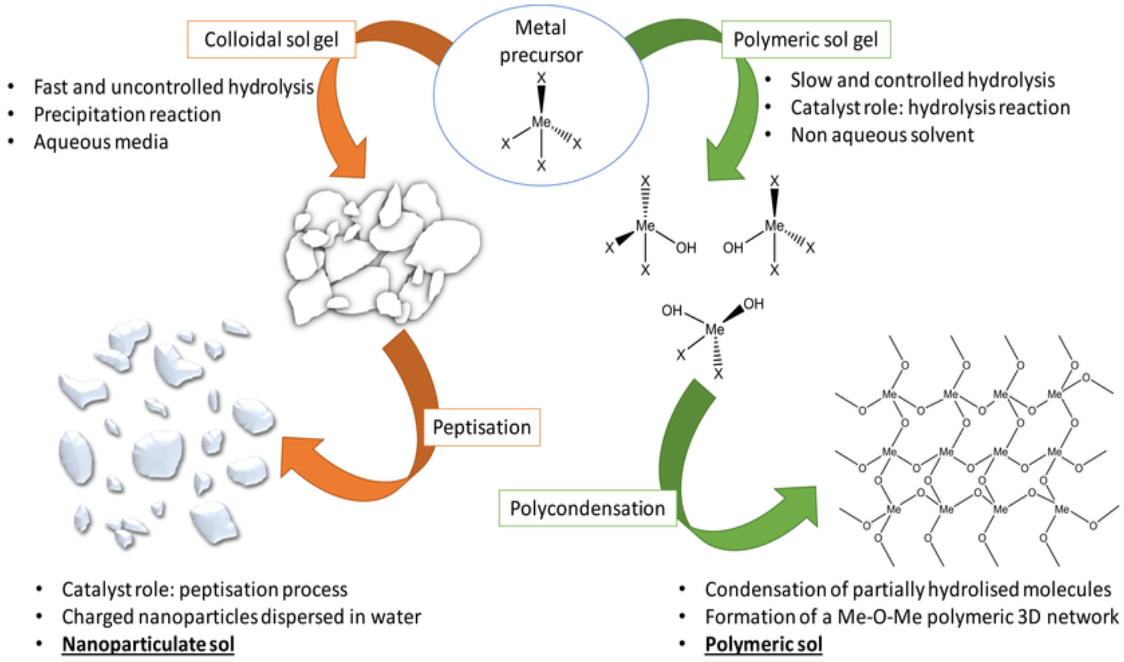

Fig. II.1 Comparison between colloidal and polymeric Sol-gel methods [8].

This process allows the development of a wide variety of oxides in different configurations (monoliths, thin films, fibers, powders) this great diversity, both in terms of materials and shaping has made this process very attractive in technological fields such as optics [9], electronics [10], biomaterials [11], sensors (detection), separation supports (chromatography). It also has the advantage of using mild chemistry and being able to produce very pure or doped materials depending on the intended application [12].

This process can be used in various fields such as encapsulation and the development of hyper-porous materials, but it is in the production of thin layer deposits that it finds its main application [9-12].

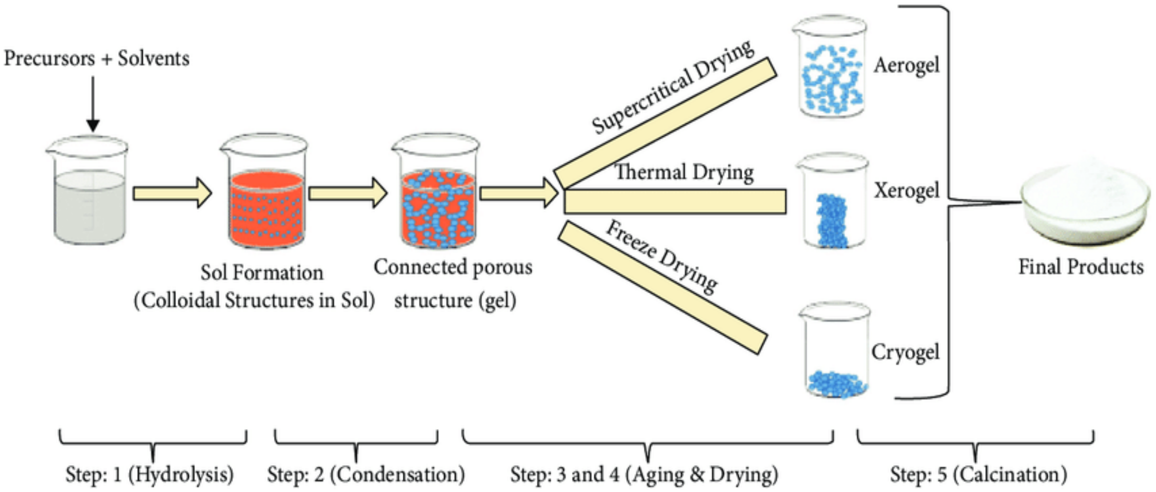

Fig. II.2 Sol-gel process [13].

II.2. Sol-gel process principle

The reactivity of the inorganic part is due to the presence of alkoxy groups (-OR´) which lead to a mineral network by the sol-gel process. It is a low-temperature synthesis process that allows us to go from the sol state to the gel state through hydrolysis and condensation reactions [14].

II.2.1. Sol

Sol is defined as a suspension of solid particles in a solvent. Depending on the size of the species, it will be a true sol (molecular species), or a stable dispersion of colloidal particles within a liquid colloidal solution (1-100nm) [16,17], these colloids are animated by a Brownian movement which keeps them in suspension [18]. These interactions are of three types: • electrostatic: Coulomb forces between charged species; • chemical: hydrogen bonds with complexation of the solute and the solvent; • physical: weak Van Der Waals bonds between neutral species [15-18].

II.2.2. Gel

Jabbour [19], reports that the term colloid was introduced in 1861 by Graham [20] by analogy with glues, to designate any substance whose solution cannot dialyze, as opposed to crystalloids. A gel is an interconnected three-dimensional network in which the solvent is trapped in pores. If the network is made up of colloidal particles, it is called a “colloidal gel” while if it is made up of macromolecules, it is called a “polymeric gel”.

In 1949, Bungenberg de Jong [21] defined a gel as a solid-state system in which the colloidal particles are arranged to form a coherent structure and in the same year, Herman [21] gave gels a three-point definition: A gel is a coherent system composed of at least two components; A gel has mechanical properties characteristic of the solid-state; In a gel, both the dispersed component and the dispersant continuously expand through the entire system.

Overall, the authors agree in recognizing that gels have a continuous structure with macroscopic dimensions. So they defined two types of gels [19-21]:

Physical gels (destabilization of a colloidal solution)

The system is frozen by electrostatic interactions. Under the effect of mechanical action (agitation), the inter-particle bonds can be broken to return to the ground state. This promotes the formation of gels with thixotropic properties (reversible transition from gel to sol) [22].

The precursors are metal oxides or hydroxides. In an aqueous medium, these precursors lead to colloidal particles dispersed by peptization (addition of electrolyte in the medium). They are subjected to electrostatic repulsions which prevent their aggregation and are at the origin of the stability of the soil. When the state of equilibrium is broken (destabilize), the neighboring particles can assemble, and increase the viscosity of the soil until the system freezes in the gel state. This gel can be obtained by reducing the interparticle space either by evaporation of the solvent or by increasing the coordination spheres which bring the particles closer together. This gel is of a physical type. The pH of the medium plays an essential role, as do other parameters such as the consultation of the medium and the nature of the anions provided by the electrolytes [22-24].

Chemical gels (polymeric routes)

The particles constituting the solid network are linked by chemical bonds: the sol state is then irreversible. They use precursors such as alkoxides or alkoxides. These compounds have been extensively described by Bradley et al. Their chemical formula is M(OR)n, OR being a hydrolyzable organic group and M a metal. They come in liquid form which is miscible in a suitable organic solvent. These chemical gels are formed by hydrolysis and condensation reactions that we have chosen to illustrate by those occurring in the well-known case of silicon (OR’) n [25].

II.2.3. The sol-gel transition

The first state is that of hydrolyzed and/or condensed sols: a liquid solution of metal alkoxides partially dissolved in a solvent. The addition of water leads to hydrolysis and polymerization reactions, oligomers and polymers are formed in the solution [26].

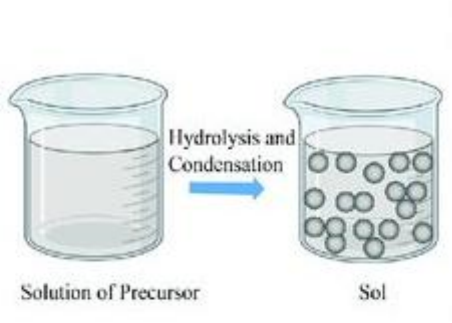

Fig. II.3 hydrolysis and condensation [27].

The viscosity of the solution increases until a gel at "t gel" is obtained (time required to obtain gel after adding water at the conditions considered). The word gel only has meaning at the macroscopic level, where it appears as a solid, although still containing a large amount of interstitial fluid. At the molecular level, nothing changes. The mesh of the gel remains very loose just after the gel point, and species not bound to the gel can still diffuse and react (polymerization, depolymerization, and grafting to the network) [28].

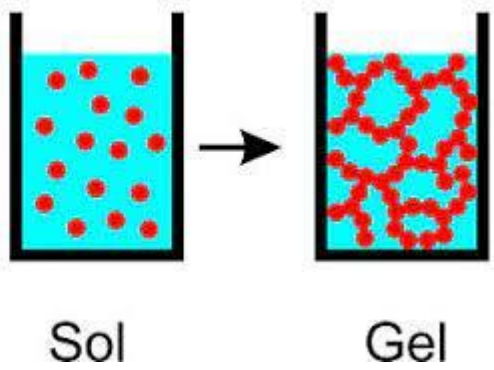

Fig. II.4 sol-gel transition [29].

Then the gel ages, and by successive graftings, its mesh becomes denser, and the molecules, and especially the macromolecules diffuse much more difficultly. This period can last several tgel. He can sometimes observe a "syneresis" (i.e. an expulsion of the solvent).

Various drying methods can then be used:

- The gel can be dried under mild conditions. It hardens by compacting:
- The solvent can be evaporated under supercritical conditions (high and constant evaporation rate) to form a very loose gel: it is an airgel. When we are still only at the sol stage, it is possible to spread the sol on a surface to form films of xerogels in thin layers (for example the techniques of spin-coating or dip-coating) [30].

Fig. II.5 Main steps in the synthesis of a material by the sol-gel route [31].

II.3. The chemical aspect of the sol-gel process

The development of oxide networks (oxo- or hydroxo-polymers), by sol-gel process, takes place via inorganic polymerization reactions in solution from molecular precursors, generally metal alkoxides: M(OR)n where M is a metal of oxidation state n (for example: Si, Ti, Zr, Al, Sn<) and OR an alkoxide group corresponding to deprotonated alcohol [32].

This polymerization takes place in two stages: hydrolysis and condensation. Hydrolysis and condensation of metal alkoxides are equivalent to nucleophilic substitution of alkoxy ligands by hydroxylated XOH species [33].

II.3.1. The formation of gels:

Typically, the process starts with a monomeric alkalized solution of metal or alkoxide precursors M(OR)n where "M" represents a metal and "R" typically represents a CxH2x+1 alkyl group eg (CH3) and ethyl (C2H5). Alcohol is a molecule obtained by the addition of several hydroxyl groups (OH) to an alkyl molecule; such as methanol (CH2OH) or ethanol (C2H5OH) [34]. Alkoxide metals are compounds of the organometallic family that have an organic radical attached to the metal or metalloid atom. The most common organometallic compounds studied and most used are tetraethoxysilane or tetraethyl ortho-silicate (TMOS, Si(OC2H5)4) and tetra-methoxy-silane or tetra-methyl ortho-silicate (TMOS, Si(OC2H5)4) [34]. An alkoxy is a radical formed by the removal of a proton from an alcohol hydroxide, such as methoxy (-OCH3) or ethoxy (-OC2H5), [35] See the most alkoxy radicals site commonly used, in Table II.1

Table II.1. Commonly used radicals [36].

Alkyle		alkoxy	
Méthyle	CH3	Méthoxy	OCH3
Ethyle	CH3 CH2	Ethoxy	OCH 2CH 2
n-propyle	CH3 CH2 CH 2	n-propoxy	O (CH 2)2 CH3
Iso –propyle	CH(C) HCH3	Iso-propoxy	CH3(O)

II.3.2.1. Hydrolysis

The hydrolysis step represents the conversion of alkoxyl functions into reactive hydroxyl functions, thus making the condensation process possible.

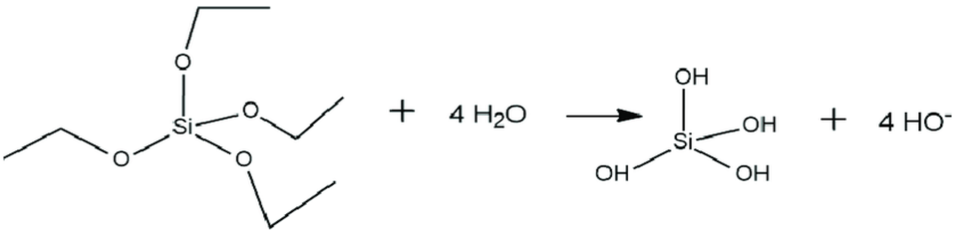

Fig. II.6 Example of hydrolysis of an organosilane [37].

The reaction follows a nucleophilic SN2 substitution mechanism through the pentacoordinate silicon transition state. This reaction is favored by the electronegative alkoxyl groups which make the silicon atom very prone to the nucleophilic attack of water.

The OH- ions initially attack the silicon according to an SN2 mechanism; The OH- group replaces OR- with an inversion of configuration [38].

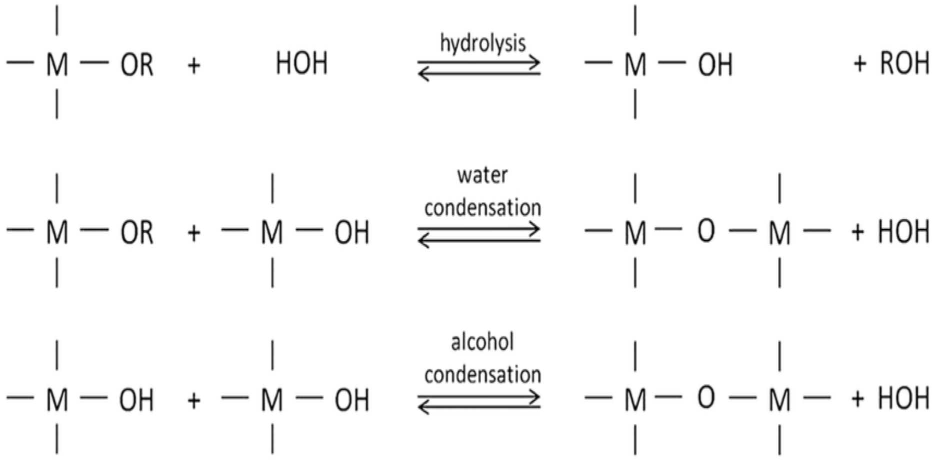

Fig. II.7 Mechanism of hydrolysis of metal alkoxides M(OR) (neutral medium, without catalyst) [39].

The hydrolysis reaction is facilitated by the addition of a catalyst, acid, or base, of organic or inorganic nature [40].

In the case of the acid catalyst, an alkoxide group is easily protonated. The electron density of the metal center is reduced which makes it more electrophilic. Protonation thus increases the nucleofuge character of the leaving group. At the kinetic level, the proton transfer between the entering group and the leaving group is no longer necessary [41].

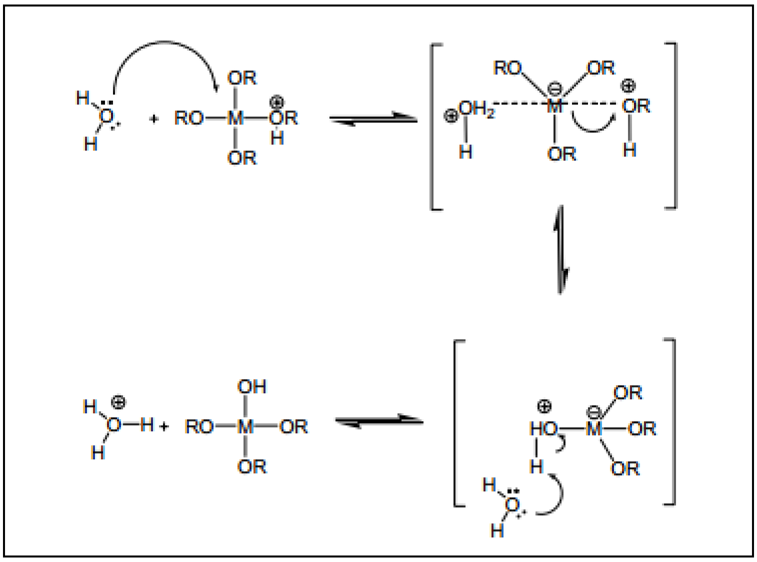

Fig. II.8 Mechanism of hydrolysis by acid catalysis of metal alkoxides [42].

Alcohol and water are undesirable in the final material, which is why they must be extracted. The volume of the gel begins to shrink during the shaking step due to the evaporation of water and alcohol. When the gelation is completed, the volume decreases more and there is often the appearance of cracks which are due to capillary forces. These forces are proportional to the evaporation rate and inversely proportional to the pore size [43].

The decrease in volume of the gel depends on the physical and chemical conditions leading to its formation. This reduction depends above all on the gelation temperature and the composition of the precursor. Thus, the type of catalyst used and the molar proportions of alkoxide, alcohol, and water are important parameters [44].

For basic catalyzes, the hydroxide ion replaces water as a nucleophilic agent because it is much more reactive, the first step is accelerated (figure II-5) [44].

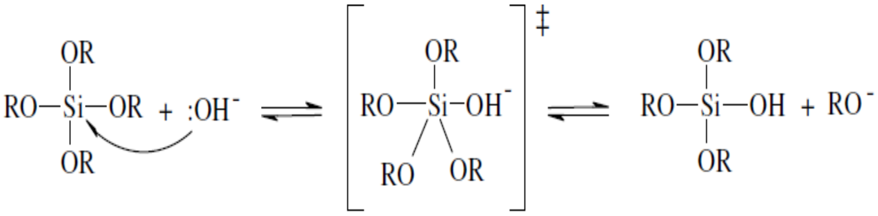

Fig. II.9 Mechanism of hydrolysis by base catalysis of metal alkoxides (OR)n (organo-silane) [45].

The mechanisms of the catalytic processes are very diverse for the silicon alkoxides. In certain cases, the inversion of the tetrahedron is observed, witnesses of nucleophilic substitution of the "SN2" type (acid and base). In other cases, it can be mechanisms by disproportionation (acid), flank attack (acid), or using a stable penta-coordinated intermediate (base) [46]. For silicon-based sol-gels, the gel time is the isoelectric point of the hydroxyl precursor pH= 2.2

II.3.2.2. Condensation

Hydrolysis and condensation being concomitant, the reaction system is very complex. On the one hand, there is competition between the hydrolysis of the alkoxyl groups and the condensation reactions (and their inverse reactions: esterification and alcoholysis). On the other hand, the oligomers in formation comprise SiOH and SiOR groups which present different electronic and steric environments which results in different hydrolysis and condensation rates for each type of group.

Thus, even if the mechanisms are similar, depending on the catalyst, the solvent, and the steric and electronic effects, the rates can change notably between hydrolysis and condensation, with important repercussions on the structure of the material formed [47].

A condition for condensation is generally at least partial hydrolysis of the precursors. [48] This hydrolysis generates a much better nucleophilic hydroxyl group than the alkoxide group. It follows that the hydroxyl group reacts by nucleophilic substitution with a mechanism analogous to hydrolysis. It consists of the conversion of hydroxy functions into M-O-M species with a temporary increase in the coordination of the metal. This corresponds to the formation of the mineral macromolecular network which can then take place via polycondensation reactions by two competing mechanisms: alcoxolation and oxolation with the elimination of water or alcohol [49].

II.3.2.3. Alcoxolation

This reaction occurs between two metal alkoxides, only one of which has been

Partially hydrolyzed. This reaction is favored when the H_2O/alkoxide molar ratio of the starting formulation is less than unity. Its reaction mechanism is similar to that of hydrolysis (Figure II. A [50]

II.3.2.4. oxolation

This mechanism occurs between two partially hydrolyzed alkoxides. The mechanism remains the same except that the leaving group is a water molecule (Fig.II B)

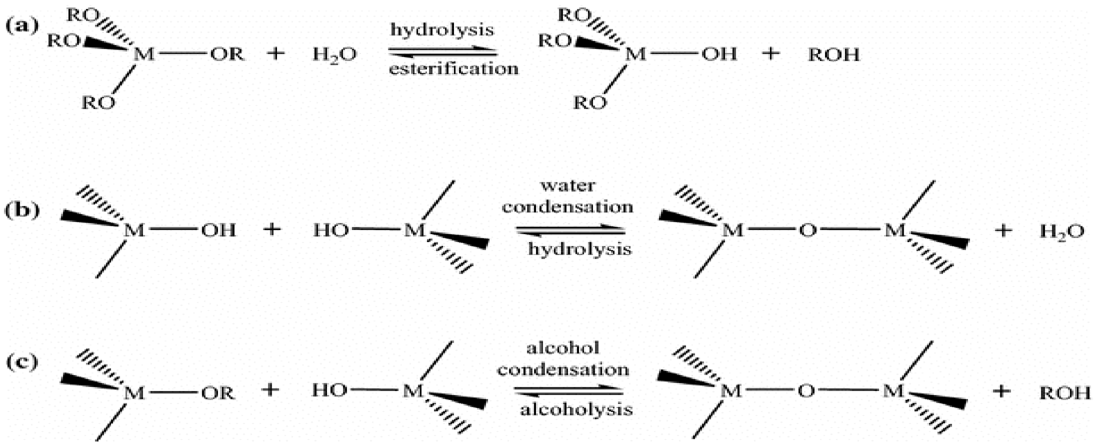

Fig. II.10 A, B Mechanism of oxolation of metal alkoxides M(OR) n [51].

The –OH groups generated during hydrolysis are good nucleophiles and, during condensation, leading to the creation of metelloxaneM-O-M bridges [51].

(a) hydrolysis

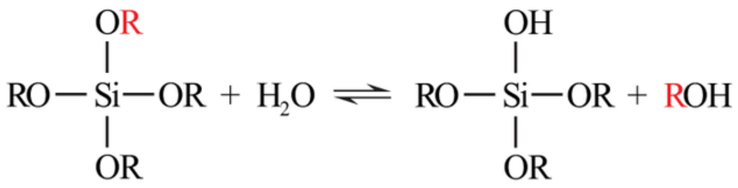

$$RO-Si(OR)_2-OR + H_2O \rightleftharpoons RO-Si(OH)(OR)-OR + ROH$$

(b) water condensation

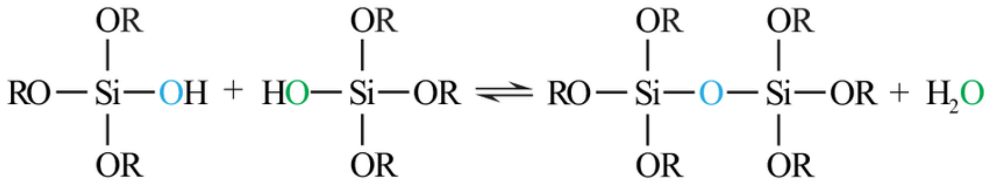

$$RO-Si(OR)_2-OH + HO-Si(OR)_2-OR \rightleftharpoons RO-Si(OR)_2-O-Si(OR)_2-OR + H_2O$$

(c) alcohol condensation

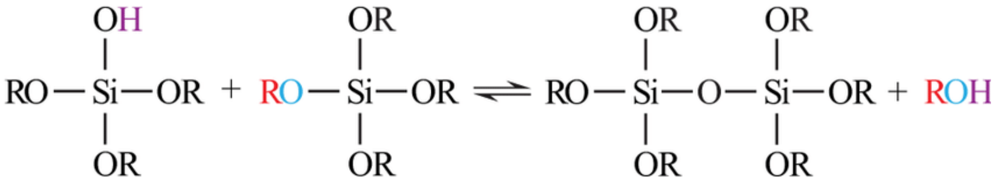

$$RO-Si(OH)(OR)-OR + RO-Si(OR)_2-OR \rightleftharpoons RO-Si(OR)_2-O-Si(OR)_2-OR + ROH$$

Fig. II.11 Example of condensation for silicon [52].

II.3.2.5. Gelification and gel structure

The two previous reactions (alcoxolationoxolation) lead to gelation and the formation of a gel made up of M-OM (or M-OH-M) chains whose viscosity increases over time. This gel still contains unreacted solvents and precursors. The "gel" phase in the sol-gel process is defined and characterized by a solid 3D "skeleton" included in a liquid phase. The solid phase is typically a condensed polymeric sol where the particles have entangled to form a three-dimensional network (figure 1.12) [53].

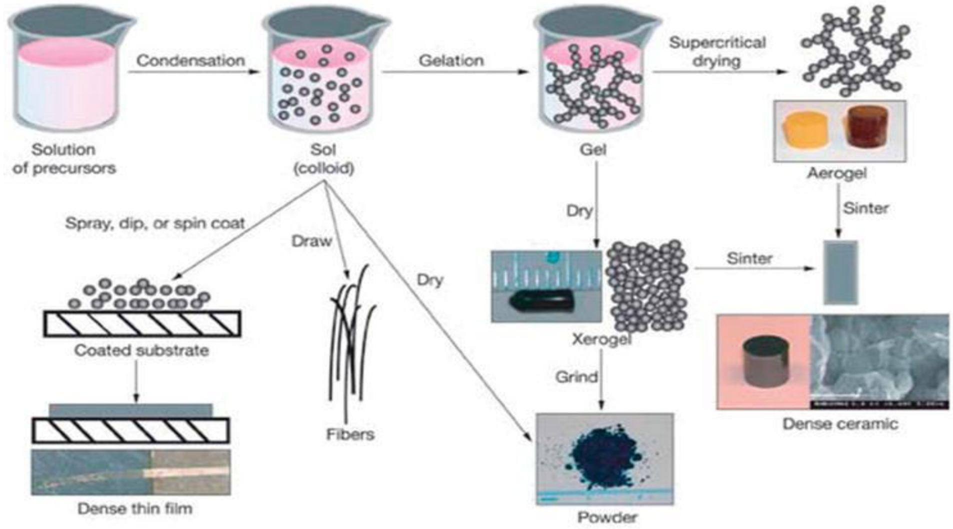

Fig. II.12 The different stages of gel formation [54].

The reactions allowing this material to be obtained are carried out at room temperature. The parameters influencing the reactions are the temperature, the pH, the nature of the precursor and the solvent, and the concentrations of the reagents [55].

II.3.2.6. Aging of the gel:

The reaction that causes gelation does not stop at the freezing point;
She continues. This entire process of gel evolution over time is called aging.
The aging of the gel results in physico-chemical modifications which take place after the gelation. Three processes can occur:

- polymerization (step of reinforcement of the network thanks to new bonds),
- ripening (the process of dissolution and reprecipitation),

- phase transformation or syneresis.

When the gel ages, the phenomenon of reticulation leads to the shrinkage of the material with the expulsion of the solvent: this is called "syneresis". Independently of the syneresis, it is possible to dry the gel, either under atmospheric conditions or under supercritical conditions. In both cases, a less dense network is obtained without solvent [56].

II.3.2.7. Gel drying

Once gelled, the material undergoes drying due to capillary forces in the pores and this drying causes volume shrinkage. The drying process for obtaining the sol-gel material requires that alcohol or water can escape at the same time as the gel solidifies. The evaporation process occurs thanks to the holes and channels existing in the porous sol-gel material. There are several types of drying allowing to obtain different types of materials:

- **Xerogel:**

conventional drying (normal evaporation) leading to a reduction in volume ranging from 5 to 10%. The evaporation of the solvent allows the formation of a xerogel which can be subjected to a heat treatment at a moderate temperature to densify the material. Densification temperatures strongly depend on the type of material and the properties sought. Drying the gel is a delicate step. The solvent must evaporate very slowly to avoid fragmentation of the xerogel. The realization of solid material is therefore difficult because of the internal tensions appearing during the drying and which can lead to the cracking of the material.

- **Airgel:**

drying under critical conditions (in an autoclave under high pressure) resulting in little or no volume shrinkage. The evacuation of the solvent under supercritical conditions leads to the formation of an aerogel that has not undergone any densification. This results in a very porous material with exceptional insulation properties. The transition from a sol to a gel, the viscosity of which can be controlled, also allows the production of fibers and films of various supports by dipping or vaporization. Xerogels are generally denser than aerogels. From the same solution and depending on the drying mode of the gel, the final material takes very different forms: dense or massive materials (glass or ceramic monoliths), powders, aerogels (supercritical drying), fibers, composites, porous gels or membranes, and, of course, films or thin layers (figure 1.13) [57-59].

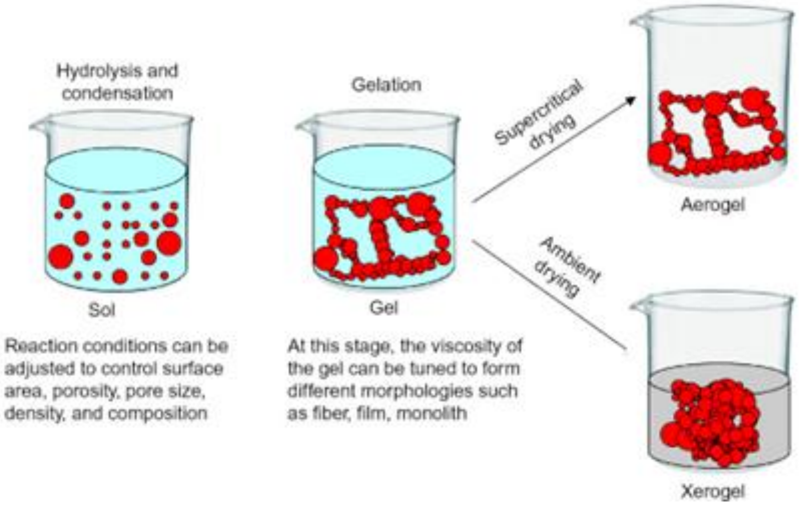

Fig. II.13 Diversity of sol-gel materials and their shaping [60].

These reaction rates depend on several parameters which must be taken into account when implementing the process:

i. Temperature: this is the first parameter to consider, which is involved in any chemical reaction. In our case, it has an influence on the rates of hydrolysis and condensation from the preparation of the soil, then during aging or storage. The higher it is, the faster the reactions.

ii. The type and concentration of alkoxide: this choice is made according to the reactivity of the alkoxide (or precursor) and the type of sample to be produced. The concentration in the soil, for its part, is especially important during condensation: the lower it is, the further the molecules capable of binding are from each other, which delays the reactions.

iii. The solvent: the alkoxides are generally little or not miscible in water. It is, therefore, necessary to mix these precursors, water (and possibly the catalyst) in a common solvent. It is then preferable to use as a solvent the alcohol corresponding to the –OR ligand of the alkoxide, to avoid possible reactions between the different components likely to modify the reaction kinetics. The starting sol is therefore generally an alcoholic solution. The choice of solvent is also dictated by process requirements (ease of drying, integrity of the final material), possible toxicity, or environmental constraints (emission of volatile organic compounds).

iv. The pH of the soil (choice of catalyst): given the mechanisms involved during gelling, the pH will play an important role in the evolution of the reactions: The H3O+ and OH- ions do not have the same influence on the two types of reaction. The cation H3O+, attracted by oxygen, facilitates the substitution of OR groups and therefore hydrolysis, while the anion OH-, attracted by the electronegative metal M, favors the formation of M-O-M bonds by condensation [61-64].

II.4. Reagents to be used in training

The objective of this paragraph is to present the principles of physico-chemical parameters involved in obtaining a sol-gel.

The starting solution generally consists of: One or more precursor(s); A co-solvent (usually alcohol); Optionally a catalyst (acid, base, or fluorine ions); Water [65].

Each compound must be dosed precisely to achieve the properties of the desired gel. The nature of the desired material dictates the precursor. The choice of solvent and catalyst is therefore dictated not only by the chemical properties of the precursor but also by environmental constraints [65]. The precursor is the central compound of the formulation and is also the one that dictates the cost of the product produced. Added to this are other elements in the formulation such as ionic or non-ionic surfactants, grafting or encapsulating agents (medicine, pigments, aromas), complexing agents (acetic acid or citric acid) which allow the formulation to modulate gelation rates [66, 68].

II.5. advantages and disadvantages

II.5.1. advantages

The sol-gel process is particularly attractive because it presents advantages such as high purity of reactants and final products, Control of the structure of the composition at the molecular level; Synthesis of new crystalline phase from non-crystalline solids; The losses by vaporization are minimized, as well as the pollution of the area; The synthesis of materials is done at relatively low temperatures compared to the solid method, hence saving thermal energy; Possibility of relatively simple doping in the ground phase, and it is possible to control connectivity and morphology by suitable choice of reactants, catalyst, and reaction conditions. Additionally, it is transparent due to the nanosized organic and inorganic domains, easy to apply on any kind of substrates and easy inclusion of suitable organic or inorganic active substances for the preparation of functional hybrid materials [69].

II.5.2. Disadvantages

The disadvantage of the sol–gel process is that long reaction times are required to achieve a high cross-linking degree as sol–gel reactions are carried out under mild conditions. However, Geppi et al. [69] have proposed that the long reaction times of sol–gel could be reduced from 7 h to 1 min using microwave heating.

The use of sol–gel has the potential to modify the surface of polymer films without using any pretreatment, and the coated materials have good adhesion to the polymer film surface. Hydroxyl groups remain after heat treatment; Significant shrinkage during drying; Very high cost of precursors; Need to precisely control the surface condition of the substrate [70].

II.6. Dispersion method of TiO_2 nanoparticles in PVA/SiO_2 Hybrid solution

Due to the inter-particle adhesion forces, nanoparticles become agglomerated and their settlement can be observed due to the gravity forces.

To start with a stable and usable condition of nanofluids, it is desired to have an aggregate- and sediment-free structure where all the nanoparticles contribute to the dispersion, which will give the maximum benefit from the nanoparticles

Currently, there are several dispersion devices available that are capable of meeting this requirement, including ultrasonication, rotor-stator systems, static mixers, and high-pressure homogenizers. ultrasonication has been widely utilized and has been accepted as an essential step in the production of nanofluids The use of ultrasonic energy–ultrasonication – for wet chemical methods has become a growing area of research for the preparation of nanoparticles of metals, oxides, etc [72].

II.6.1. Ultrasonication principle

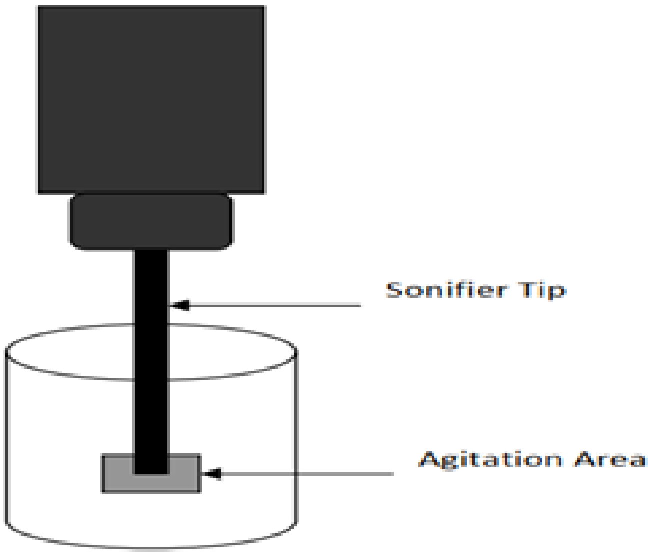

Fig. II.14 Schematic representation of a sonifier [73].

Emulsification using ultrasound was first reported in 1927 and the first patent was granted for this type of system in 1944 in Switzerland. A schematic diagram of an ultrasonic system is illustrated in Figure II.14 The sonifier produces ultrasonic waves that cause the molecules to oscillate about their mean position as the waves propagate. During the compression cycle, the average distance between the molecules decreases, whilst during rarefaction the distance increases. The rarefaction results in a negative pressure that may cause the formation of voids or cavities (cavitation bubbles) that may grow in size. High-frequency vibrations applied to a diphasic liquid system provides a different means of breaking and dispersing a bulk phase [74].

II.7. Conclusion

Sol-Gel synthesis leads to the elaboration at a low temperature of transparent and dense amorphous solids in which organic molecular species can be introduced. The wealth of precursors allows the development of new organic-inorganic hybrid materials whose optical properties can be controlled at will. Indeed, depending on the nature of the alkoxides used, it is easy to control the interactions between the polymeric network of the Sol-Gel matrix and the molecular system depending on the field of application of the material [71].

References

[1] Navas, D.; Fuentes, S.; Castro-Alvarez, A.; Chavez-Angel, E. Review on Sol-Gel Synthesis of Perovskite and Oxide Nanomaterials, *Gels. 7,* 275 (2021).

[2] K. Katagiri, K. Ariga, J. Kikuchi, Novel class of organic-inorganic hybrid vesicle “Cerasome” derived from various amphiphiles with alkoxysilyl head, Studies in Surface Science and Catalysis. Volume 132 (2001) Pages 599-602

[3] Ryan Yarbrough et al, A sol–gel synthesis to prepare size and shape-controlled mesoporous nanostructures of binary (II–VI) metal oxides, RSC Adv. 10 (2020) 14134–14146.

[4] Arvind Varma, Solution Combustion Synthesis of Nanoscale Materials, Chemical Reviews. 116 (23) (2016) 14493-14586.

[5] Landau, M.V, Sol–Gel Process. In Handbook of Heterogeneous Catalysis. (2008) 80-88.

[6] Yichao Xu, Qinfeng Rong, Tianyi Zhao, Mingjie Liu, Anti-Freezing multiphase gel materials: Bioinspired design strategies and applications, Giant. Volume 2 (2020) 100014.

[7] Guo Feng et al, A novel green nonaqueous sol-gel process for preparation of partially

stabilized zirconia nanopowder, Processing and Application of Ceramics 11. 3 (2017) 220–224.

[8] Mario Borlaf, Rodrigo Moreno, Colloidal sol-gel: A powerful low-temperature aqueous synthesis route of nanosized powders and suspensions, Open Ceramics, Volume 8, (2021) 100200.

[9] Dr. David Levy, Dr. Luis Esquivias, Sol–gel processing of optical and electrooptical materials, Volume7, Issue2, February (1995) Pages 120-129.

[10] Mihaela Aleksandrova, Bojidar Jivov, Lyuben Lakov, Summary of sol-gel synthesis of materials with electronic applications, International Scientific Journal. 3 (2020) 83-85.

[11] Gareth J. Owens, et al, Sol–gel based materials for biomedical applications, Progress in Materials Science. 77 (2016) 1-79.

[12] Tatiana N. Myasoedova et al, Sol-Gel Materials for Electrochemical Applications: Recent Advances, Coatings. 12, 1625 (2022).

[13] Dmitry Bokov et al, nanomaterial by Sol-Gel Method: Synthesis and Application, advances in Materials Science and Engineering. (2021) 21.

[14] C. Sanchez, et al, “Chimie douce”: A land of opportunities for the designed construction of functional inorganic and hybrid organic-inorganic nanomaterials, Comptes Rendus Chimie. Volume 13, Issues 1–2, (2010) Pages 3-39.

[15] Jarosław Kaszubkiewicz, Krzysztof Papuga, Equation for determining cumulative particle size distribution using the pressure of a sedimenting suspension, Measurement, Volume 209 (2023) 112493.

[16] Víctor Duarte Alaniz, Humberto Híjar, Anisotropic active colloidal particles in liquid crystals: A Multi-particle Collision Dynamics simulation study, Physica A: Statistical Mechanics and its Applications. Volume 609 (2023) 128298.

[17] Xiangqiong He, Bing Yu, Xiulan Zhang, Hailin Cong, pH-sensitive colloidal crystals built from monodisperse poly(St-MMA-SPMAP-AA) microspheres via air-liquid interface assembly, Optical Materials, Volume 135 (2023) 113350.

[18] Shima Ito, Akihiro Nishiguchi, Tetsushi Taguchi, Effect of particle size on the tissue adhesion and particle floatation of a colloidal wound dressing for endoscopic treatments, Acta Biomaterialia, (2023).

[19] Yuan Y, Basu S, Lin MH, Shukla S, Sarkar D. Colloidal Gels for Guiding Endothelial Cell Organization via Microstructural Morphology. ACS Appl Mater Interfaces. (2019) 4;11(35):31709-31728.

[20] Dickinson E. Structure and rheology of colloidal particle gels: insight from computer simulation. Adv Colloid Interface Sci. 199-200 (2013) 114-27.

[21] Douglas, J.F. Weak and Strong Gels and the Emergence of the Amorphous Solid State. *Gels. 4* (2018) 19.

[22] Correa S, Grosskopf AK, Lopez Hernandez H, Chan D, Yu AC, Stapleton LM, Appel EA. Translational Applications of Hydrogels. Chem Rev. 22;121(18) (2021) 11385-11457.

[23] Mario Borlaf, Rodrigo Moreno, Colloidal sol-gel: A powerful low-temperature aqueous synthesis route of nanosized powders and suspensions, Ceramics, Volume 8, (2021) 100200.

[24] Marion J. et al, Interactions between Metal Oxides and Biomolecules: from Fundamental Understanding to Applications, Chemical Reviews. (2018) 118 (22), 11118-11193

[25] Kessler, V.G. The chemistry behind the sol–gel synthesis of complex oxide nanoparticles for bio-imaging applications. J Sol-Gel Sci Technol. **51** (2009) 264–271.

[26] Esposito, S. “Traditional” Sol-Gel Chemistry as a Powerful Tool for the Preparation of Supported Metal and Metal Oxide Catalysts. Materials. 12 (2019) 668.

[27] J. Singh, K. Sahu, A. Pandey, M. Kumar, T. Ghosh, B. Satpati, et al., Atom beam sputtered Ag-TiO_2 plasmonic nanocomposite thin films for photocatalytic applications, Appl. Surf. Sci. 411 (2017) 354.

[28] Ghebremedhin M, Seiffert S, Vilgis TA. Physics of agarose fluid gels: Rheological properties and microstructure. Curr Res Food Sci. 22;4 (2021) 436-448.

[29] R. Jones, "Soft Condensed Matter," Oxford University Press Inc., New York (2002).

[30] Şahin, İ.; Özbakır, Y.; İnönü, Z.; Ulker, Z.; Erkey, C. Kinetics of Supercritical Drying of Gels. *Gels. 4* (2018) 3.

[31] Shirsath, S.E., Wang, D., Jadhav, S.S., Mane, M.L., Li, S. Ferrites Obtained by Sol-Gel Method. In: Klein, L., Aparicio, M., Jitianu, A. (eds) Handbook of Sol-Gel Science and Technology. Springer, Cham. (2018).

[32] Styskalik, A.; Skoda, D.; Barnes, C.E.; Pinkas, J. The Power of Non-Hydrolytic Sol-Gel Chemistry: A Review. *Catalysts. 7* (2017) 168.

[33] Ye, Chao-Qun. “Sol-Gel Processes of Functional Powders and Films.” Chemical Reactions in Inorganic Chemistry, May. InTech. (2018).

[34] Haryadi, Haryadi, Porous hybrid organic-inorganic silica materials: preparation,structural and transport properties.(2005)

[35] Tadros, Tharwat F. Basic Principles of Formulation Types. Berlin, Boston: De Gruyter. (2018).

[36] S. Girish Kumar, K. S. R. Koteswara Rao, Polymorphic phase transition among the titania crystal structures in solution based approach:

From precursor chemistry to nucleation process, ***Nanoscale***. **6** (2014) 11574-11632.

[37] A. E. Danks, S. R. Hall, and Z. Schnepp, The evolution of ‘sol–gel’ chemistry as a technique for materials synthesis, Mater. Horiz. **3** (2016) 91-112.

[38] Hamlin TA, Swart M, Bickelhaupt FM. Nucleophilic Substitution (S_N 2): Dependence on Nucleophile, Leaving Group, Central Atom, Substituents, and Solvent. Chemphyschem. 5;19(11) (2018)1315-1330.

[39] Giancarlo C. Righini, Andrea Chiappini, "Glass optical waveguides: a review of fabrication techniques," Opt. Eng. 53(7) 071819 (2014).

[40] Intramolecular Catalysis of Hydrolytic Reactions. II. The Hydrolysis of Phthalamic Acid1,2, Myron L. Bender, Yuan-Lang Chow, and Frank Chloupek, Journal of the American Chemical Society. 80 (20) (1958)5380-5384.

[41] Charles L. Perrin et al, Glossary of terms used in physical organic chemistry (IUPAC Recommendations 2021), Pure Appl. Chem. 94(4) (2022) 353–534.

[42] Mario Borlaf, Rodrigo Moreno, Colloidal sol-gel: A powerful low-temperature aqueous synthesis route of nanosized powders and suspensions, Open Ceramics. Volume 8 (2021) 100200.

[43] Jonschker, Gerhard. "6. Application, drying and densification". Sol-Gel-Technology in Praxis, Hannover, Germany: Vincentz Network, (2014) pp. 133-201.

[44] Esposito S. "Traditional" Sol-Gel Chemistry as a Powerful Tool for the Preparation of Supported Metal and Metal Oxide Catalysts. Materials (Basel). 23;12(4):668 (2019).

[45] Cecilia Agustín-Sáenz, et al, Broadband antireflective coating stack based on mesoporous silica by acid-catalyzed sol-gel method for concentrated photovoltaic application, Solar Energy Materials and Solar Cells, Volume 186, (2018) Pages 154-164.

[46] Phosphorus-Based Catalysis, Changmin Xie, Andrew J. Smaligo, Xian-Rong Song, and Ohyun Kwon, ACS Central Science. 7 (4) (2021) 536-558.

[47] Muhammad Sohail, et al, Synthesis and Hydrolysis–Condensation Study of Water-Soluble Self-Assembled Pentacoordinate Polysilylamides, Organometallics. 32 (6) (2013) 1721-1731.

[48] Sinkó K. Influence of Chemical Conditions on the Nanoporous Structure of Silicate Aerogels. Materials (Basel). 26;3(1) (2010) 704–40.

[49] Juliette Blanchard et al, Hydrolysis and Condensation Reactions of Transition Metal Alkoxides: Calorimetric Study and Evaluation of the Extent of Reaction, Volume 8, (1998) Pages 1115-1127.

[50] George M. Whitesides, John S. Sadowski, and Jennifer Lilburn, Copper(I) alkoxides. Synthesis, reactions, and thermal decompositions, Journal of the American Chemical Society. 96 (9) (1974)2829-2835.

[51] Ismail, W.N.W. Sol–gel technology for innovative fabric finishing—A Review. *J Sol-Gel Sci Technol*. 78 (2016) 698–707.

[52] M. Zielecka, E. Bujnowska, K. Suwala, and M. Wenda, “Sol-Gel-Derived Silicon-Containing Hybrids,” Recent Applications in Sol-Gel Synthesis. Jul. (2017)

[53] Yamamoto K, Suzuki S, Kitamura S, Yuguchi Y. Gelation and Structural Formation of Amylose by In Situ Neutralization as Observed by Small-Angle X-ray Scattering. Gels. (2018) 26;4(3):57.

[54] Aguilar G. V. Sol-Gel Method - Design and Synthesis of New Materials with Interesting Physical, Chemical and Biological Properties, London: IntechOpen. (2019)106 p.

[55] Jie Yang, Yanhui Li, Digby D. Macdonald, Effects of temperature and pH on the electrochemical behaviour of alloy 600 in simulated pressurized water reactor primary water, Journal of Nuclear Materials. Volume 528 (2020) 151850.

[56] Mad-Ali S, Benjakul S, Prodpran T, Maqsood S. Characteristics and gelling properties of gelatin from goat skin as affected by drying methods. J Food Sci Technol. 54(6) (2017) 1646-1654.

[57] Lichun Li, Baris Yalcin, Baochau N. Nguyen, Mary Ann B. Meador, and Miko Cakmak, Flexible Nanofiber-Reinforced Aerogel (Xerogel) Synthesis, Manufacture, and Characterization, ACS Applied Materials & Interfaces (2009) 1 (11), 2491-2501.

[58] Highly Absorbent Silk Fibroin Protein Xerogel Kang Cheng, Xiaosheng Tao, Zhenzhen Qi, Zuqiang Yin, Subhas C. Kundu, and Shenzhou Lu, ACS Biomaterials Science & Engineering. (2021) 7 (8), 3594-3607.

[59] Tatiana S. Babicheva, Anastasiya A. Konduktorova, Sergei L. Shmakov, and Anna B. Shipovskaya, Formation of Liesegang Structures under the Conditions of the Spatiotemporal Reaction of Polymer-Analogous Transformation (Salt → Base) of Chitosan, The Journal of Physical Chemistry B (2020) 124 (41), 9255-9266.

[60] Aboualigaledari, N., & Rahmani, M, A review on the synthesis of the TiO_2-based photocatalyst for the environmental purification. *Journal of Composites and Compounds*. *3*(6) (2021) 25–42.

[61] An LY, Dai Z, Di B, Xu LL. Advances in Cryochemistry: Mechanisms, Reactions and Applications. Molecules. (2021) Feb 1;26(3):750.

[62] Augustin S, Fröhlich T. Temperature Dependence of the Dynamic Parameters of Contact Thermometers. Sensors (Basel). (2019) May 18;19(10):2299.

[63] Tätte T, Hussainov M, Paalo M, Part M, Talviste R, Kiisk V, Mändar H, Põhako K, Pehk T, Reivelt K, Natali M, Gurauskis J, Lõhmus A, Mäeorg U. Alkoxide-based precursors for direct drawing of metal oxide micro- and nanofibres. Sci Technol Adv Mater. (2011) Jun 28;12(3):034412.

[64] C. Stewart Slater & Mariano Savelski, A method to characterize the greenness of solvents used in pharmaceutical manufacture, Journal of Environmental Science and Health, Part A, 42:11 (2007) 1595-1605.

[65] S.P. Mukherjee, Sol-gel processes in glass science and technology, Journal of Non-Crystalline Solids, Volume 42, Issues 1–3 (1980) Pages 477-488.

[66] Munish Gupta, Manik Gupta, B.S. Randhawa, Influence of Mg concentration on physico-chemical properties of Cd ferrites (CdMg1.5xFe2−xO4) synthesized by sol–gel combustion method, Journal of Alloys and Compounds. Volume 626 (2015) Pages 421-427.

[67] Gibin George and S. Anandhan, A comparative study on the physico–chemical properties of sol–gel electrospun cobalt oxide nanofibres from two different polymeric binders, *RSC Adv.* 5 (2015) 81429-81437.

[68] T. Surendar et al, Influence of La-doping on phase transformation and photocatalytic properties of ZnTiO3 nanoparticles synthesized via modified sol–gel method, *Phys. Chem. Chem. Phys.* 16 (2014) 728-735.

[69] Sols, Gels, and Organic Chemistry. In: Ceramic Materials. Springer, New York, NY. (2007).

[70] David Joseph Sullivan, Shafrina Azlin-Hasim, Malco Cruz-Romero, Enda Cummins, Joseph P. Kerry, Michael A. Morris, 11 - Natural Antimicrobial Materials for Use in Food Packaging, Editor(s): Atul Tiwari, Handbook of Antimicrobial Coatings. (2018) Pages 181-233.

[71] J.-P. Boilot, T. Gacoin, S. Perruchas, Synthesis and sol–gel assembly of nanophosphors, Comptes Rendus Chimie. Volume 13, Issues 1–2, (2010) Pages 186-198.

[72] Bondy, C.; Sollner, K., Mechanism of emulsification by ultrasonic waves. Trans Faraday Soc. 31 (1935) 835-43.

[73] Mason, T. J., Industrial sonochemistry: potential and practicality. Ultrason Sonochem. 30, (3) (1992) 192-6.

[74] Li, M. K.; Fogler, H. S.; , Acoustic emulsification. Part 1. The Instability of the oil-water Interface to form the initial droplets. J.Fluid. Mech. 88, (3) (1978) 499.

Chapter III

Overviews of the used materials

Chapter III Overviews of the used materials

In this chapter, we will provide an overview of the materials used, highlighting their wide range of applications and properties

III.1. Polyvinyl alcohol (PVA)

Poly (vinyl alcohol) (PVA) or Poly(1-hydroxy-ethylene) are semi-crystalline, colorless, synthetic, and biodegradable polymer. PVA is water-soluble, and its linear structure allows its molecules to align through hydrogen bonds, giving it excellent film-forming and adhesive properties. However, like other polymers, the physical properties of PVA generally depend on the method of preparation. PVA has very low transmission rates of oxygen, nitrogen, and helium, making it suitable as a barrier coating for other thermoplastics or when co-extruded with them. The water solubility of PVA films can be adjusted to some extent. The "standard" type, made from higher-molecular-weight polymers and plasticized with glycerin, is only weakly soluble in cold water. PVA is extrudable and moldable, and it is commonly used in fabric sizing, adhesives, emulsifying agents, and packaging films. [1, 3].

III.1.1. synthesis of polyvinyl alcohol (PVA)

Polyvinyl alcohol cannot be synthesized directly from its vinyl alcohol monomer; this is due to the instability of vinyl alcohol which tautomerizes to the more stable acetaldehyde [4]. Polyvinyl alcohol is obtained by partial or complete hydrolysis of polyvinyl acetate with methanol or water. The alcoholysis of polyvinyl acetate in acid or base catalysis by the reaction:

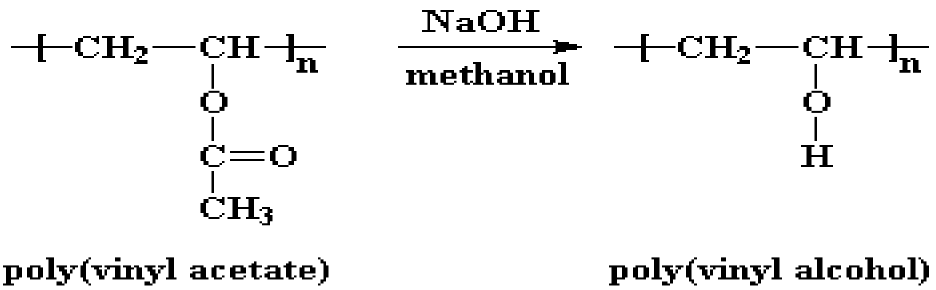

Fig. III.1 Formation of polyvinyl alcohol [5].

Industrially, the alcoholysis reaction occurs in basic catalysis, using alkali metal hydroxides or their alkoxides as catalysts. In the case of basic alcoholysis in methanolic solution, the true catalyst of the reaction is sodium methoxide [6],

III.1.2. Properties of polyvinyl alcohol

Polyvinyl alcohol (PVA) has several notable properties, including:

1. Water-solubility: PVA is readily soluble in water, which makes it useful for applications where a water-soluble polymer is required.
2. Film-forming and adhesive properties: PVA's linear structure allows its molecules to align through hydrogen bonds, which gives it excellent film-forming and adhesive properties.
3. Biodegradability: PVA is biodegradable, which means it can be broken down by microorganisms in the environment.
4. Barrier properties: PVA has very low transmission rates of oxygen, nitrogen, and helium, which makes it suitable as a barrier coating on other thermoplastics or when co-extruded with them.
5. Adjustable water solubility: The water solubility of PVA films can be adjusted to some extent by varying the molecular weight and degree of hydrolysis of the polymer.
6. Extrudable and moldable: PVA can be extruded and molded into a variety of shapes, which makes it useful in many manufacturing applications.

Overall, these properties make PVA a versatile polymer with a wide range of applications, including fabric sizing, adhesives, emulsifying agents, and packaging films [7-10].

III.1.3. Some applications of PVA

Polyvinyl alcohol (PVA) has many applications across various industries due to its unique properties, some of which include:

1. Adhesives: PVA is used as an adhesive in many industries, including paper and packaging, woodworking, and textiles.

2. Packaging films: Due to its barrier properties, PVA is used as a coating or as a film in food packaging, pharmaceutical packaging, and other applications where a barrier to oxygen or other gases is required.
3. Textiles: PVA is used as a sizing agent in the textile industry to improve the strength, stiffness, and crease resistance of fabrics.
4. Emulsifying agents: PVA is used as an emulsifying agent in a wide range of applications, including paint, ink, and personal care products.
5. Paper coatings: PVA is used as a coating on paper to improve its strength, printing quality, and water resistance.
6. Medical applications: PVA is used in medical applications, such as wound dressings, due to its biocompatibility and water solubility.

Overall, the versatility and unique properties of PVA make it a valuable polymer with many applications in various industries [11-14].

III.2. Silicon Dioxide (SiO_2)

Silica, also known as silicon dioxide, is a naturally occurring mineral solid with the chemical formula SiO_2. The mineral is composed of [SiO_4] tetrahedrons linked by their vertices, and can exist in different forms including crystalline (quartz, tridymite, and cristobalite) or amorphous. Silica is found in a wide range of materials including natural sources such as minerals (for example, quartz sand) and plants (such as bamboo). However, for industrial applications, synthetic amorphous silica is typically used [15].

III.2.1. Structure of SiO_2

Silica can be found in three allotropic forms (same chemical composition, but different atomic arrangements): crystalline (long-range crystallographic order), vitreous (short-range order), and amorphous (absence of order). The structure obtained by thermal oxidation is vitreous silica. It is amorphous in the case of poor control of oxide growth. The basic structural unit of silica is a silicon atom surrounded by four oxygen atoms forming the vertices of a tetrahedron [16, 17].

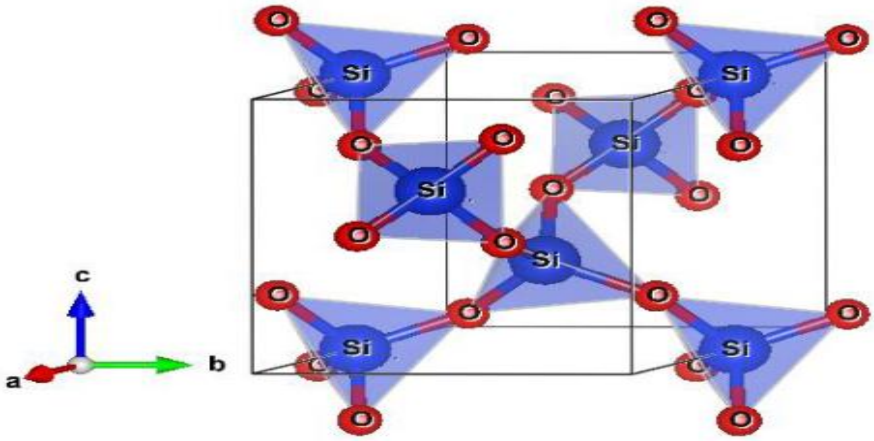

Fig. III.4 Crystal structure of SiO_2 [18].

Silica is made up of an arrangement of SiO_4 tetrahedrons linked together via the oxygen vertices. These tetrahedrons are characterized by the Si-O atomic distance (from 1.6 to 1.63 Å), and by the value of the angle θ between the O -Si-O bonds (θ varies from 110° to 180°, with an average value of 144° for amorphous silica) [19].

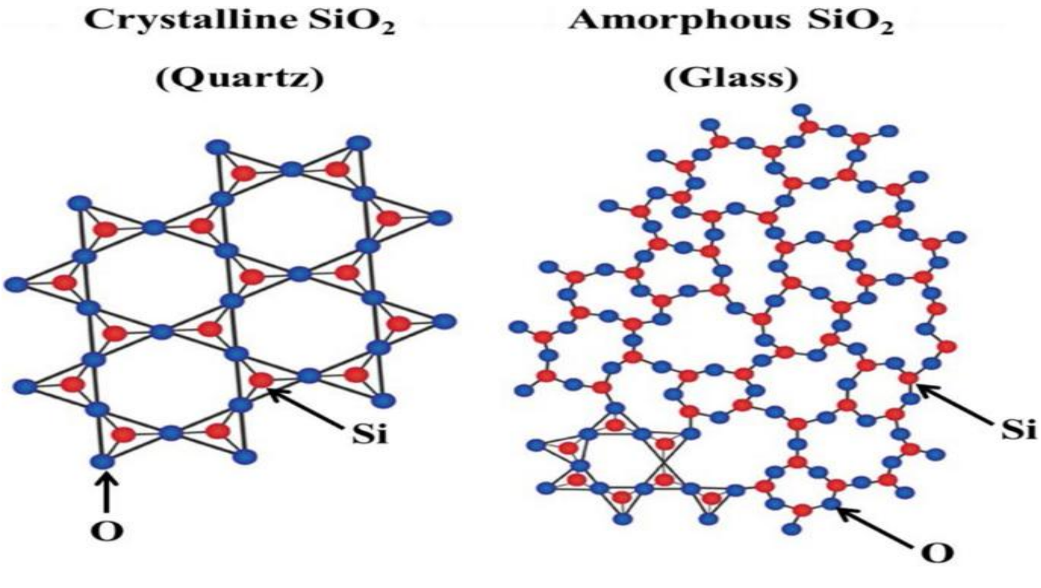

Fig. III.5 Planar representation of the lattice of (a) crystalline and (b) amorphous silica [20].

Silica nanoparticles are commonly used as fillers for hybrid inorganic-organic UV-curable materials. Their importance is because they are optically inert, low toxic, highly abundant, thermally and chemically stable, and permeable to template molecules. Their surface is highly rich in silanol groups, so they are extremely hydrophilic and are not adequate for a homogeneous dispersion in the [21].

III.2.2. Natural silicas

In its natural state, silica exists mainly in crystalline form. The latter is characterized by a high degree of organization and a dense structure. In this case, the active surface of the material, which is involved in the processes of chemical and physical interactions with the external environment, is limited to the outer surface of the particles. The specific surface of silica is of the order of some 2m/g and can be less. Silica is found in its natural form in minerals such as quartz, or in plants. In its natural state, silica occurs mainly in crystalline form. Several phases can exist, depending on temperature, pressure, and degree of hydration. Thus, at atmospheric pressure, crystalline silica exists in four different phases depending on the temperature. Quartz is the most stable form below 1143K, tridymite between 1143K and 1743K, and cristobalite between 1743K and 1973K. Above 1973K the cristobalite transforms into amorphous silica glass [22,23].

III.2.3. Synthetic silicas

Unlike natural silicas, these silicas are mainly produced in amorphous form. Their major interest lies in their porosity, which makes it possible to introduce a large surface inside the particles. They thus have a specific surface of the order of (30 up to 800 $m^2.g$-1) and a much larger active surface than crystalline silicas, this confers interesting surface properties, in particular in terms of reactivity or physico-chemical interactions. The specific surface, the particle size, the volume, and the pore size are all factors governing the reactivity of silica and can be controlled independently of each other by the choice of the method of preparation and the specific parameters of this method. this. There is a big difference between crystalline and amorphous silica. Crystalline silica has a dense and ordered structure, and its active surface allows chemical and physical interactions which are limited. Only the external surface can participate in these interactions, the specific surface is therefore limited to the geometric surface. It is quite the opposite for amorphous silicas due to the random arrangement of SiO_4 tetrahedrons and their porosity. Thus, the specific surface is more important and the surface properties become much more interesting in terms of reactivity. Synthetic silicas are obtained mainly by two main routes:

- wet process: precipitated silicas and silica sols;

- thermal route: thermal or pyrogenation silicas (smoked silica) [24-26].

III.2.4. Silica gels

The sol-gel process is the one best described in the literature. One of its advantages is that it leads to a pure and homogeneous product at low temperatures. The sol-gel process involves two common chemical reactions, hydrolysis, and condensation to form a siloxane network. [30] A silicate such as sodium silicate is commonly used as a raw material, although more recently the use of alkoxysilanes with the general formula $Si(OR)_4$(R can be CH_3, C_2H_5, or C_3H_7). It is by the hydrolysis of these molecules that silanols are obtained which can then give rise by condensation to siloxane bonds. Hydrolysis and condensation take place simultaneously in the aqueous solution, forming stable particles of colloidal size [27, 28].

It is thus possible to favor either the growth of the particles or the bridging of the particles to give rise to chains. In the latter case we can, from a certain point, pass from a sol to a gel, where we have an elastic behavior. This gel is called hydrogel in the case where the solvent is water or alcogel in the case where the solvent used is alcohol. The structure of the hydrogel is controlled by the temperature, the pH of the medium, the nature of the solvent, the type of electrolyte used, and the type of silicate or alkoxide [30].

The family of granular silicas mainly includes xerogels and aerogels. Xerogels (from the Greek Xêros: dry) are obtained by drying hydrogel silicas (silica impregnated with water), while aerogels are formed after heating organogels (silica impregnated with organic solvent) [31].

III.2.5. Properties of silicon dioxide

For the various forms of silica, the specific surface varies from 25 to 1000 $m^2.g-1$ [32]. Porosity This factor is important for the reactivity of silica. Indeed, the higher the porosity and the more homogeneous the distribution, the more the silanols of the pores are accessible, thus increasing the total number of surface silanols. Depending on the pore size, silica can be microporous (diameter less than 2 nm), meso-porous (diameter between 2 and 50 nm), or macroporous (diameter greater than 50 nm). Primary particle size According to the types of silica, the sizes vary from a few nanometers to 500 nm. These primary particles can also agglomerate together to give aggregates whose sizes are between 1 and 40 µm. We then obtain supports with various shapes [33, 34].

III.2.5.1. Viscosity

As the viscosity of a fluid increases, its ability to flow decreases. The introduction of colloidal particles into a liquid increases its viscosity. For example, silica is mixed with paint as well as certain pharmaceutical or cosmetic products [35].

III.2.5.2 Hardness

Hardness describes the ability of a material to resist deformation. The great hardness and the abrasive properties of silica gels and powders justify their interest as a reinforcing agent. Indeed, the ability to resist abrasion, scratching, or deformation makes it possible to increase the applications, particularly in the field of mechanics. The specificity and the porosity are to be taken into account for large applications such as chromatography using adsorption properties, while the hardness and viscosity are highlighted for applications where the mechanical properties are important. From a chemical point of view, silica has a high melting temperature (above 1500°C) and zero oxidation-reduction reactivity, which makes it a very stable material. Its potential at zero charges equal to two is explained by the presence of silanols on the surface. These groups justify the ionization and hydrophilic properties of silica. These are the reactive sites allowing chemical functionalization by organic or inorganic compounds [36-38].

III.3. Titanium dioxide (TiO_2)

III.3.1. Introduction

Titanium dioxide is a molecule composed of oxygen and titanium atoms with the formula TiO_2. It is a wide bandgap semiconductor (gap = 3.2 eV). It has a high refractive index (at 590 nm): nrutile = 2.70, nanatase = 2.55) and a high scattering coefficient (96% of incident light is reflected in the visible). Its theoretical density, high for an oxide, is 4.25 (measured between 3.9 and 4.2). It has a melting point of 1855°C. TiO_2 is chemically and biologically inert. It is an abundant material on Earth in the form of ilmenite (oxide of titanium and iron) and erutile. TiO_2 is obtained by the treatment of ilmenite ores by the sulfate process directly or by the chlorine process (for rutile ores), a fairly simple processes. This material is not expensive. TiO_2 is found in three crystallographic forms: rutile, anatase, and brookite. Rutile is the most stable form of titanium dioxide and is produced at high temperatures, brookite forms at lower temperatures, and anatase at even lower temperatures [39, 40]. Titanium oxide is the most widely used white pigment. It is non-toxic and replaced white lead. It is obtained from titanium ore. About 95% of the quantity of ore extracted is used for the production of the pigment and only 5% for the preparation of the metal. Titanium oxide is widely produced around the world, with an annual sales volume of more than 3.5 million tons and global consumption increasing at around 2% per year. The main producers are Canada, Norway, Australia, and South Africa. The sectors of use are very varied: paint, plastic, and paper. This enthusiasm is explained by its exceptional properties [41, 42].

III.3.2. Different Forms of Titanium Dioxide

Natural titanium oxide exists in the crystalline state in three allotropic forms: rutile, anatase, and brookite. These varieties are placed according to a regular filiation in the temperature scale. Anatase, gradually heated, is converted into rutile. Brookite is an intermediate form that has a very narrow domain of stability [43].

III.3.2.1. Rutile

It forms the most abundant part, takes its name from its red color, and it's a high density of 4.3, sometimes forming large alluvial deposits that can be industrially exploited. It is from this mineral that titanium is usually used, this type is thermodynamically stable, although this mineral can also be represented by yellow or black individuals. This product is used in the manufacture of many colors and may contain up to 10% iron. It strongly refracts light, with a high refractive index of value between (2.7-3.1), and is not very hard, it is also known under the following names: Cajuelite, Rutilite, Crispite, and Edisonite. [44]

III.3.2.2. Anatas

It is a tetragonal mineral, it has a theoretical density of 3.893, and its refractive index is between (2.55-2.75), heated to 700 C° it turns into rutile. The crystalline structure of anatase is much more complex than that of rutile, the octahedra have been "distorted" there.

Anatase is mainly used as a pigment and opacifier for all kinds of applications:

paint: titanium white, but also as an opacifying agent for all dyes, paper, plastics, ceramics, and toothpaste [45].

III.3.2.3. Brookite

Orthorhombic crystal structure, it is the hydrated oxide found in ore deposits, usually dark blue, black, very dark brown to brownish-red, well-formed, stubby complex prismatic crystals; isometric pseudo-hexagonal bipyramids and rarely in tabular form, with density of

4.1 g/cm3. Generally, this substance is not used as a photo-catalyst in the photo-degradation process [46, 47].

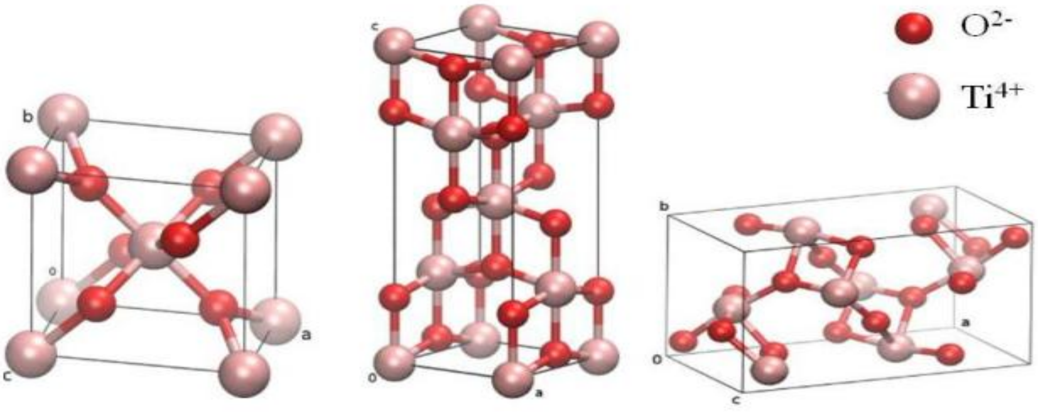

Fig. III.6 Phase structure of TiO_2**:** a: Rutile**;** b: Anatase**;** c: Brookite [48].

III.3.3. Titanium Dioxide Elaboration Processes

There are two major titanium dioxide production processes in industry: the sulfuric process and the chloride process.

III.3.3.1. sulfuric process

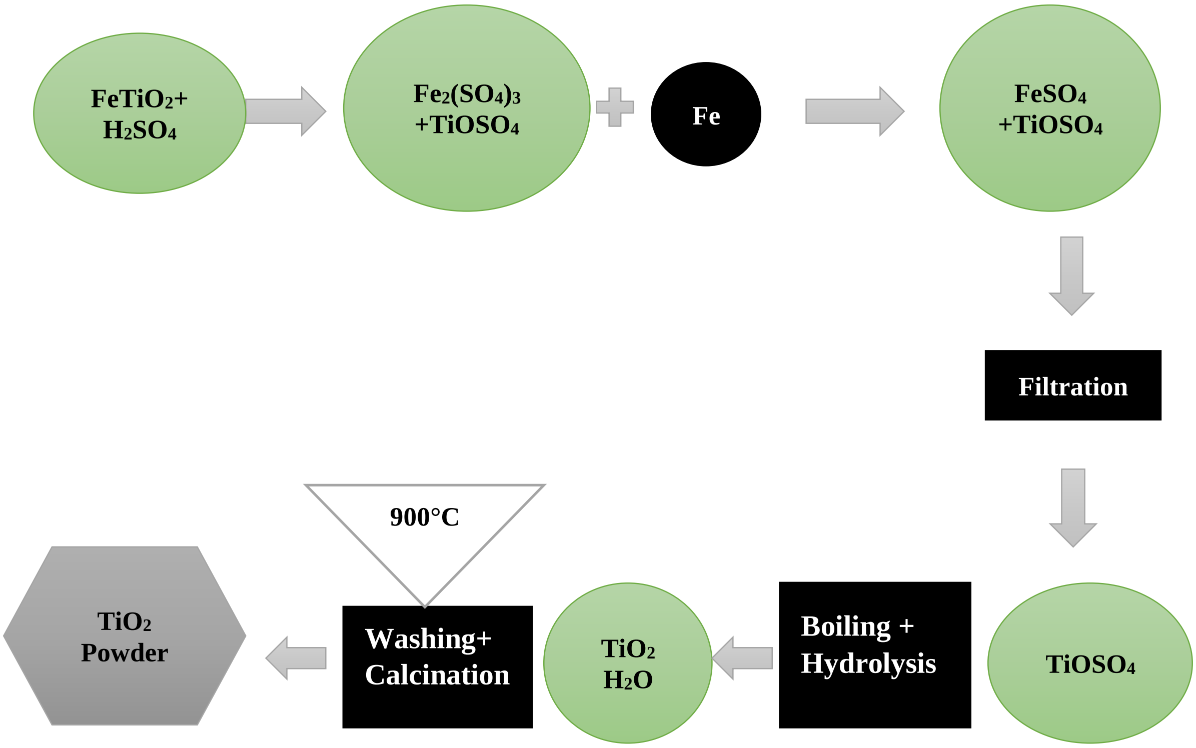

Fig. III.7 Diagram of the sulfuric process relating to the production of titanium dioxide [49].

III.3.3.2. Chloride process

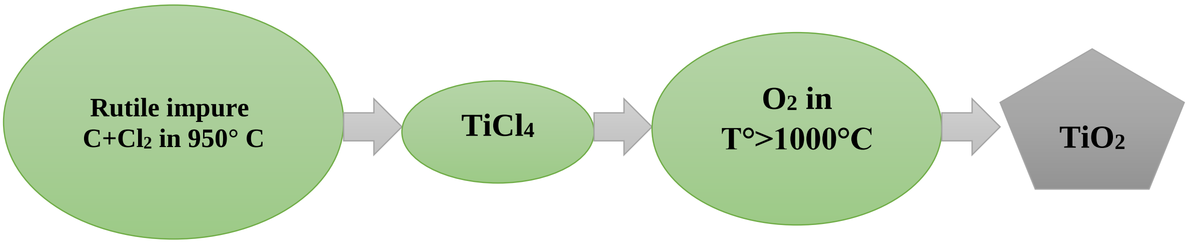

Fig. III.8 Diagram of the chloride process relating to the production of titanium dioxide [50].

III.3.4. Properties of TiO_2

III.3.4.1. Chemical properties

Titanium dioxide is very stable thanks to very strong bonds between Ti+4, tetravalent cations, and O^{2}-, divalent anions; it is therefore very chemically inert. It is insoluble in all liquids except concentrated sulfuric acid and hydrofluoric acid [51].

III.3.4.2. Physical properties

Table III.1 present a comparison between the properties of the three phases of TiO_2 [52].

Property	*Rutile*	*Anatase*	*Brookite*
Band gap (eV) [ZALLEN R]	***3,06***	***3,3***	***1,9***
Density (g/cm3)	***4,27***	***3,90***	***4,08 – 4,2***
Refractive index (à 589 nm)	***2,61 – 2,90***	***2,49 – 2,55***	***2,58 – 2,70***
Melting temperature (° C)	***1843***	***1843***	***1830 – 1850***
Hardness (Mohs scale)	***7,0 – 7,5***	***5,5 – 6,0***	***5,5 – 6,0***

III.3.5. Some applications of TiO_2

In the field of photochemistry, titanium dioxide allows the initiation of reactions such as the photolysis of water, the photo-reduction of nitrogen, and the purification of liquid and gaseous effluents. In optics, titanium dioxide coatings have favorable properties for modifying the refractive index of the surface of lenses. TiO_2 applications also concern microelectronics, solar energy conversion, and gas sensors. TiO_2 is also used as a coating for protection against corrosion, in photovoltaics with the development of a new generation of sensitized solar cells called Grätzel type and in photochromic materials [53-55].

I.4 Conclusion

The first section of this thesis focused on the problematic of hybrid materials produced through the sol-gel route. This was achieved through a comprehensive literature review, spanning Chapters I, II, and III. The review covered generalities on hybrid materials, including methods of their elaboration, their properties, and resulting applications. The chemical reactions involved in the process comprise two mechanisms, namely hydrolysis and condensation. These reactions are influenced by several factors such as the nature of the precursor, its concentration, pH, among others. To determine the best process for developing the hybrid film, a comparative analysis of the different development methods was carried out. While the literature offers limited insight into the properties of the material, we have summarized the few available results. It is noteworthy that thin hybrid films have a wide range of applications. Additionally, we presented generalities on the materials used in this study (PVA, silicon dioxide, and titanium dioxide), including their properties, preparation methods, fields of application, and drawbacks. Our contribution will be to develop a hybrid material with superior properties to those reported in the literature, we will now proceed to the experimental part.

References

[1] Sapalidis A A, Porous Polyvinyl Alcohol Membranes: Preparation Methods and Applications, Symmetry. 12 (2020) 960.

[2] Nihed Ben Halima, Poly(vinyl alcohol): review of its promising applications and insights into biodegradation, RSC Adv. 6 (2016) 39823-39832.

[3] Chen X, Taguchi T, Enhanced Skin Adhesive Property of Hydrophobically Modified Poly(vinyl alcohol) Films, ACS Omega. 10 (2020) 1519-1527.

[4] Mirela Teodorescu, Maria Bercea & Simona Morariu, Biomaterials of Poly(vinyl alcohol) and Natural Polymers, Polymer Reviews. 58:2 (2018) 247-287.

[5] Giannelis, E P, Applied Organometallic Chemistry. 12 (1998) 675-680.

[6] Paralikar S, Poly (vinyl alcohol) / Cellulose Nanocomposite Barrier Films, OregonState University, Oregon, US. (2006).

[7] Usurelu CD, Badila S, Frone AN, Panaitescu DM, Poly(3-hydroxybutyrate) Nanocomposites with Cellulose Nanocrystals, Polymers (Basel). 10 (2022) 12-14.

[8] Chen, Nx., Zhang, Jh, The role of hydrogen-bonding interaction in poly(vinyl alcohol)/poly(acrylic acid) blending solutions and their films, Chin J Polym Sci. 28 (2010) 903-911.

[9] Yu Bao, Xiaobo Huang, Jun Xu, and Shuxun Cui, Effect of Intramolecular Hydrogen Bonds on the Single-Chain Elasticity of Poly(vinyl alcohol): Evidencing the Synergistic Enhancement Effect at the Single-Molecule Level, Macromolecules. 54 (2021) 7314-7320.

[10] Brough C, Miller DA, Keen JM, Kucera SA, Lubda D, Williams RO 3rd. Use of Polyvinyl Alcohol as a Solubility-Enhancing Polymer for Poorly Water Soluble Drug Delivery (Part 1). AAPS PharmSciTech. 17 (2016) 167-79.

[11] Punjataewakupt A, Reddy N, & Aramwit, P. Enhancing clinical applications of PVA hydrogel by blending with collagen hydrolysate and silk sericin, J Polym Res. 29 (2022) 110.

[12] Goodship, Vannessa and Jacobs, D. K, Polyvinyl alcohol: materials, processing and applications, Rapra review reports. 16 (2009) 12.

[13] Baker MI, Walsh SP, Schwartz Z, Boyan BD. 2012. A review of polyvinyl alcohol and its uses in cartilage and orthopedic applications. J Biomed Mater Res, Part B, 100B (2012)1451–1457.

[14] Gaaz, T.S.; Sulong, A.B.; Akhtar, M.N.; Kadhum, A.A.H.; Mohamad, A.B.; Al-Amiery, A.A. Properties and Applications of Polyvinyl Alcohol, Halloysite Nanotubes and Their Nanocomposites, *Molecules*, *20* (2015) 22833-22847.

[15] M. Schaible, Empirical Molecular Dynamics Modeling of Silicon and Silicon Dioxide: A Review, Critical Reviews in Solid State and Materials Sciences, 24:4 (1999), 265-323.

[16] Albert Rimola, Dominique Costa, Mariona Sodupe, Jean-François Lambert, and Piero Ugliengo, Silica Surface Features and Their Role in the Adsorption of Biomolecules: Computational Modeling and Experiments, Chemical Reviews, 113 (6) (2013), 4216-4313,

[17] I M Joni *et al*, Characteristics of crystalline silica (SiO2) particles prepared by simple solution method using sodium silicate (Na2SiO3) precursor, *J. Phys.: Conf. Ser.* 1080 (2018) 012006.

[18] Siti Mariyah Ulfa *et al* Structural Characterization of Ni/ZrO2/SiO2 Nanocomposites Prepared by Wet Impregnation Route, *IOP Conf. Ser.: Mater. Sci. Eng,* **515** (2019) 012014.

[19] Shchipalov Y K, Surface Energy of Crystalline and Vitreous Silica, *Glass and Ceramics* **57** (2000) 374–377.

[20] Atif, R.; Khaliq, J.; Combrinck, M.; Hassanin, A.H.; Shehata, N.; Elnabawy, E.; Shyha, I. Solution Blow Spinning of Polyvinylidene Fluoride Based Fibers for Energy Harvesting Applications: A Review. *Polymers*, 12 (2020) 1304.

[21] Rita Zakhia Douaihy, Igor Telegeiev, Hussein Nasrallah, Oleg Lebedev, Philippe Bazin, Alexandre Vimont, Jean-François Chailan, Armand Fahs, Mohamad EL-Roz, Synthesis of silica-polymer core-shell hybrid materials with enhanced mechanical properties using a new bifunctional silane-based photoinitiator as coupling agent, Materials Today Communications, Volume 27 (2021) 2352-4928.

[22] Croissant, J.G., Butler, K.S., Zink, J.I. et al. Synthetic amorphous silica nanoparticles: toxicity, biomedical and environmental implications, Nat Rev Mater 5 (2020) 886–909.

[23] Gonçalves, M.C. Sol-Gel Silica Nanoparticles in Medicine: A Natural Choice. Design, Synthesis and Products, *Molecules*, *23* (2021).

[24] Imai, H. and Arai, K. and Isoya, J. and Hosono, H. and Abe, Y. and Imagawa, H. Generation of E' centers and oxygen hole centers in synthetic silica glasses by ensuremath\gamma irradiation, Phys. Rev. B, American Physical Society, 48 (1993) 3116—3123.

[25] E.J. Friebele, D.L. Griscom, M.J. Marrone, The optical absorption and luminescence bands near 2 eV in irradiated and drawn synthetic silica, Journal of Non-Crystalline Solids, Volume 71 (1985) 133-144.

[26] Otto W. Flörke et al, Silica, Ullmann's Encyclopedia of Industrial Chemistry, (2008).

[27] Ferri, Fabio and Frisken, B. J. and Cannell, David S, Structure of silica gels, Phys. Rev. Lett, 67, 25 (1991) 3626—3629.

[28] Nassif, N., Bouvet, O., Noelle Rager, M. *et al.* Living bacteria in silica gels. Nature Mater 1 (2002) 42–44.

[29] Antoine Bisson, Arnaud Rigacci, Didier Lecomte, Elisabeth Rodier & Patrick Achard, Drying of Silica Gels to Obtain Aerogels:Phenomenology and Basic Techniques, Drying Technology. 21:4 (2003) 593-628.

[30] Li-Chih Hu et al, Organo–silica hybrid functional nanomaterials: how do organic bridging groups and silsesquioxane moieties work hand-in-hand, *Chem. Soc. Rev.*. 40 (2011) 688-695.

[31] Selay Sert Çok, Fatoş Koç, Firuz Balkan, Nilay Gizli, Revealing the pore characteristics and physicochemical properties of silica ionogels based on different sol-gel drying strategies, Journal of Solid State Chemistry. 278 (2019) 0022-4596.

[32] Nekrashevich, S.S., Gritsenko, V.A. Electronic structure of silicon dioxide (a review). *Phys. Solid State.* **56** (2014) 207–222.

[33] H.R. Philipp, - Silicon Dioxide (SiO_2) (Glass), Editor(s): Edward D. Palik, Handbook of Optical Constants of Solids, Academic Press. (1997) 749-763.

[34] N. M. Ravindra *and* J. Narayan, Optical properties of amorphous silicon and silicon dioxide, Journal of Applied Physics. **60** (1986) 1139.

[35] David E. Tambe, Mukul M. Sharma, The effect of colloidal particles on fluid-fluid interfacial properties and emulsion stability, Advances in Colloid and Interface Science. Volume 52 (1994) 1-63.

[36] Xu, Yong-Nian and Ching, W. Y. Electronic structure and optical properties of \ensuremath\alpha and \ensuremath\beta phases of silicon nitride, silicon oxynitride, and with comparison to silicon dioxide, Phys. Rev.. volume 51 (1995) 17379—17389.

[37] G. Carlotti, L. Doucet, M. Dupeux, Elastic properties of silicon dioxide films deposited by chemical vapour deposition from tetraethylorthosilicate, Thin Solid Films. Volume 296 (1997) Pages 102-105.

[38] D.R. Lamb, Some electrical properties of the silicon-silicon dioxide system, Thin Solid Films. Volume 5 (1970) Pages 247-276.

[39] O. Carp, C.L. Huisman, A. Reller, Photoinduced reactivity of titanium dioxide, Progress in Solid State Chemistry. 32 (2004) 33–177.

[40] D Reyes-Coronado, G Rodrıguez-Gattorno, M E Espinosa-Pesqueira, C Cab, R de Coss and G Oskam, Phase-pure TiO_2 nanoparticles: anatase, brookite and rutile, Nanotechnology 19 (2008) 145605 (10pp).

[41] Juergen H. Braun, Andrejs Baidins, Robert E. Marganski, TiO_2 pigment technology: a review, Progress in Organic Coatings, Volume 20 Issue 2 (1992) Pages 105-138.

[42] O. Carp, C.L. Huisman, A. Reller, Photoinduced reactivity of titanium dioxide, Progress in Solid State Chemistry. Volume 32 Issues 1–2 (2004) Pages 33-177.

[43] Wenfu Yan et al, Preparation and Comparison of Supported Gold Nanocatalysts on Anatase, Brookite, Rutile, and P25 Polymorphs of TiO2 for Catalytic Oxidation of CO, The Journal of Physical Chemistry B, 109 (21) (2005) 10676-10685.

[44] Comotti, M., Weidenthaler, C., Li, WC. *et al.* Comparison of gold supported catalysts obtained by using different allotropic forms of titanium dioxide. *Top Catal.* **44** (2007) 275–284.

[45] Annalisa Palmieri et al, Comparison between titanium and anatase miRNAs regulation, Nanomedicine: Nanotechnology, Biology and Medicine. Volume 3 Issue 2 (2007), Pages 138-143.

[46] Xiangchun Liu, Preparation and characterization of pure anatase nanocrystals by sol–gel method, Powder Technology. Volume 224 (2012), Pages 287-290.

[47] D. Velten et al , Preparation of TiO_2 layers on cp-Ti and Ti6Al4V by thermal and anodic oxidation and by sol-gel coating techniques and their characterization, Journal of Biomedical Materials Research Volume59, Issue1, January (2002) Pages 18-28.

[48] MOELLMANN J. et al. Jonas Moellmann, Stephan Ehrlich, Ralf Tonner and Stefan Grimme, A DFT-D study of structural and energetic properties of TiO_2 modifications**,** J. Phys.: Condens. Matter. 24 (2012) 424206.

[49] Thambiliyagodage, C., Wijesekera, R. & Bakker, M.G. Leaching of ilmenite to produce titanium based materials: a review. *Discov Mater* **1**. 20 (2021)

[50] Argex Titanium Inc. Argex Process: Third Generation Process to Manufacture Titanium Dioxide. Montreal, Canada: TiO_2 World Summit. October 7-9, (2014) Page 14.

[51] M. F. Yan *and* W. W. Rhodes, Preparation and properties of TiO_2 varistors, Appl. Phys. Lett. 40, 536 (1982).

[52] R. Zallen, M.P. Moret ; The optical absorption edge of brookite TiO_2, Solid State Communications 137 (2006) 154–157.

[53] Swagata Banerjee, Dionysios D. Dionysiou, Suresh C. Pillai, Self-cleaning applications of TiO_2 by photo-induced hydrophilicity and photocatalysis, Applied Catalysis B: Environmental. Volumes 176–177 (2015) Pages 396-428.

[54] Adawiya J. Haider, Riyad Hassan AL– Anbari, Ghadah Rasim Kadhim, Chafic Touma Salame, Exploring potential Environmental applications of TiO_2 Nanoparticles, Energy Procedia. Volume 119 (2017) Pages 332-345.

[55] Zhenhuan Zhao et al, Structure, Synthesis, and Applications of TiO_2 Nanobelts, Advnced materials. Volume27, Issue16, April 24, (2015) Pages, 2557-2582.

Chapter IV

Materials, Methodology and Experimental Techniques

Chapter IV *Materials, methodology, and experimental techniques*

After having described in the literature review part (Chapter I, II, and III) the hybrid materials, the methods of elaboration and deposition of hybrid materials in general as well as the sol-gel method in particular, and generalities on the materials used, in this experimental part we will now devote the chapter IV to present in the first part all the materials used for the preparation of the samples, in the second part of this chapter, the different experimental techniques used will be presented.

IV.1. General characteristics of the materials used and methodology

IV.1.1 General characteristics of the materials used

All of these materials were supplied by Sigma-Aldrich. Deionized water (DI) was used throughout all the experiments. All chemicals and materials were obtained and used as received without any further purification.

IV.1.1.1 Polyvinyl alcohol (PVA)

Poly (vinyl alcohol) degree of polymerization = 1800, 98% hydrolyzed with Mw= 15000g/mol**,** presented in the form of a crystalline white powder resulting from the hydrolysis of polyvinyl acetate.

Table IV.1 Properties of the used PVA [1].

Properties	
General formula	$(C_2H_4O)_n$
Density	1.19
melting point	230°C
Solubility (solvent)	Water

IV.1.1.2. Titanium dioxide (TiO_2)

The titanium dioxide TiO_2 with an average particle size of 10-25 nm, with a purity of 93%, is used as a nanofiller for the reinforcement of the polymer matrices, the characteristics described by the supplier are given in Table III.2.

Table IV.2 Main characteristic of the used TiO_2 [2].

Specification	Value
Shape of crystals	Rutile
Molecular weight (g/mol)	79.90
Average particle size	10-25 nm
Chemical stability	Stable
Relative density	3.4 – 4.3

IV.1.1.3. TEOS as a source of silica (SiO_2)

Tetraethyl orthosilicate precursor was used as a source of silica (SiO_2) using the sol-gel method

Table IV.3 Characteristics of the used TEOS [3].

Product	Property	
TEOS	General formula	$Si(OC_2H_5)_4$
	Molecular weight	208.33 g/mol
	Density	0.933 g/ml
	Purity	98. %

IV.1.1.4. Reagents and solvents

IV.1.1.4. Ethanol

Table IV.4 Characteristics of the used Ethanol [4].

Product	Property	
Ethanol	General formula	(C_2H_5OH)
	Molecular weight	46.07 g/mol
	Density	0.789 g/ml
	Purity	96%

IV.1.1.4.b Hydrochloric acid (HCl)

Table IV.5 Characteristics of the used HCL [5].

Product	Property	
hydrochloric acid	Molecular weight	36.46
	Density	1.19 g/ml
	Purity	38%

IV.1.2. Materials Development Methodology

IV.1.2.1 Choice of the precursor

The hybrid materials that we have developed result from the combination of a precursor and a polymer powder. The precursor used, supplied by Sigma Aldrich, is: tetraethoxysilane (TEOS, 98%) and the polymer is the PVA, their chemical formulas are given in Chapter III. precursors of the organosilane type of formula Rn'SiX4-n (n = 1, 2, 3) where X denotes a hydrolyzable group (alkoxide, halide, carboxylate, etc.), and R' an organic group. The index n linked to the term functionality designates the number of hydrolyzable groups present in the molecule [6,7]. The choice of the precursor is guided by the nature of the hybrid that one wishes to obtain (class I or II) as described in chapter I. The class II of the hybrids that we have developed has the advantage, by comparison to class I, to be derived from a precursor itself containing a strong bond between its mineral part and its organic part. On the other hand, and independently of the nature of the precursor, it is necessary to ensure during the synthesis process, the stability of the organometal interface initially established by the Si-R chemical bond. This property, which depends on the nature of the inorganic element and the organic group, is achieved in the case of the precursor that we have chosen. Indeed, for chemical elements that are not very electropositive such as silicon, covalent bonds of the Si-C type, stable to hydrolysis, will make it possible to synthesize materials. Class II hybrids [8]. The stability of organic groups linked to the inorganic network makes it possible to avoid a drawback of class I hybrid compounds: the possible departure of organic entities during the use of the material [8].

The other advantage of the chosen precursor is to lead to hybrids having a better definition of the organic-inorganic interface and consequently a better understanding of the material and the microstructure-mechanical properties relationship, as well as an easier adjustment of the hydrophilic or hydrophobic character.

IV.1.2.2. Experimental Flow Chart

A general flow chart for the sol-gel process leading to the preparation of the hybrid films using tetraethyl orthosilicate is shown in Fig.1.

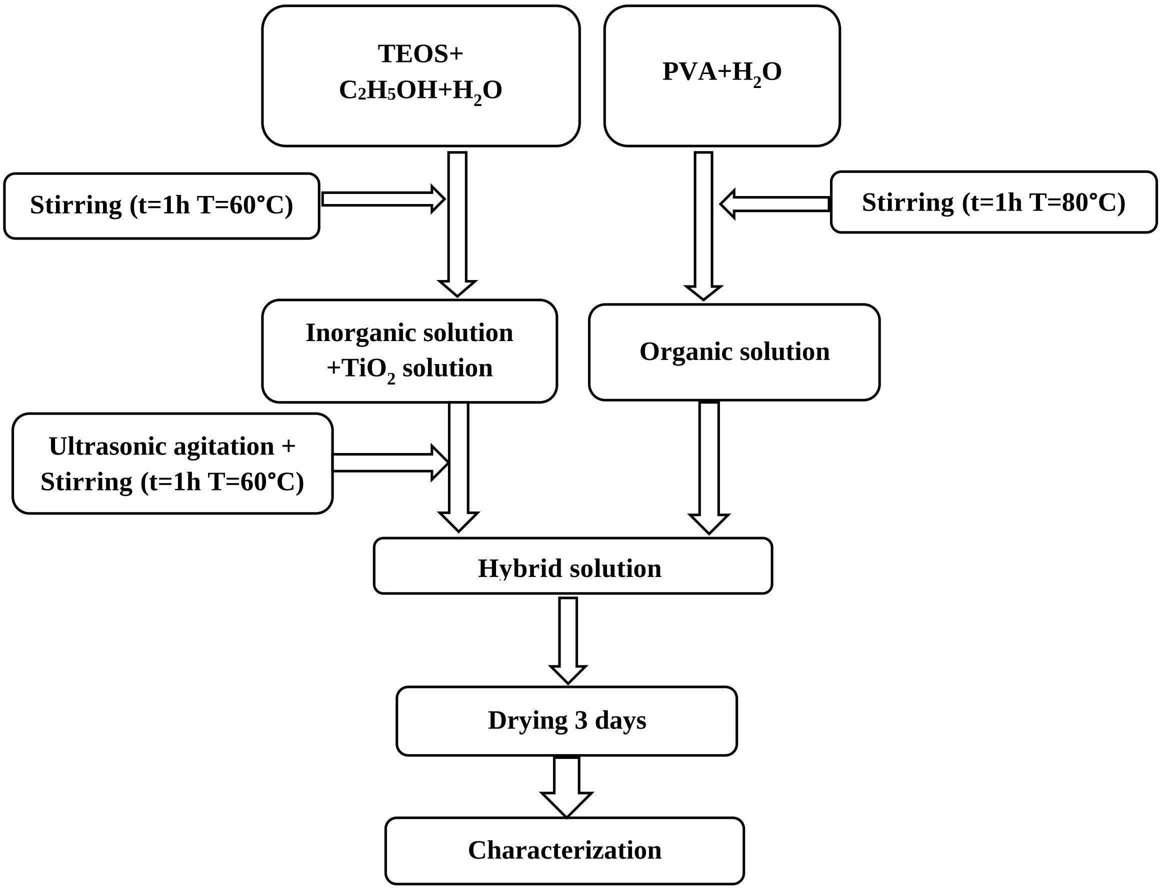

Fig. IV.1 Flow chart showing the synthesis of hybrid PVA-Silica-Nano TiO_2 sol-gel steps

IV.1.2.3. Neat PVA Films:

First, a sufficient amount of PVA (5 g) was dissolved in 100 ml of deionized water (5 percent). Then the mixture was magnetically mixed and heated for 1 hour at 80 °C until the mixture appeared homogeneous and viscous. The gel was placed into a petri dish for three days allowing it to solidify at room temperature.

IV.1.2.4. PVA/SiO_2 Films:

5 g of PVA was dissolved in the same manner as indicated above. 40% of TEOS was dissolved in ethanol and deionized water and hydrochloric acid at a molar ratio of 1: 4: 1: 0.04 of TEOS/Ethanol/Water/HCl, respectively. This mixture was heated at 60 °C and stirred for 1 hour. Then, the PVA solution was gradually added separately to each solution of the TEOS and the resulting mixture was thoroughly mixed for 1 hour by stirring at 60 °C. The solution obtained was poured into a Petri dish and allowed to solidify at room temperature for 3 days.

IV.1.2.5. PVA/SiO_2/TiO_2 Films:

The PVA/SiO_2 solution was prepared using the same experimental procedure as described above. To avoid nanoparticle agglomeration, TiO_2 nanoparticles were added to water and magnetically stirred vigorously for 3 hours before sonication for 1 hour. The mixture was mixed with the PVA solution and TEOS under magnetic stirring for 1 hour and then sonicated again for 1 hour to ensure a good dispersion. Finally, the mixture was poured into a petri dish and left for 3 days to solidify at room temperature. All compositions of the hybrid films are presented in Table IV.6.

Table IV.6 Compositions and Preparation of PVA/SiO_2/TiO_2 hybrid solutions. P: Neat PVA, PS: PVA/SiO_2, PST1: PVA/SiO_2/TiO_2 (1wt %), PST3: PVA/SiO_2/TiO_2 (3wt %), PST5: PVA/SiO_2/TiO_2 (5wt %).

Sample	**PVA (Wt %)**	**TEOS (Wt %)**	**Silica (W %)**	**TEOS (wt %) in Solution**	**PVA (wt %) in the solution**	**silica: PVA ratio in solution (by wt)**	**H_2O/TEOS (mol) ratio**	**HCL/TEOS (mol) ratio**	***TiO_2 (g)***	***Appearance of the films***
P	100	0	0	0	5	0:1	0	0	0	Transparent
PS	60	40	16	3	4.5	1:1.5	1	0.04	0	Transparent
PST1	60	40	16	3	4.5	1:1.5	1	0.04	0.5	opaque white
PST3	60	40	16	3	4.5	1:1.5	1	0.04	0.15	opaque white
PST5	60	40	16	3	4.5	1:1.5	1	0.04	0.25	opaque white

IV.1.3. Conclusion

This first part of chapter IV was devoted to the preparation of hybrid films with an explanation of the experimental conditions used in this work as well as their flowchart, the PVA/SiO_2/TiO_2 hybrid material was successfully synthesized. We will now present in the second part the different characterization techniques used.

IV.2. Experimental techniques

In this second part of chapter IV, we will describe the characterization techniques (FTIR, ATG, XDR) implemented during this work as well as the associated instruments. It is not a question, here, of describing in detail each technique but of giving the main lines used to obtain and interpret the results. The techniques listed have made it possible to analyze the morphology, the physico-chemical and thermal properties of hybrid materials in thin films.

IV.2.1. Fourier Transform Infrared Spectroscopy (FT-IR):

infrared spectra were recorded using a Perkin Elmer FTIR Spectrum 1000 spectrophotometer in the transmission mode at room temperature. After an average of 32 scans, the samples were scanned from 4000 to 400 cm^{-1} with a resolution of 2 cm^{-1}.

IV.2.2. X-ray Diffraction (XRD):

Measurements were performed with a Phillips X'PERT Pro diffractometer at room temperature using a CuKα radiation source and 1.54 Å X-ray wavelength, 30 mA current, and 40 kV generator voltage. The 2θ scanning range was 5–70 in fixed time 0 mode with a step interval of 0.02.

IV.2.3. UV-VIS Spectrophotometry:

The UV-VIS absorption and transmission spectra of the samples were recorded using a Perkin Elmer 4B spectrophotometer in the range of 200-800 cm^{-1}.

IV.2.4. TGA Analysis:

Thermogravimetric analysis was performed using a Mettler Toledo Star System in an N_2 atmosphere from 30 to 700° C at a heating rate of 10°C per min.

IV.2.5. Differential Scanning Calorimetry:

Thermal analysis was performed in a Perkin-Elmer differential scanning calorimeter (DSC), in an N_2 atmosphere. The temperature range studied was -50 to 270°C. The heating rate was 20 C/min. Typical sample weights were 6 mg.

IV.2.6. Water absorption:

The relative rate of water absorption under saturated conditions was determined by drying films for 12 hours in a vacuum oven at 50°C, after immersing them in distilled water. The water absorption of the films under saturated conditions was calculated according to the ASTM-D570-81 procedure. The composites' water (W) was calculated using the following equation and plotted against time:

$$\mathbf{W}(\%) = \left[\frac{\boldsymbol{m_t - m_0}}{\boldsymbol{m_0}}\right].100 \quad \textbf{\textit{(1)}}$$

where W is the water uptake (in percent), m_0 is the initial dry weight of the film, and m_t is the dry weight of the swollen film.

IV.2.7. Contact Angle:

5µl of water was dropped on the film surface at room temperature at a relative humidity of 30%± 5%, using a rame-hart contact angle goniometer and tensiometer instrument. A (speed digital CCD camera) was used to capture the picture of the droplet of water. The contact angle is the angle created by the baseline and the tangent line at the point where the water droplet makes contact with the surface.

IV.2.8 Conclusion

The different characterization techniques used in this work as well as the associated experimental devices were exposed. For our studies, the basic principle of each technique has been recalled and the corresponding instrumentation has been described. We are now going to present all the results obtained thanks to the implementation of all the techniques mentioned above.

References

[1]. PVA powder from Sigma Aldrich **[online],** Available on: https://www.sigmaaldrich.com/DZ/fr/product/aldrich/348406

(Consulted on 06/01/2022)

[2]. TiO_2 nanoparticles from Sigma Aldrich **[online],** Available on: https://www.sigmaaldrich.com

(Consulted on 06/01/2022)

[3]. TEOS from Sigma Aldrich **[online],** Available on: https://www.sigmaaldrich.com/DZ/fr/product/aldrich/131903 (Consulted on 06/01/2022)

[4]. ETHANOL from Sigma Aldrich **[online],** Available on: https://www.sigmaaldrich.com/DZ/fr/product/mm/159010

(Consulted on 06/01/2022)

[5]. HCL from Sigma Aldrich **[online],** Available on: https://www.sigmaaldrich.com/DZ/fr/product/sigald/258148

(Consulted on 06/01/2022)

Chapter V
Results and Discussions

Chapter V Results and Discussions

In this chapter, we present and discuss the results obtained from our study. The chapter is structured into two key sections. Firstly, we investigate the influence of SiO_2 on the properties of PVA, analyzing its impact on various physical and chemical characteristics. Secondly, we examine the effect of TiO_2 content on the physicochemical and thermal properties of PVA/SiO_2 hybrids, exploring how this component affects the behavior of the materials under different conditions. Together, these two sections provide a comprehensive analysis of the properties and behavior of PVA/SiO_2/TiO_2 hybrids, shedding light on important factors that can impact their performance in various applications.

V.1. Structure and Morphology of the Hybrid Films

V.1.1. Fourier Transform Infrared Spectroscopy

Fourier Transform Infrared Spectroscopy (FT-IR) was used to characterize the presence of specific chemical groups in the hybrid materials, neat PVA, PVA-SiO_2, and PVA-SiO_2-TiO_2 were analyzed using the FT-IR transmittance mode in the wavenumber range of 4000 to 400 cm^{-1}.

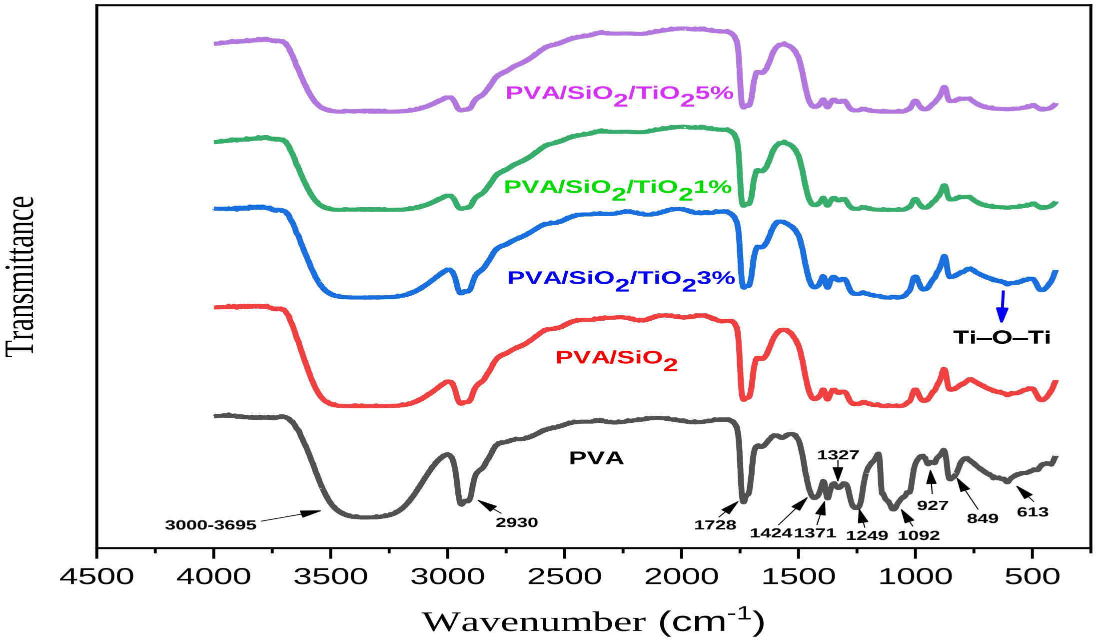

Fig.V.1 FTIR spectra of neat PVA and PVA/SiO_2 and PVA/SiO_2 films with different TiO_2 concentrations: 1%, 3%, 5%.

Fig. V.1 presents FT-IR spectra. For all samples, a broad absorption peak is centered on 3000–3660 cm^{-1}, which is due to the presence of the hydroxyl group of PVA molecules and adsorbed water (HOH) and the stretching vibrations of Si-OH groups resulting from the incompleteness of the condensation reaction of TEOS [1].

The vibrational band observed between 2816 and 2990 cm^{-1} refers to the stretching of νas (CH_2) and symmetric νs(CH_2) band of CH_2 from alkyl groups of PVA [2].

A weak band is observed at 2285 cm^{-1} and has been attributed to the frequency of the combination of (C-H) and (C-C) [3]. The peaks between 1623–1763 cm^{-1} have been assigned to C=C stretching mode and/or C=O stretching from the acetate group remaining after the preparation of PVA from hydrolysis of poly (vinyl acetate) [4]. Two strong bands observed at 1424 and 849 cm^{-1} have been attributed to bending and stretching modes of the CH_2 group, respectively [3,5]. The weak band at 1328 cm^{-1} is assigned to the combined frequency of the (CH + OH) group [3]. The band around 1249 cm^{-1} is assigned as υw (CH) wagging vibration.

The strong band at 1092 cm^{-1} and sharp band at 927 cm^{-1} are attributed to the C-O and C-C groups stretching in the crystalline and the amorphous phase of the PVA matrix, respectively [6]. The intensity of the strong band at 1092 cm^{-1} increases as the degree of crystallinity increases [7].

For the samples which contain silica**,** the peaks between 920–950 $cm^{-1}$are assigned to Si-OH stretching (silanol), and Symmetric C-O stretching (ether) [8].

The broadband in the region 1052–1100 cm^{-1} which might be attributed to Si-O-Si stretching vibration, indicates that the silica network has successfully been formed [8,9]. It is to be noted that the peak at 1092 cm^{-1} became flattered in the sample containing the silica, which indicates the diminution of crystallinity and that the silica/PVA network has successfully been formed.

The peak at 1085 cm^{-1} due to Si–O–C stretching vibrations shows that the organic process was covalently connected to the inorganic phase [10]. It is striking that the large band between 3000-3695 cm^{-1}(3660) shows a broadening in comparison to the hydroxyl stretching vibration of neat PVA. This is due to the appearance of new bands at 3100-3200 cm^{-1} which are attributed to the hydrogen bonding between PVA and silica through their hydroxyl groups, but also the H-bonded hydroxyl group having a polymeric association [9].

Compared with neat PVA and PVA-SiO_2, new broad absorption bands around 450–800 cm^{-1} are present in the FT-IR spectra of PVA/SiO_2 at different contents of TiO_2, which are attributed to Ti-O-Ti and Ti-O-O bonds. The intensity of these peaks increases with the increase of TiO_2 content [11–13]. The intensity of PVA's OH groups decreased as the concentration of TiO_2 nanoparticles increased. It is also noticed that the peak of crystallinity at 1092 cm^{-1} becomes flattered with the increase of the amount (1, 3, and 5%) of nano-TiO_2 suggesting the diminution of the crystallinity. This is due to the OH groups of PVA chains associated with the OH groups of TiO_2 nanoparticles. The observed FT-IR band positions and their assignments are presented in Table 2.

Table V.1 FTIR peaks assignment and their corresponding Wavenumber.

Band Assignment	Wavenumber (cm^{-1})
O-H stretching	625
CH_2 stretching	852
C-C stretching	917
C-O stretching	1100
C-H +OH combination frequencies	1328
CH_2 bending	1429
C=C stretching vibration	1660
-	1710
C-H+C-C stretching	2169
CH_2 stretching	2938
O-H stretching	3127
-	3493
Si-O + C-O stretching	920–950
Si-O-Si stretching	1052–1100 and 460
Si-O-C stretching	1085
Ti-O-O + Ti-O-Ti stretching	450
C–C stretching; increase in the intensity can be related to the decrease of the crystallinity, i.e., represents noncrystalline conformation of the PVA carbon backbone	920

These results were also confirmed by XRD analysis [14]. Nakane et al [14] have observed that the crystallinity of PVA considerably decreased in the PVA/Silica hybrid composites. This behavior may be imputable to the drop of crystallinity and hydrogen bonding at the PVA-silica particle interface. These data confirm the results obtained by DSC, water contact angle, and water absorption, which will be further discussed.

V.1.2. X-Ray Diffraction Analysis

Fig. V.2 presents the X-ray diffraction (XDR) patterns of the doped PVA/SiO_2 hybrid films.

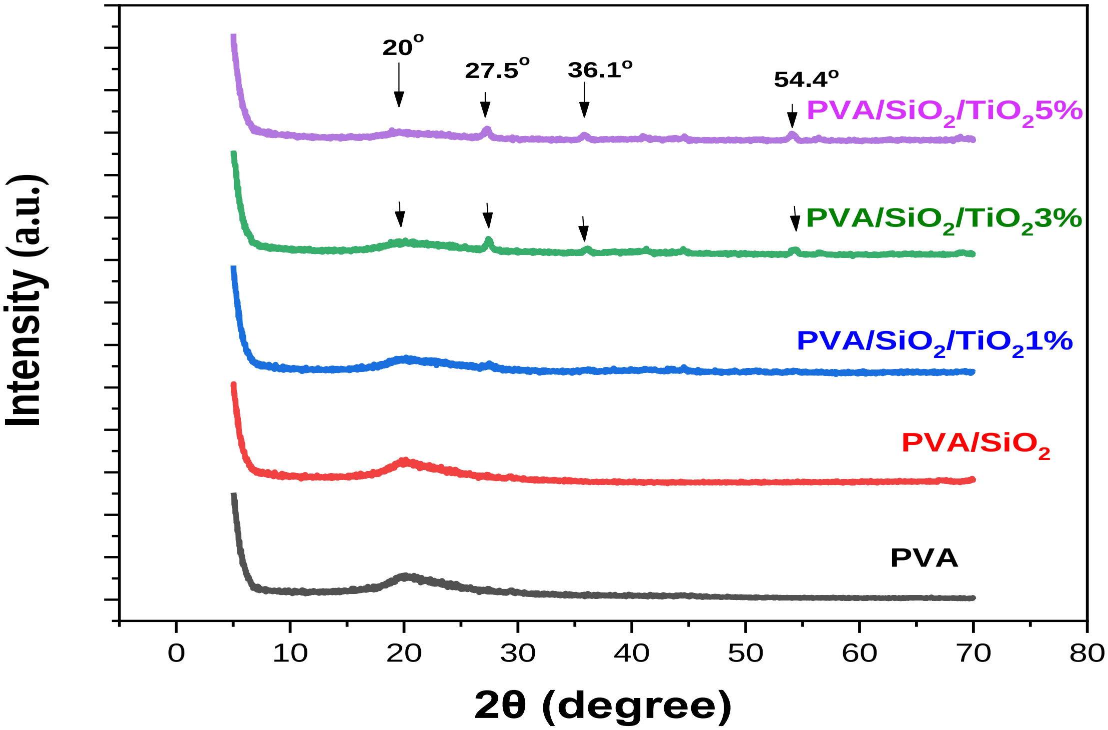

Fig. V.2 X-ray patterns of hybrid films.

The neat PVA sample exhibits one peak around 2θ equal to 20°, corresponding to the (101) plane of semi-crystalline PVA [15]. This peak becomes much broader and shifts in the sample which contains silica. These findings show that the presence of SiO_2 in hybrid films affects the crystallinity of PVA.

For the sample containing 1% of TiO_2, the diffraction peak becomes flattered with the absence of any sign of Anatase, Rutile, or Brookite; which confirms its interaction with PVA/SiO_2.

For the samples containing 3 and 5%, new peaks are observed at 27.5, 36.1, and 54.4° suggesting the presence of (110), (101), and (211) planes respectively. These peaks are in agreement with the tetragonal structure of the TiO_2 rutile phase (JCPDS 21-1276) [16]. The results confirm also the existence of nano-sized TiO_2 particles in the samples which did not react especially at high concentrations.

V.2. Optical Transparency Analysis of the Films

V.2.1. UV-VIS Spectroscopy

UV-VIS spectroscopy may be used to measure the absorption, transmission, and reflectivity of a wide range of substances and technologically significant materials.

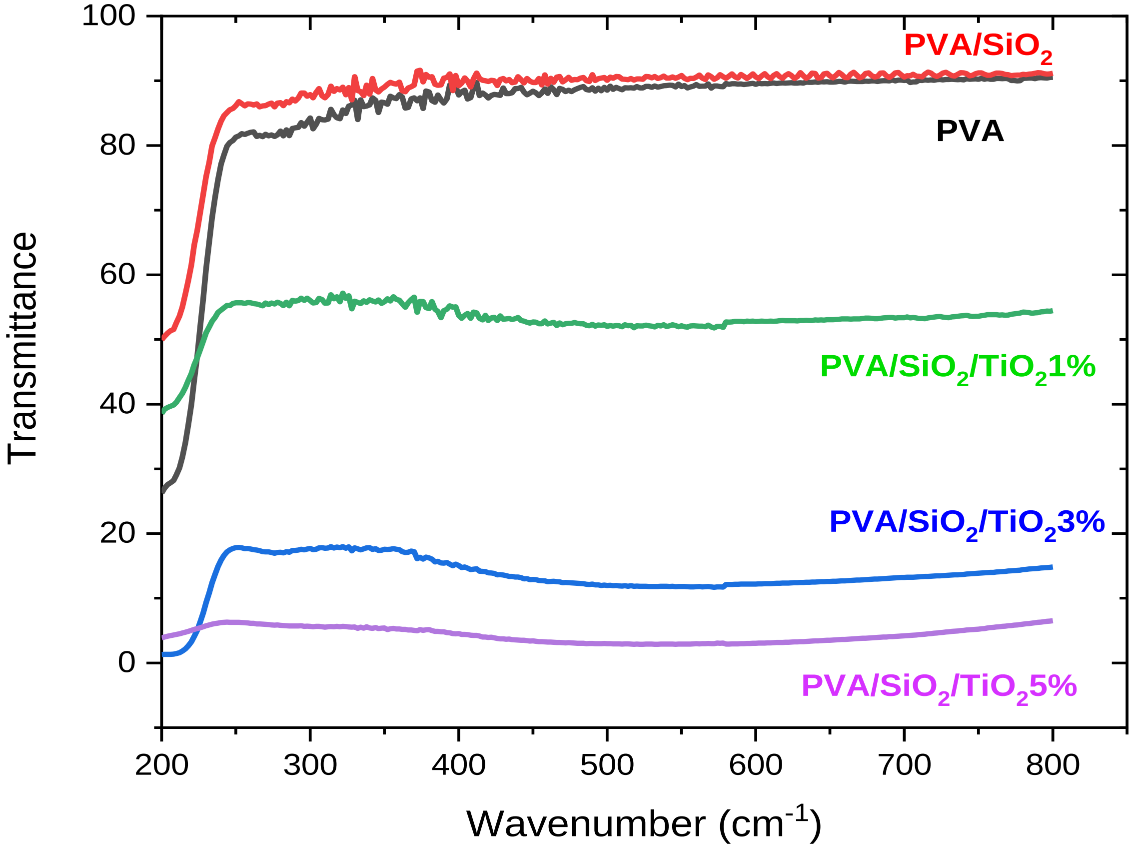

Fig. V.3 UV–VIS transmittance spectra of Neat PVA and PVA/SiO_2 and PVA/SiO_2 films with different TiO_2 content:1%, 3%, 5%.

Fig. V.3 shows the UV-VIS transmittance spectrum in the range between 200–800 nm for neat PVA, PVA/silica, and PVA-silica-TiO_2 composites with different TiO_2 contents.

Neat PVA exhibits good transparency (88–90%) in the visible region (400-780 nm). Furthermore, it is observed that increasing SiO_2 content results in higher transparency (91–92%) in the same region due to the smaller particle size and higher dispersity. It can be noticed also that the transmittance decreases in general with increasing TiO_2 content up to (4.69-6.80%) for the sample containing 5 wt%. This is because TiO_2 particles absorb and scatter the light from the composites film [17]. These results are similar to those described by Chiang, and Mallakpour et al [18].

The appearance of the absorption peaks around 250 nm was noticed in all samples containing TiO_2. This observation suggests the presence of a titanium portion in the composites, and the intensity of these peaks is dependent on the loading of TiO_2 in the core of the composites; it decreases with increasing the filler concentration. However, no absorption peaks were observed in the samples that do not contain TiO_2 [19]. So, the existence of conjugated structures was verified by peaks varying from 200 to 300 nm, as investigated by the FT-IR technique. The characteristic bands present at 288 and 236 nm in neat PVA and PVA/silica samples are due to the $\pi \rightarrow \pi^*$ transition of the unsaturated bond Si=O from silica, C=O, and/or C=C primarily in the tail-head of neat PVA polymer [20]. Because of the presence of lone pairs of electrons on the hydroxyl substituent and Si-O-Si, the absorption bands at 298.50 nm and 290.50 nm are due to $n \rightarrow \pi^*$ transitions [21].

V.3. Thermal Properties

V.3.1. Thermogravimetric Analysis

The thermogravimetric thermograms of neat PVA, PVA/SiO_2, and PVA/SiO_2/TiO_2 composites are shown in Fig. V.4a, Fig. V.4b, and Fig.V. 4c, respectively.

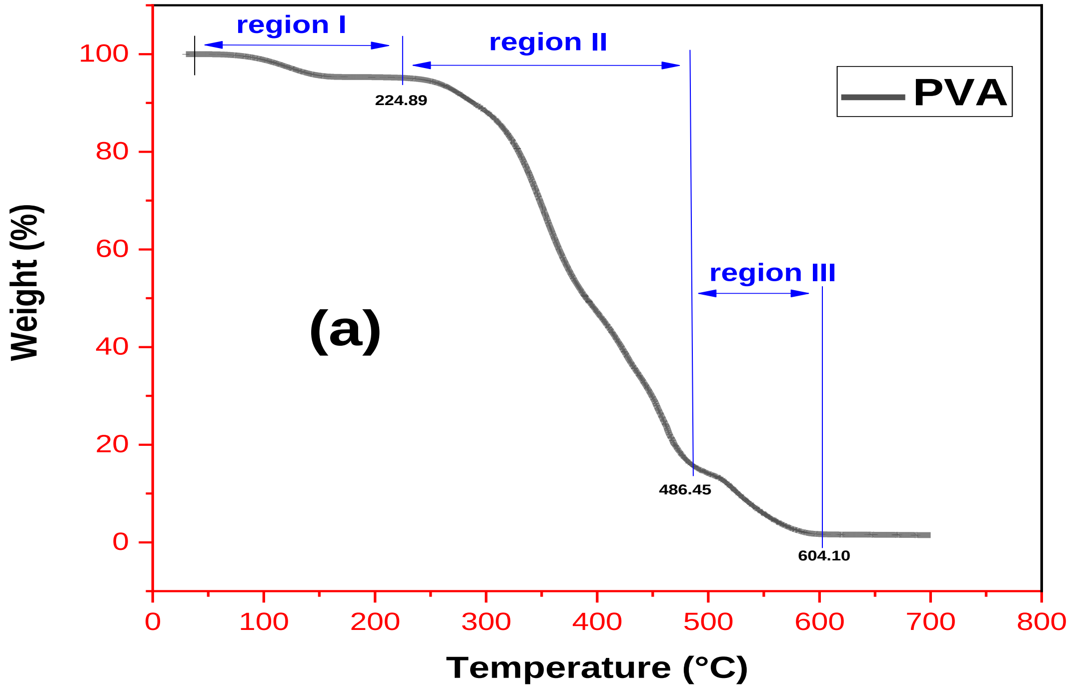
region I
region II
region III
224.89
486.45
604.10
PVA
(a)
Weight (%)
Temperature (°C)
100
80
60
40
20
0
0
100
200
300
400
500
600
700
800

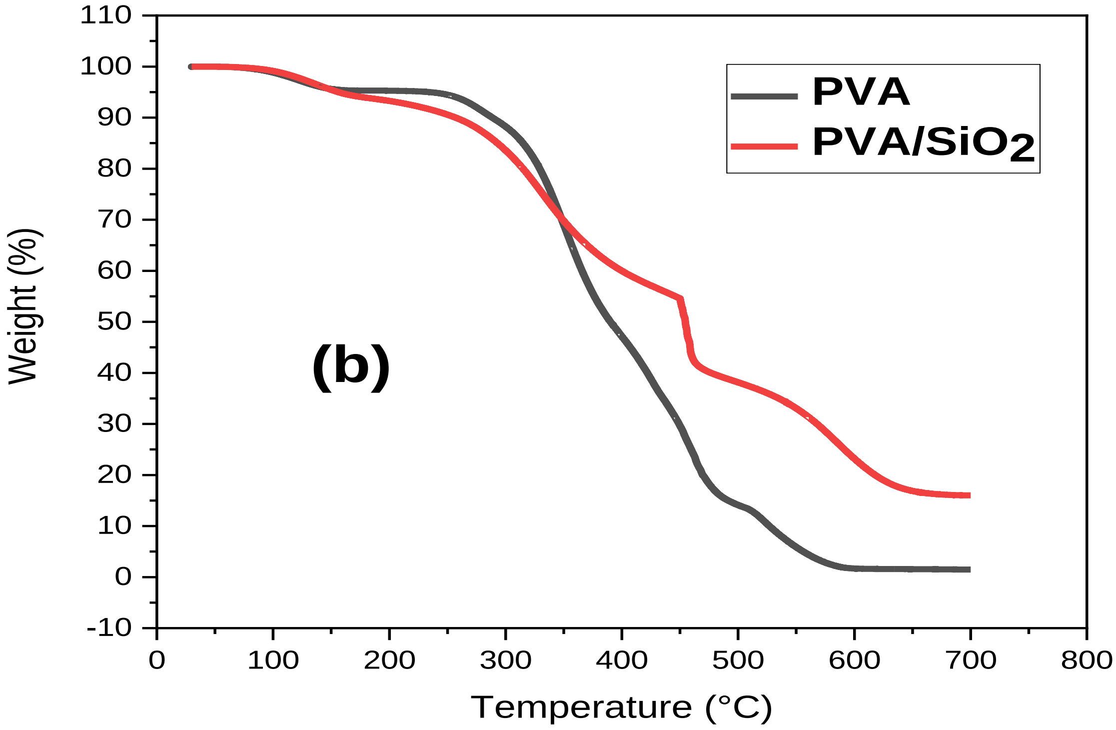
PVA
PVA/SiO2
(b)
Weight (%)
Temperature (°C)
110
100
90
80
70
60
50
40
30
20
10
0
-10
0
100
200
300
400
500
600
700
800

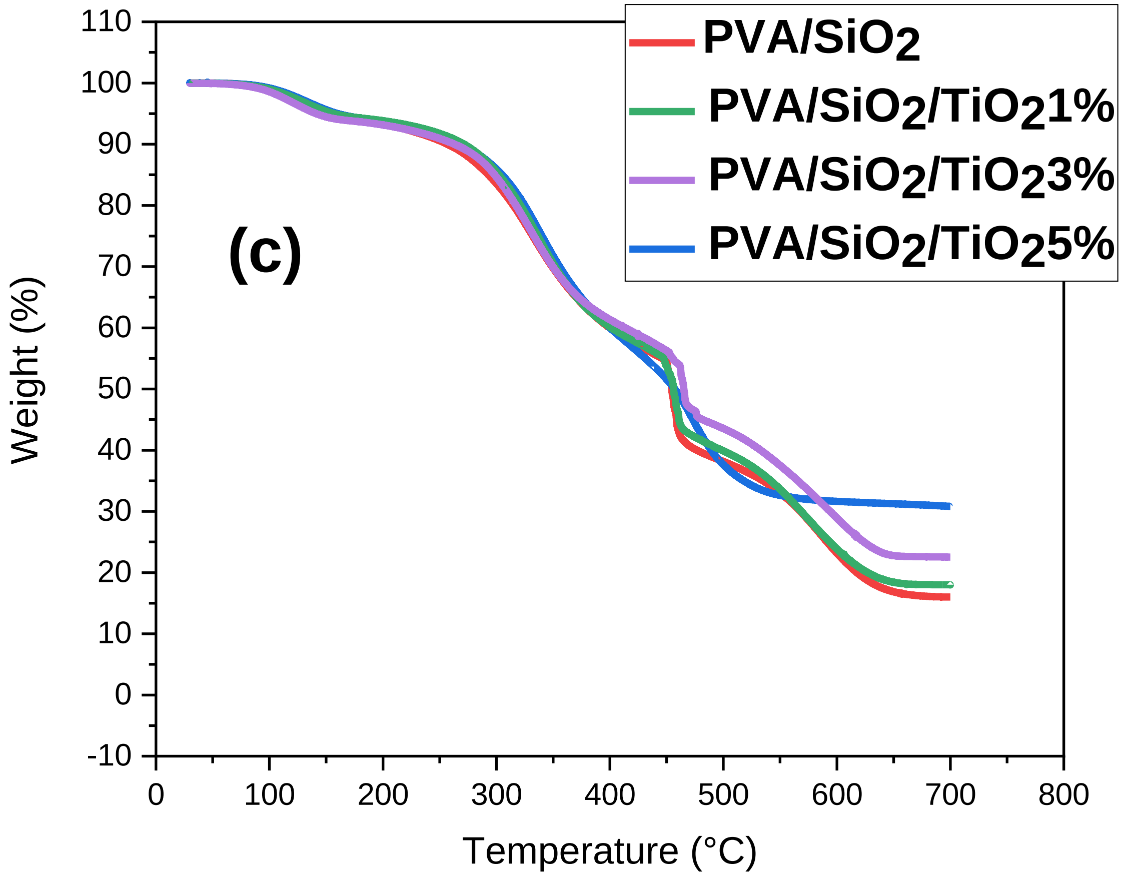

Fig. V.4 (a, b and c) TGA thermograms of neat PVA (a), PVA/SiO_2 (b), and PVA/SiO_2 films with different TiO_2 contents:1%, 3%, 5% (c).

As shown in Fig. V.4a, the thermal degradation of neat PVA shows three major weight loss regions [22]. The small first region occurs at temperatures between 80–150 °C with a maximum weight loss temperature at Tmax, step1 = 95 °C. This is due to the evaporation of free and bound water molecules. In this stage, a small weight loss can be observed (5%). This weight loss can be attributed to the removal of residual solvent molecules [23].

The second region, presenting a maximum decomposition rate, occurs in the temperature range from 224 to 486°C. This weight loss was estimated to be 15 % and corresponds to the degradation of the (-OH) side group leading to the formation of a polyene at Tmax, step2 =270 °C. The third step, observed at 410–450 °C range where Tmax, step3 =430 °C, can be related to the decomposition of the main chain of PVA polymer (cleavage of C–C backbone) which is currently called carbocation or so-called carbonation

[22]. This last step, occurring at 600 °C, induces a weight loss of 95 wt.% corresponding to a total residue of 05 %.

After adding silica to the PVA matrix an improvement in the thermal stability of the PVA/SiO_2 membranes was observed (See Fig. V.4b), in this case, the PVA/SiO_2 thermogram shows four weight-loss regions with a slow and gradual degradation [24]. It may be due to the loss of the crystalline structure which changes to a more amorphous state, caused by hydrogen bonding between PVA chains and silanol ends of the silica [24]. This explanation was early discussed and confirmed above by the FT-IR and DSC sections. The first weight loss is estimated at 6%. This is due to the silanol groups implicating the self-condensation reaction associated with the removal of the residual solvent molecules (water and ethanol) at temperatures of 30-170 °C [25].

The remaining regions of weight loss occurred in the temperature ranges as follows: 170–390 °C, 390–490 °C, and 490–690 °C with maximum weight loss temperatures of 120, 330, 455, and 590 °C, respectively. These temperatures indicate the degradation of hydroxyl groups with other organic residues of PVA and silica networks. The final residual weight corresponds to 76.9%–83.6% of the global weight with a total residue of 20 %. It can be inferred that attaching a silica network to the PVA matrix polymer increases the thermal stability of the films.

Fig. V.4c presents the TGA curves of PVA/SiO_2 with different nano-TiO_2 content. It can be observed that the heat tolerance of neat PVA was increased after integration with the silica network.

The TGA thermograms of PVA/SiO_2/TiO_2(1%), PVA/SiO_2/TiO_2(3%), and PVA/SiO_2/TiO_2(5%) show a similar behavior towards the thermal degradation as those of PVA/SiO_2 hybrid films. The thermograms show four major weight loss regions, and the difference lies in the amount of the final residual weight. Sample PVA/SiO_2/TiO_2 (1%), has a final residual weight of 17.84 % concerning the global weight at a temperature of 700° C. The PVA/SiO_2/TiO_2 (3%) sample and PVA/SiO_2/TiO_2 (5%), have a final residual weight of 22.73 % and 31.12 % respectively. This indicates that there is an enhancement of thermal stability of PVA/SiO_2 with increasing the content of nano-TiO_2 (1, 3, 5%). It can be concluded that the TiO_2 nanoparticles as a reinforcing filler led to an enhancement of the thermal stability of PVA/SiO_2 nanocomposite films.

V.3.2. Differential Scanning Calorimetry

DSC analysis is an important technique for measuring the thermal properties of materials. In this work, DSC was used to measure the crystallization and melting temperatures (Tc, Tm).

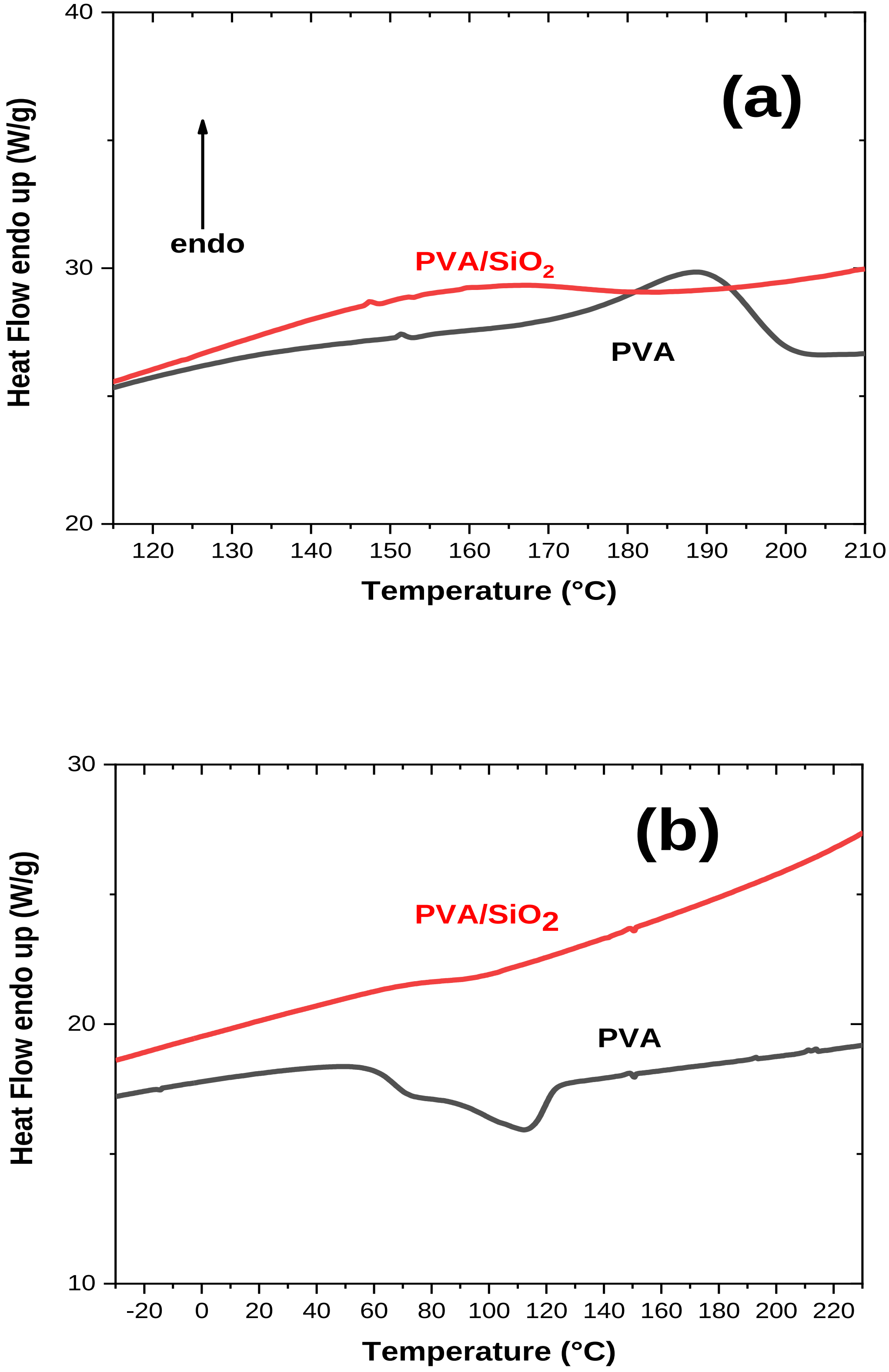
(a)
endo
PVA/SiO$_2$
PVA
Heat Flow endo up (W/g)
20
30
40
120
130
140
150
160
170
180
190
200
210
Temperature (°C)
(b)
PVA/SiO$_2$
PVA
Heat Flow endo up (W/g)
10
20
30
-20
0
20
40
60
80
100
120
140
160
180
200
220
Temperature (°C)

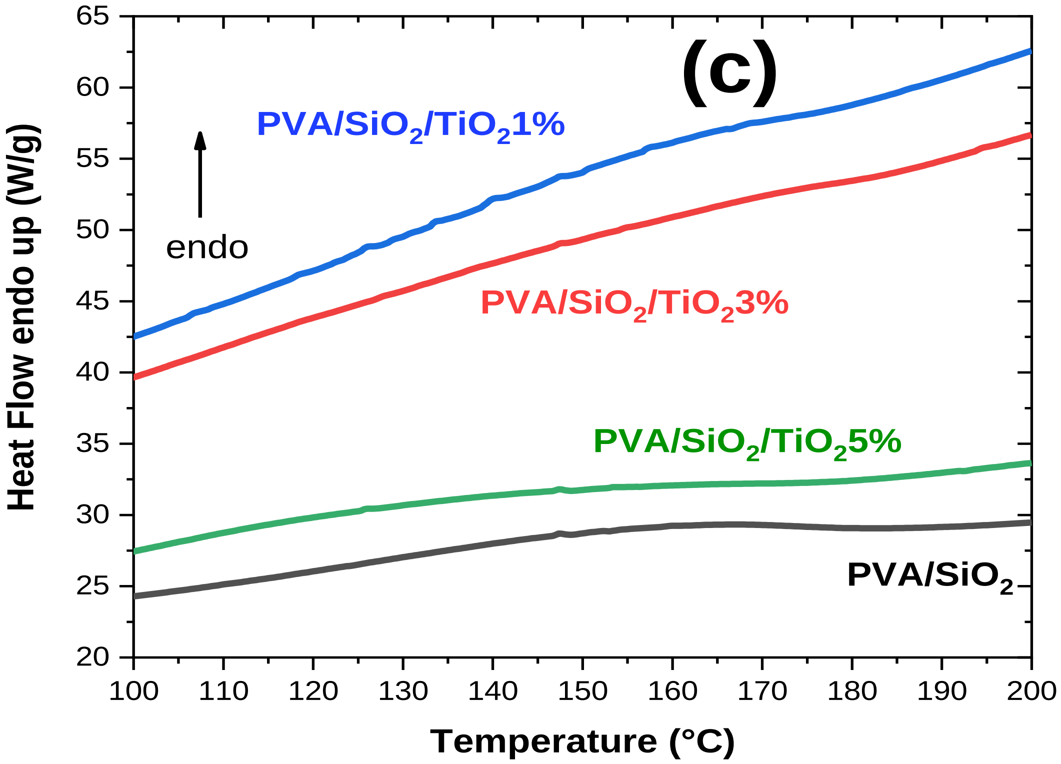

Fig. V.5 (a, b, c) DSC curves of (a): melting peaks for neat PVA and PVA/SiO_2, (b): crystallization peaks for neat PVA and PVA/SiO_2, (c): melting peaks for PVA/SiO_2, and PVA/SiO_2 films with different TiO_2 contents:1%, 3%, 5%.

Fig. V.5 (a, b, c) shows the DSC curves of neat PVA, PVA/SiO_2, and PVA/SiO_2/TiO_2 nanocomposites with different contents of nano-TiO_2 (1%, 3%, and 5%). The curves show both exothermic and endothermic reactions. PVA reveals a relatively large and sharp melting endothermic peak at 193°C corresponding to the melting point (Fig. V.5a), while a larger and less sharp very weak, and broad melting endothermic peak of PVA/SiO_2 is observed at around 167°C with a decrease by 26°C compared to neat PVA.

On the other hand, there is an exothermic peak that corresponds to the crystallization region (Tc) and is observed for Neat PVA at a temperature of 112°C (Fig. V.5b) but does not appear for PVA/SiO_2: This Loss of crystallization is caused by the crosslinking reaction between PVA chains and the silanol ends of silica as was already explained in the previous results. Other works also provided similar discoveries

[26]. For example, Bin et al [27] reported this kind of behavior for PVA–VGCF (vapor growth carbon fiber) and PVA–MWNT (multi-wall carbon nanotubes) composites.

Fig. V.5c shows the DSC curves of PVA/SiO_2/TiO_2 nanocomposites, it can be observed that the endothermic peak of PVA segments decreased rapidly and disappeared for all samples containing TiO_2 nanoparticles. These results are in contrast with what is generally reported in the literature [28]. It can be concluded that the depression of the melting temperature and broadening of the peak indicates that the regular structure of the PVA molecules was altered by the presence of silica and nanoparticles of TiO_2.

V.4. Physical Properties

V.4.1. Water absorption.

It is to be recalled that dried films were immersed in distilled water at room temperature (25° C) Fig. V.6 (a, b, c) shows the extent of water absorption for neat PVA, PVA/SiO_2 composite, as a function of titanium percentage (1, 2, and 3%).

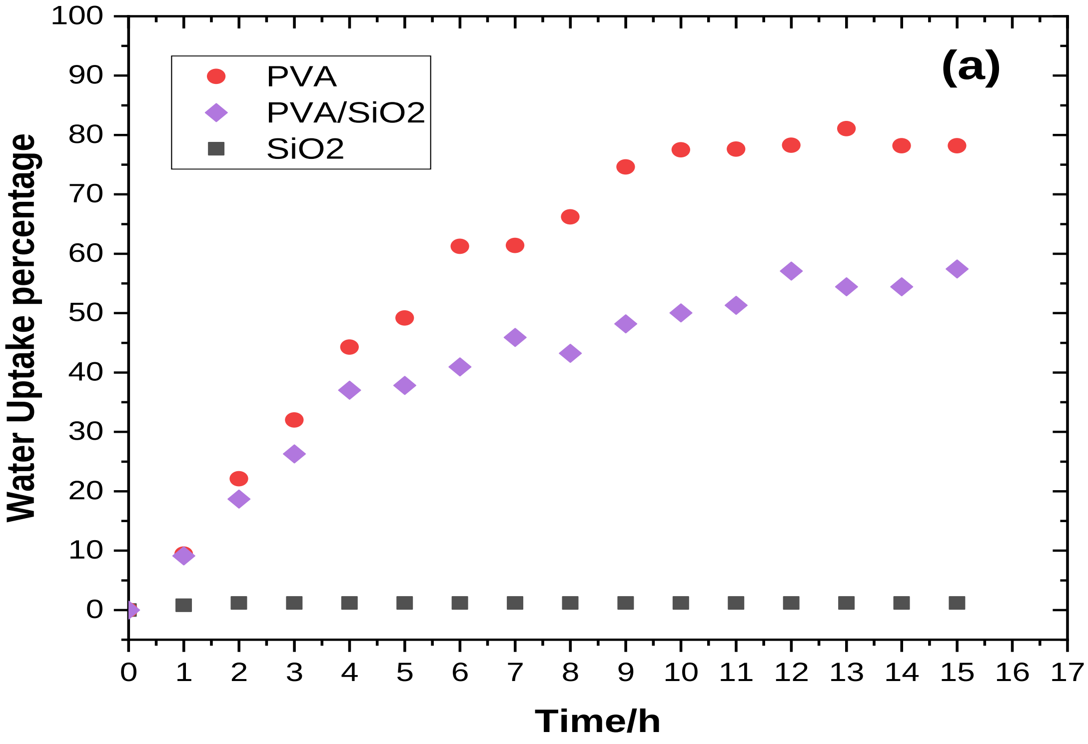

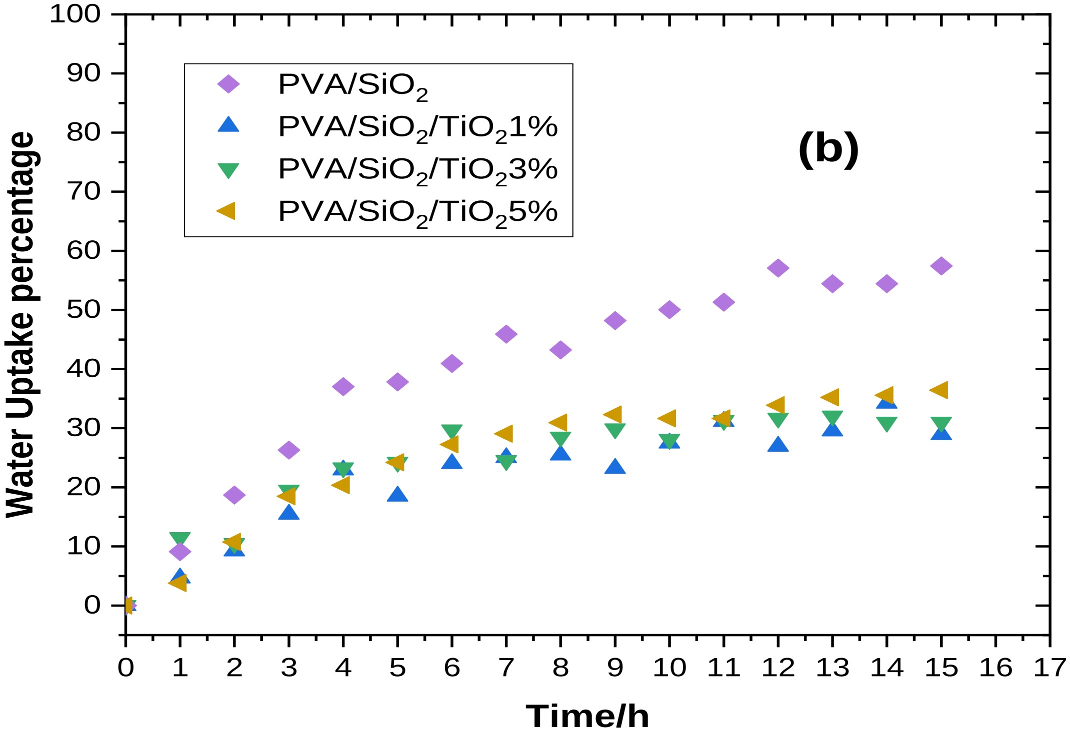

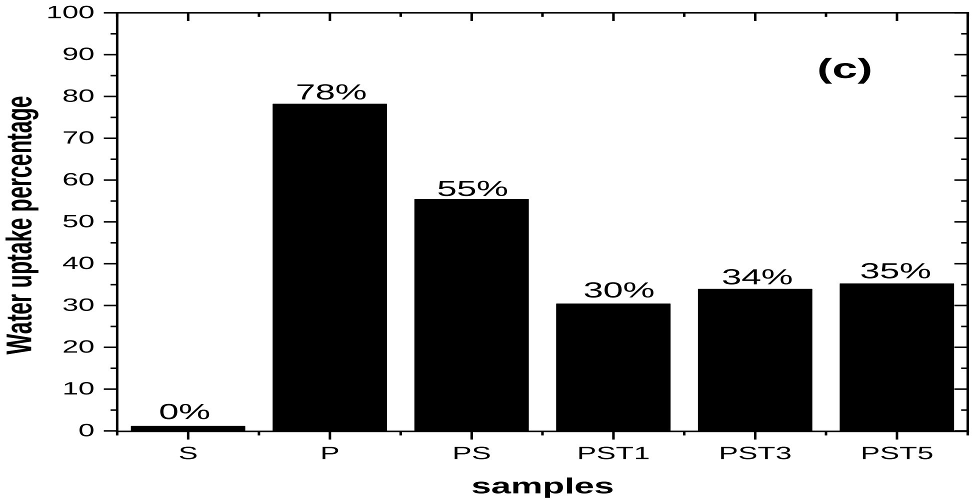

Fig. V.6 (a, b, c) Extent of water absorption of Neat PVA and PVA/silica hybrid and PVA/silica hybrid as a function of TiO_2 content. S: Neat SiO_2, P: Neat PVA, PS: PVA/SiO_2, PST1: PVA/SiO_2/TiO_2 (1%), PST3: PVA/SiO_2/TiO_2 (3%), PST5: PVA/SiO_2/TiO_2 (5%).

PVA absorbs much water through its hydroxyl groups. There is a considerable decrease in the water absorption (from 78 to 55%) for the films containing silica compared to neat PVA. The silica may create hydrogen bonds with the PVA chain; which decreases the volume of water consumed by the polar hydroxyl groups. Based on these observations, it can be concluded that these hybrid films may be used as water perm selective membranes [29]. Pereira et al [23] and Nakane et al [14] investigated the rate of hydrolysis of PVA/silica hybrid materials and have also reported that the solubility and degree of swelling in water decreased linearly with silica content in the composites [29]. A reduction in water uptake capacity was observed at low nano-TiO_2 content (1%). This is due to The TiO_2 composition which would form a wall of hybrid films, being non-porous and by filling its empty spaces, therefore, a reduction in water uptake capacity may have occurred.

The reaction between TiO_2 and PVA through its available hydroxyl groups enhanced the resistance of water leading to a further decrease. In this case, these results seem to be very similar to those reported by Chen et al [30]. But, when increasing the amount of nano-TiO_2 (3 and 5%) an increase in the water absorption was also observed suggesting aggregation of the particles.

Since PVA is currently used as a biomaterial, it can be proposed that these novel hybrid materials can be considered potential candidates for biomedical applications.

V.4.2. Water Contact Angle

Contact angle measurements are the best way to verify whether a surface is hydrophilic or hydrophobic. A high water contact angle implies a more hydrophobic surface. The water droplet and contact angle of the specimens are presented in Table V.2 and Fig.V.7.

Table V.2 The contact angle of PVA and PVA/SiO_2/TiO_2 nanocomposites incorporated at various TiO_2 concentrations.

Sample	TiO_2 content (%)	Contact angle (degree)
PVA	0	50.82±0.01
PVA/SiO_2	0	63.86±0.03
PVA/SiO_2/TiO_2	1	72.08±0.50
PVA/SiO_2/TiO_2	3	67.12±0.04
PVA/SiO_2/TiO_2	5	64.04±0.04

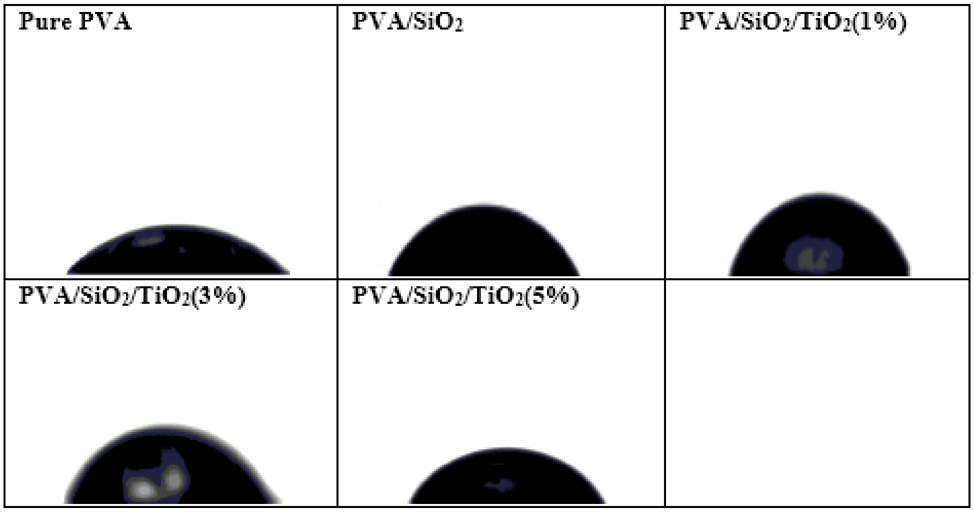

Fig. V.7 Images of Deionized water droplets on Neat PVA and hybrid films

Since PVA contains a lot of hydroxyl groups in its structure, it consequently exhibits higher hydrophilicity. Thus, PVA has a lower contact angle than other samples in which fewer hydroxyl groups are present. When 40% silica was added to PVA, the contact angle increased dramatically going from 64.04° to 72.08°. This behavior is essentially attributed to the decrease in the number of hydroxyl groups on the surface of PVA, which can interact with silanol groups of silica (condensation reaction) as was explained in FT-IR, DSC, and water absorption results.

As shown in Table 3, the contact angle of the films increased after adding 1% nano-TiO_2, suggesting that the nanoparticles are uniformly distributed in the core of the polymer and are well linked to the PVA chains. However, a reduction in the contact angle was detected in samples containing 3 and 5% nano-TiO_2. This is attributable to the agglomeration and migration to the surface. This has a consequence to render the material surface more hydrophilic. These results are consistent with those obtained by El-Wail et al [31] and Vahid Goudarzi et al [32].

V.5. Conclusion

The results obtained from our study lead us to draw several important conclusions. Firstly, we successfully synthesized PVA/SiO_2/TiO_2 hybrids using the sol-gel method, and found that the addition of TiO_2 nanoparticles to the PVA-SiO_2 composite resulted in significant improvements to the material's properties. In particular, the hybrid films showed enhanced water uptake, thermal stability, and optical properties compared to both neat PVA and PVA/SiO_2. Furthermore, we observed that the addition of

40% TEOS (SiO_2) had a positive impact on the properties of PVA, and that the water absorption of the films improved with the inclusion of the inorganic component.

Our results indicate that PVA/SiO_2 hybrids filled with TiO_2 nanoparticles hold great potential for use as UV masks, due to their selective absorbance of UV light, transparency, and ability to form fibers. In addition, these films could be used in various applications such as filtration, separation, and tissue engineering, among others. Overall, our study highlights the promising properties and potential applications of PVA/SiO_2/TiO_2 hybrids, and suggests avenues for future research and development in this field.

References

[1] Unger K K, Surface Structure of Amorphous and Crystalline Porous Silicas: Status and Prospects, The Colloid Chemistry of Silica. Advances in Chemistry, ed H E Bergna (Washington DC: American Chemical Society). 234 (1994) 165–81.

[2] Chen X, Preparation and property of TiO_2 nanoparticle dispersed polyvinyl alcohol composite materials, Journal of Materials Science Letters. 21 (2002) 1637–1639.

[3] Raju Ch L, Rao J L, Reddy B C V, Veera Brahmam K, Thermal and IR studies on copper doped polyvinyl alcohol, Bull Mater Sci. 30 (2007) 215–8.

[4] Fathi E, Atyabi N, Imani M, Alinejad Z, Physically crosslinked polyvinyl alcohol–dextran blend xerogels: Morphology and thermal behavior, Carbohydrate Polymers. 84 (2011) 145–52.

[5] Santos C, Silva C J, Büttel Z, Guimarães R, Pereira S B, Tamagnini P, Zille A, Preparation and characterization of polysaccharides/PVA blend nanofibrous membranes by electrospinning method, Carbohydrate Polymers. 99 (2014) 584–92.

[6] Jessie Lue S, Chen J, Ming Yang J, Crystallinity and Stability of Poly (vinyl alcohol) -Fumed Silica Mixed Matrix Membranes, Journal of Macromolecular Science, Part B. 47 (2007) 39–51.

[7] Tretinnikov O N, Zagorskaya S A, Effect of inorganic salts on the crystallinity of polyvinyl alcohol, J Appl Spectrosc. 78 (2012) 904–8.

[8] Que W, Sun Z, Zhou Y, Lam Y L, Chan Y C, Kam C H, Optical and mechanical properties of TiO_2/SiO_2/organically modified silane composite films prepared by sol-gel processing, Thin Solid Films. 359 (2000) 177-183.

[9] Plinio I, Infrared spectroscopy of sol-gel derived silica-based films: a spectra-microstructure overview, Journal of Non-Crystalline Solids. 316 (2003) 309-319.

[10] Tang S, Zou P, Xiong H, Tang H, Effect of nano-SiO_2 on the performance of starch/polyvinyl alcohol blend films, Carbohydrate Polymers. 72 (2008) 521–6.

[11] Panchanathan K, Bellie P N, Kanakasabai P, Prakash N B, Preparation and Characterization of Crosslinked Pva/Tio2 Hybrid Membranes Containing Sulphonic Acid Groups for Direct Methanol Fuel Cell Applications, International Journal of Engineering Technology. 3 (2015) 20.

[12] Ahmad J, Deshmukh K, Hägg M B, Influence of TiO_2on the Chemical, Mechanical, and Gas Separation Properties of Polyvinyl Alcohol-Titanium Dioxide (PVA-TiO_2) Nanocomposite Membranes. International Journal of Polymer Analysis and Characterization, 18(4) (2013) 287–296.

[13] Mohanapriya S, Mumjitha M, PurnaSai K, Raj V, Fabrication and characterization of poly (vinyl alcohol)-TiO_2 nanocomposite films for orthopedic applications, Journal of the Mechanical Behavior of Biomedical Materials. 63 (2016) 141–56.

[14] Chai JYH, Wong BT, Study of Light Scattering by TiO_2, Ag, and SiO_2 Nanofluids with Particle Diameters of 20-60 nm, Journal of Nano Research.60 (2019) 1-20.

[15] Tang C-M, Tian Y-H, Hsu S-H, Poly (vinyl alcohol) Nanocomposites Reinforced with Bamboo Charcoal Nanoparticles: Mineralization Behavior and Characterization, Materials. 8 (2015) 4895–911.

[16] Dai S, Wu Y, Sakai T, Du Z, Sakai H, Abe M, Preparation of Highly Crystalline TiO_2 Nanostructures by Acid-assisted Hydrothermal Treatment of Hexagonal-structured Nanocrystalline Titania/Cetyltrimethyammonium Bromide, Nanoskeleton Nanoscale Res Lett. 5 (2010) 1829–35.

[17] Liu X, Chen X, Ren J, Zhang C, TiO_2-KH550 Nanoparticle-Reinforced PVA/xylan Composite Films with Multifunctional Properties, Materials. 11 (2018) 1589.

[18] Mallakpour S, Barati A, Efficient preparation of hybrid nanocomposite coatings based on poly (vinyl alcohol) and silane coupling agent modified TiO_2 nanoparticles, Progress in Organic Coatings. 71 (2011) 391–8.

[19] Ma H, Shi T, Song Q, Synthesis and Characterization of Novel PVA/SiO_2-TiO_2 Hybrid Fibers, Fibers. 2 (2014) 275–84.

[20] Shehap A M, Akil D S, Structural and optical properties of TiO_2 nanoparticles/PVA for different composites thin films, Int. J. Nanoelectronics and Materials. 9 (2016) 17-36.

[21] Kaler V, Pandel U, Duchaniya R K, Development of TiO_2/PVA nanocomposites for application in solar cells, Materials Today: Proceedings. 5 (2018) 6279–87.

[22] Yang C-C, Synthesis and characterization of the cross-linked PVA/TiO2 composite polymer membrane for alkaline DMFC, Journal of Membrane Science. 288 (2007) 51–60.

[23] Betti N A, Thermogravimetric Analysis on PVA / PVP Blend Under Air Atmosphere, Eng. &Tech. Journal. 34 (2016) 2433-2442.

[24] Quan F, Chen L-L, Xia Y, Ji Q. Structure and Properties of PVA/SiO_2 Interpenetrating Polymer Network Materials Prepared by the Sol-Gel Method. Polymers and Polymer Composites. February 17 (2009) 97-100.

[25] Awada H, Daneualt C, Chemical modification of poly (vinyl alcohol) in water, applied science. 5 (2015) 840 – 850.

[26] Dodda J M, Bělský P, Chmelař J, Remiš T, Smolná K, Tomáš M, Kullová L and Kadlec J, Comparative study of PVA/SiO_2 and PVA/SiO_2/glutaraldehyde (GA) nanocomposite membranes prepared by single-step solution casting method, J Mater Sci. 50 (2015) 6477–90.

[27] Bin Y, Mine M, Koganemaru A, Jiang X, Matsuo M, Morphology and mechanical and electrical properties of oriented PVA–VGCF and PVA–MWNT composites, Polymer. 47 (2006) 1308–17.

[28] Ren M, Frimmel F H, Abbt-Braun G, Multi-cycle photocatalytic degradation of bezafibrate by a cast polyvinyl alcohol/titanium dioxide (PVA/TiO_2) hybrid film, Journal of Molecular Catalysis A: Chemical. 400 (2015) 42–8.

[29] Kotoky T, Dolui S K, Synthesis and Characterisation of Polyvinyl alcohol (PVA)/Silica Hybrid Composites Derived Through the Sol-Gel Method in Aqueous Medium: Effect of Acid Content, Silica Content and Viscosity of PVA on the Dispersion Characteristics of Silica and the Physical Properties of the Composites, Journal of Sol-Gel Science and Technology. 29 (2004) 107–14.

[30] Chen Y, Lin A, Gan F, Improvement of polyacrylate coating by filling modified nano-TiO_2, Applied Surface Science. 252 (2006) 8635–40.

[31] El-Wakil N A, Hassan E A, Abou-Zeid R E, Dufresne A, Development of wheat gluten/nanocellulose/titanium dioxide nanocomposites for active food packaging, Carbohydrate Polymers. 124 (2015) 337–46.

[32] Anon, Preparation of eco-friendly UV-protective food packaging material by starch/TiO_2 bio-nano composite: Characterization International, Journal of Biological Macromolecules. 95 (2017) 306–13.

General conclusions

General conclusions

The objective of this thesis was to prepare and characterize new organo-mineral hybrid materials based on poly (vinyl alcohol) / silica gel / Nano-TiO_2, and the study of nanoparticles of titanium dioxide (TiO_2) (from 1 to 5 %) on the properties of poly(vinyl alcohol) (PVA)/silica films. To obtain properties that conventional polymers do not possess. PVA/SiO_2/TiO_2 has been successfully synthesized by the sol-gel method.

Class II PVA/SiO_2 was synthesized. This choice has many advantages, compared to class I, namely the presence of a strong bond, Si-C, between the mineral part and the organic part of the hybrid. The protocol for the synthesis of the hybrids was established by taking inspiration from similar works found in the literature such as the temperature of the hydrolysis and condensation reaction, the water content, the mixing time, and the pH. The experimental deposition and cooling conditions were also optimized.

This new material was prepared by the sol-gel method using poly(vinyl alcohol) powder with tetraethyl orthosilicate (TEOS) as a precursor source of silica. Several characterization techniques have been used such as Fourier transform infrared (FT-IR), water absorption, the contact angle with water, ultraviolet-visible spectrometry (UV-VIS), and thermogravimetric analysis (TGA).

The few results obtained on the properties of this hybrid film are promising and encourage us to continue this study. (FTIR, XRD) were implemented and confirmed the formation of the Si-O-Si and Si-O-C bridges characteristic of this network Adding TiO_2 nanoparticles to the PVA-SiO_2 composite revealed that the properties of the resulting material were significantly improved. The properties of PVA have been improved with the addition of 40% TEOS (SiO_2). UV-VIS tests indicated that the UV protection properties of the hybrid films were significantly improved with the addition of TiO_2. According to TGA tests, hybrid films are more heat resistant than pure PVA films. The water contact angle results revealed that TiO_2 nanoparticles used as a doping compound possess a significant influence on the hydrophilicity of PVA/SiO_2 as thin films. These hybrid films showed significant improvement in water absorption, thermal stability, and optical properties compared to pure PVA and PVA/SiO_2. Finally, this thesis allowed us to develop hybrid materials with very interesting properties.

This study showed that PVA/SiO_2 filled with TiO_2 nanoparticles has the potential to be used as a UV mask, due to their selective UV absorbance. With transparency, and the ability to form fibers, the films could find applications as a means of filtration, separation, the field of food packaging, tissue engineering, and many other applications.

Recommendations

Recommendations

The current work has provided valuable insights into the development of hybrid composites. However, in order to further explore the durability performance and microstructure of the materials, several additional studies are recommended.

First, it would be beneficial to investigate the effect of Nano-TiO_2 on the mechanical properties of PVA/SiO_2 Hybrid films.

Additionally, the durability performance of the hybrid composites prepared in this study should be studied in more detail. Furthermore, studying the microstructure of the different composites both before and during the tensile test could provide a better understanding of the materials' behavior.

It is also recommended to use SEM or TEM Microscopy to study the morphology and dispersion of the TiO_2 nanoparticles.

Finally, it would be beneficial to examine the recyclability of crosslinked PVA and PVA/SiO_2, as well as crosslinked PVA/SiO_2/TiO_2 hybrid composites. These studies will provide a more comprehensive understanding of the properties of the hybrid composites and could lead to further advancements in their development.

Abstract: This thesis is focused on the preparation and characterization of poly (vinyl alcohol)/silica gel/Nano-TiO_2, and the study of titanium dioxide (TiO_2) nanoparticles (from 1 to 5%) on the properties of poly (vinyl alcohol) (PVA)/silica films. This new material was prepared by the sol-gel method using poly (vinyl alcohol) powder with Tetraethyl Orthosilicate (TEOS) as a precursor source of silica. TEOS was hydrolyzed and condensed in water and ethanol in the presence of hydrochloric acid (HCl) used as a catalyst. Fourier transform infrared (FT-IR), water absorption, water contact angle, ultraviolet-visible spectrometry (UV-VIS), and thermogravimetric analysis (TGA) were used to characterize the hybrid films obtained. The PVA/SiO_2/Nano-TiO_2 films were successfully synthesized. Owing to the FT-IR Analysis, the chemical bonds have clearly shown that the PVA backbone is linked to the (SiO_2-TiO_2) network. UV-VIS tests indicated that the hybrid films' UV shielding properties were drastically enhanced as a result of the addition of TiO_2. According to the TGA tests, the hybrid films are more heat tolerant than neat PVA films. The water contact angle results revealed that TiO_2 nanoparticles used as a doping compound possess an important influence on the hydrophilicity of PVA/SiO_2 as thin films. The film's water resistance has also been enhanced.

Keyword: Sol-Gel Method; Poly (vinyl alcohol); Silicon Dioxide; Nano-Titanium Dioxide; Hybrid Films; Spectroscopic Characterization.

Résumé : Cette thèse porte sur la préparation et la caractérisation de poly(alcool vinylique)/gel de silice/Nano-TiO_2, et l'étude de nanoparticules de dioxyde de titane (TiO_2) (de 1 à 5%) sur les propriétés du films poly(alcool vinylique)) (PVA)/silice. Ce nouveau matériau a été préparé par la méthode sol-gel en utilisant la poudre de poly(alcool vinylique) avec de l'orthosilicate de tétraéthyle (TEOS) comme source précurseur de silice. Le TEOS a été hydrolysé et condensé dans de l'eau et de l'éthanol en présence d'acide chlorhydrique (HCl) comme catalyseur. L'infrarouge à transformée de Fourier (FT-IR), l'absorption d'eau, l'angle de contact avec l'eau, la spectrométrie ultraviolet-visible (UV-VIS) et l'analyse thermogravimétrique (TGA) ont été utilisés pour caractériser les films hybrides obtenus. Les films PVA/SiO_2/Nano-TiO_2 ont été synthétisés avec succès. Grâce à l'analyse FT-IR, les liaisons chimiques ont clairement montré que le squelette du PVA est lié au réseau (SiO_2-TiO_2). Les tests UV-VIS ont indiqué que les propriétés de protection contre les UV des films hybrides étaient considérablement améliorées grâce à l'ajout de TiO_2. Selon les tests TGA, les films hybrides sont plus résistants à la chaleur que les films PVA purs. Les résultats de l'angle de contact avec l'eau ont révélé que les nanoparticules de TiO_2 utilisées comme dopant possèdent une influence importante sur l'hydrophilie du PVA/SiO_2 sous forme de couches minces. La résistance à l'eau du film a également été améliorée.

Mot clé : Méthode Sol-Gel ; Alcool Polyvinylique; Dioxyde de Silicium; Nano-Dioxyde de Titane ; Films Hybrides ; Caractérisation Spectroscopique.

ملخص: تركز هذه الرسالة على تحضير وتوصيف بولي (كحول فينيل) / هلام السيليكا / نانو ثنائي أكسيد التيتانيوم، و دراسة تأثير جزيئات ثاني أكسيد التيتانيوم النانوية (من 1 الى 5 %) على خواص بولي (كحول فينيل)/سيليكا. تم تحضير هذه المادة الجديدة بطريقة سول جل باستخدام مسحوق بولي (كحول فينيل) مع رباعي إيثيل أورثوسيليكات كمصدر أولي للسيليكا. تم تحليل رباعي إيثيل أورثوسيليكات في الماء و الكحول في ووجود حمض الهيدروكلوريك المستخدم كمحفز. تم استخدام تحويل فوريي للأشعة تحت الحمراء، زاوية الملامسة مع الماء، الطيف المرئي فوق البنفسجي، التحليل الحراري الوزني، لتوصيف الأفلام الهجينة المتحصل عليها. تم تخليق الافلام الهجينة بنجاح. طبقا لتحليل الاشعة فوق الحمراء تم تأكيد ووجود رابطة بين بولي (كحول الفينيل) و شبكة السيليكا و نانو ثنائي أكسيد التيتانيوم. تحليل الطيف المرئي أضهر أن خاصية الحماية ضد الاشعة فوق البنفسجية للأفلام تحسنت كثيرا بعد اضافة جزيئات ثنائي أكسيد التيتانيوم. طبقا لتحليل الحراري الوزني أضهرت الافلام الهجينة مقاومة حرارية أعلى لبولي (كحول الفينيل) بعد اضافة السيليكا و مقاومة أعلى للأفلام الهجينة بعد إضافة الجزيئات النانوية لثنائي أكسيد التيتانيوم. كشفت نتائج زاوية التلامس مع الماء أن الجزيئات النانوية لثنائي أكسيد التيتانيوم لها تأثير كبير على قابلية الماء كأفلام رقيقة. مقاومة الماء أيضا تم تحسينها.

الكلمات المفتاحية: طريقة سول جل ؛ بولي (كحول فينيل) ؛ ثاني أكسيد السيليكون؛ ثاني أكسيد التيتانيوم النانوي ؛ أفلام هجينة. التوصيف الطيفي